TECHNISCHE UNIVERSITÄT DRESDEN

Institut für Bioanalytische Chemie, Bergstr. 66, D-01062 Dresden

Nanoorganized biocomposites: from biomimetic potential to development of new biomaterials

by

Hermann Ehrlich

Nanoseminar, MBZ

November, 18, 2010

Content

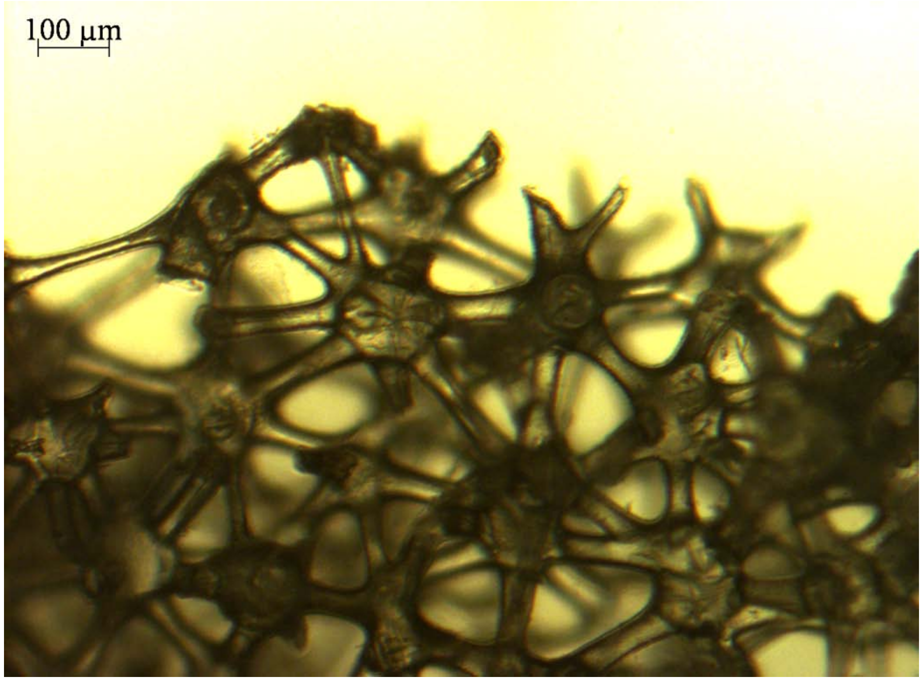

Light microscopy view: 3D skeleton of *Sarostegia oculata* glass sponge

- Silica-aragonite-chitin biocomposite
- Silica-calcite biocomposites
- Phenomenon of multiphase biomineralization
- Extreme Biomimetics

Motivation

Deep-sea *Aspidoscopulia sp.* glass sponge (up to 2 m high and 70 cm wide). It skeleton is made of silica-chitin composite.

Our discoveries of:

Silica-chitin composites in cell walls of diatoms (2010)

Silica-chitin composites in spicules and skeletal frameworks of glass sponges (2007 - 2010)

Silica-collagen composites in glass sponge spicules (2005-2010)

Sponges

(Porifera)

Glass sponges (Hexactinellida)	Horn sponges (Demospongia)	Calcareous sponges (Calcarea)
		
Silica	Silica or $CaCO_3$	$CaCO_3$

Biominerals

First evidence of the presence of chitin in sponges

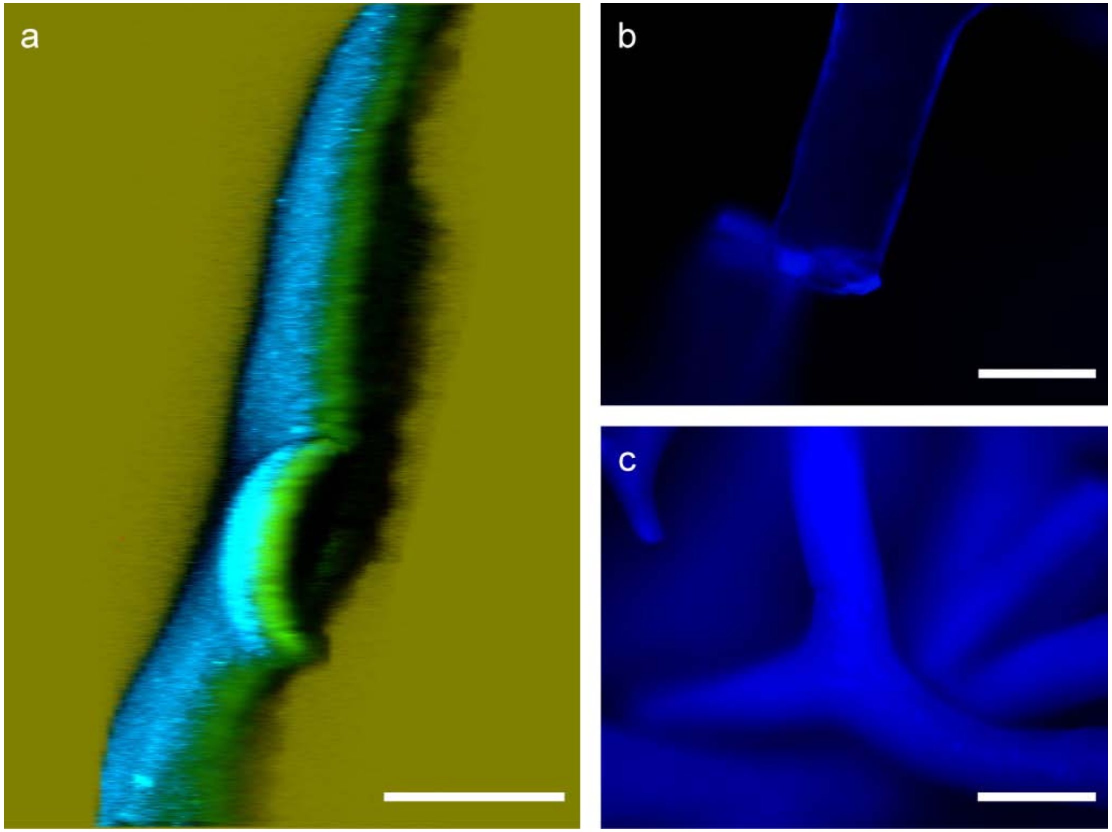

Staining indicating the presence of chitin, as shown in a 3D-reconstruction of a multichannel confocal LSM image stack (**a**) as well as in wide-field fluorescence images revealing marked difference between unstained (**b**) and stained (**c**) alkali-insoluble sponge fibers (bars: 200 µm)

In demosponges: Ehrlich et al., *J. Exp. Zool*. (Mol.Dev.Evol.), 2007, 308B, 347-356

In glass sponges: Ehrlich et al., *J. Exp. Zool*. (Mol.Dev.Evol.), 2007, 308B, 473-483

What is chitin?

Chitin, or poly-(beta-[1→4]-2-acetamido-2-deoxy-D-glucopyranose), is crystalline in its native state.

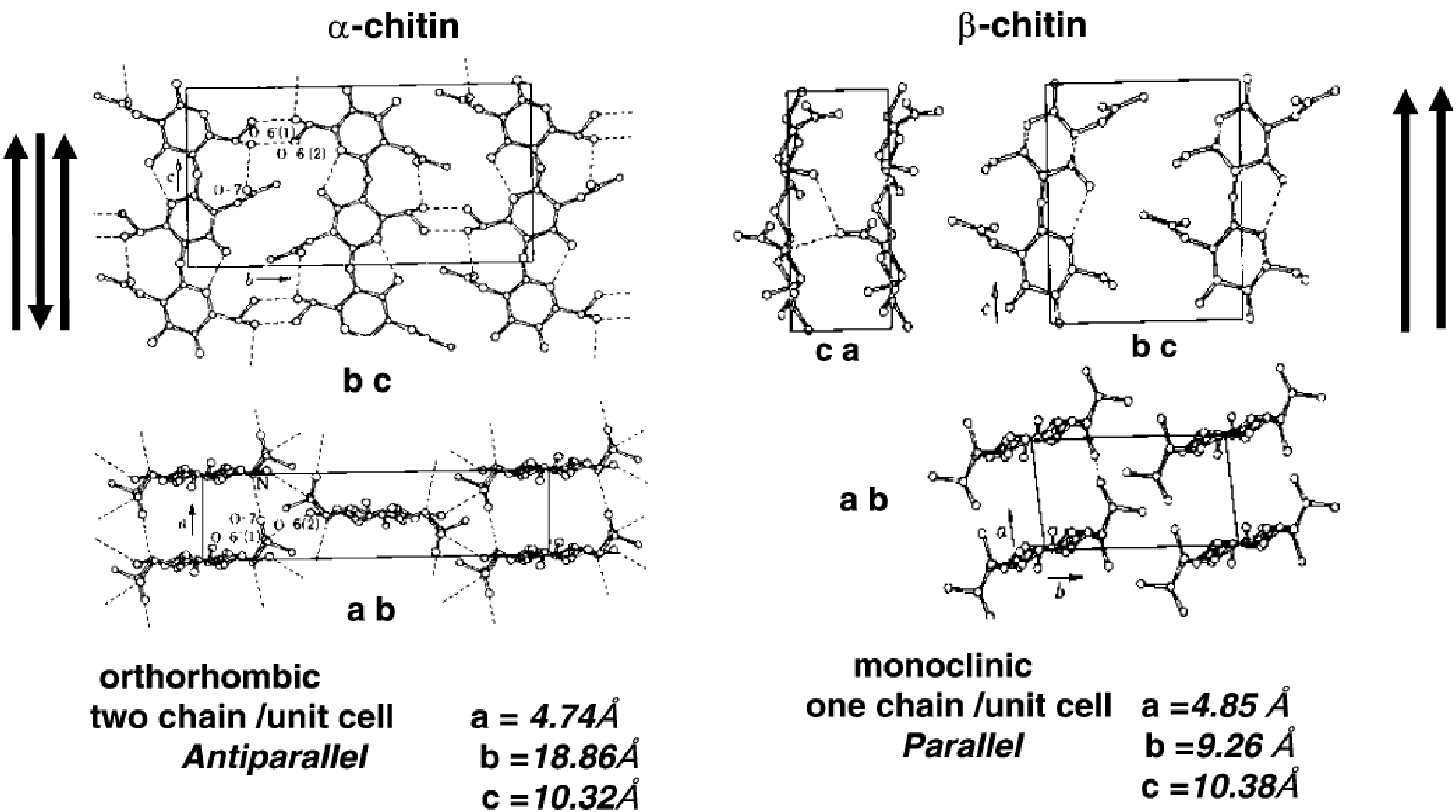

Scheme 1. Crystalline structures of chitin.

From: H. Tamura *et. al.*, Cellulose (2006) 13: 357 –364

Chitin-based Sponges: Verongida (Demospongia)

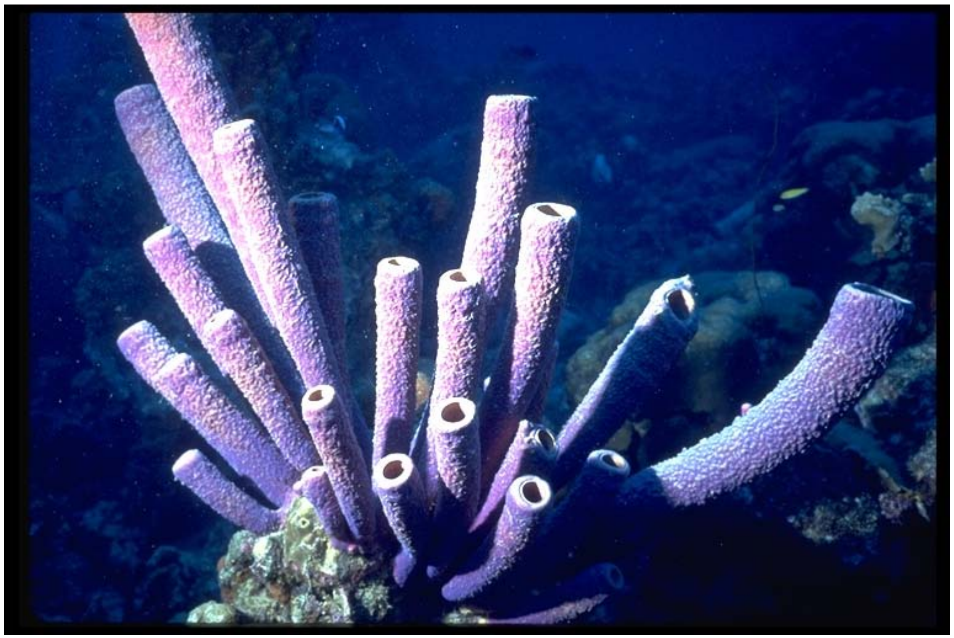

Aplysina archeri

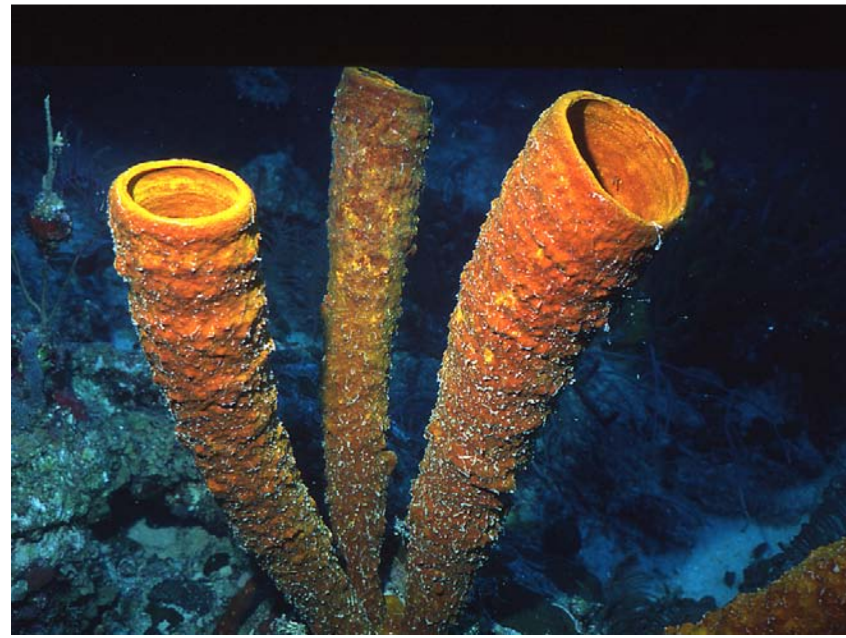

Aplysina sp.

Fibrous skeleton of *Verongula gigantea*

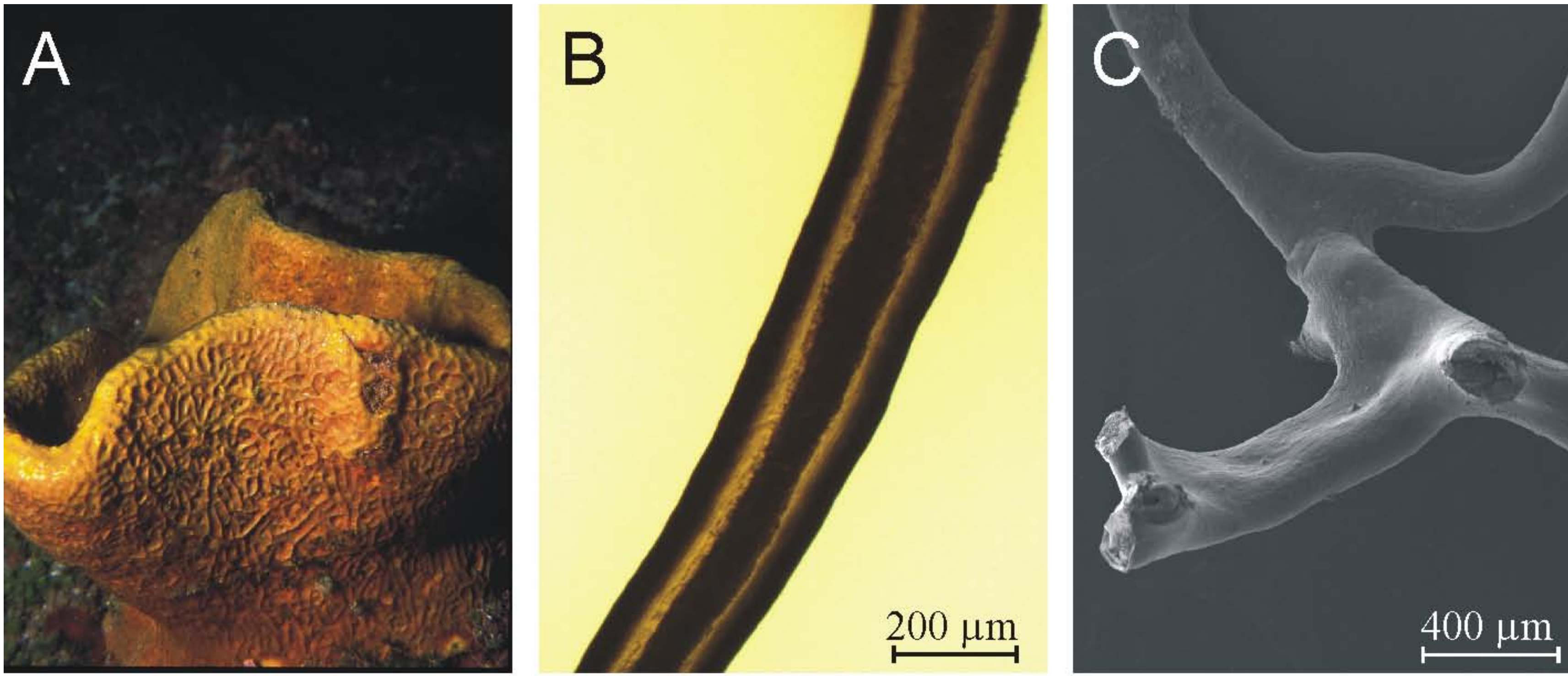

A, *Verongula gigantea* from Trindade Island, 10 cm tall.

B, Skeletal fibers of *V. gigantea* showing pith (dark coloured) and bark (yellow and dark-brown coloured).

C, reticulated fiber skeleton of *V. gigantea* seen in SEM

Fibrous skeleton of *V. gigantea*

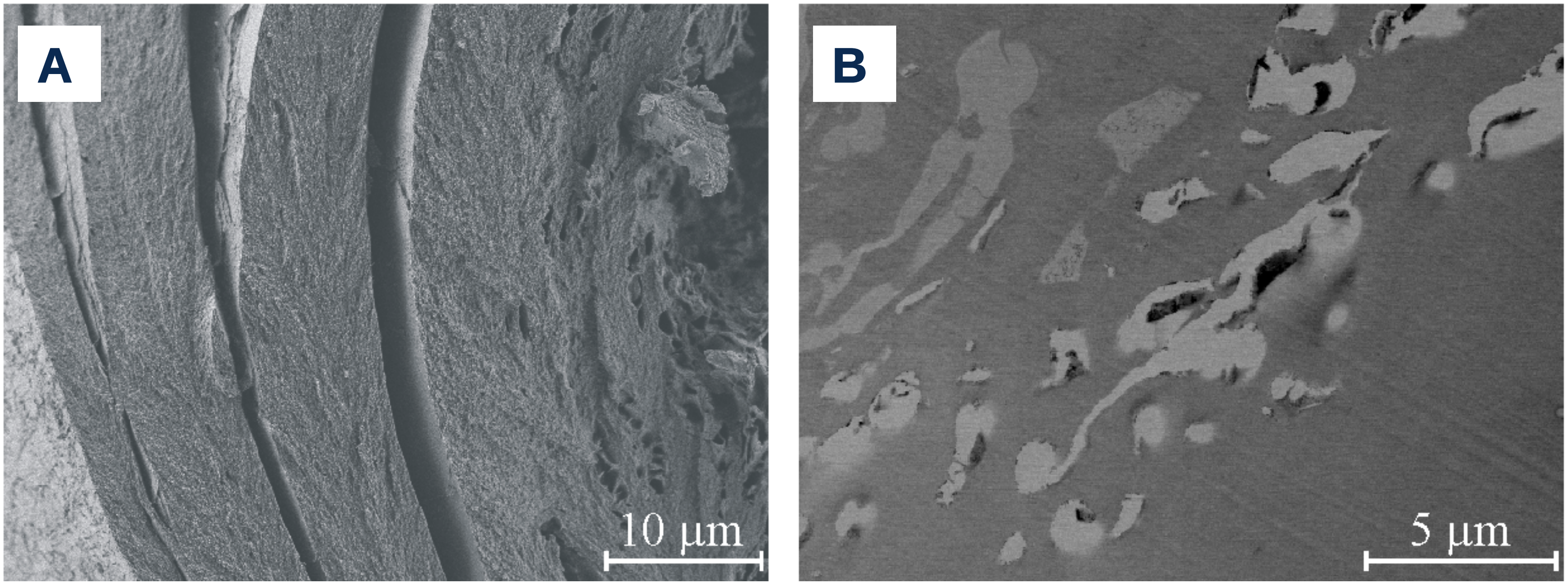

A, cross-section of a skeletal fibre showing multilayered structure, resembling silica spicules as described for hexactinellids and demosponges

B, STEM image of cross-section of inner layer of the fibre showing the presence of electron-dense inclusions (dark)

Light microscopy: *Verongula* vs. *Dysidea*

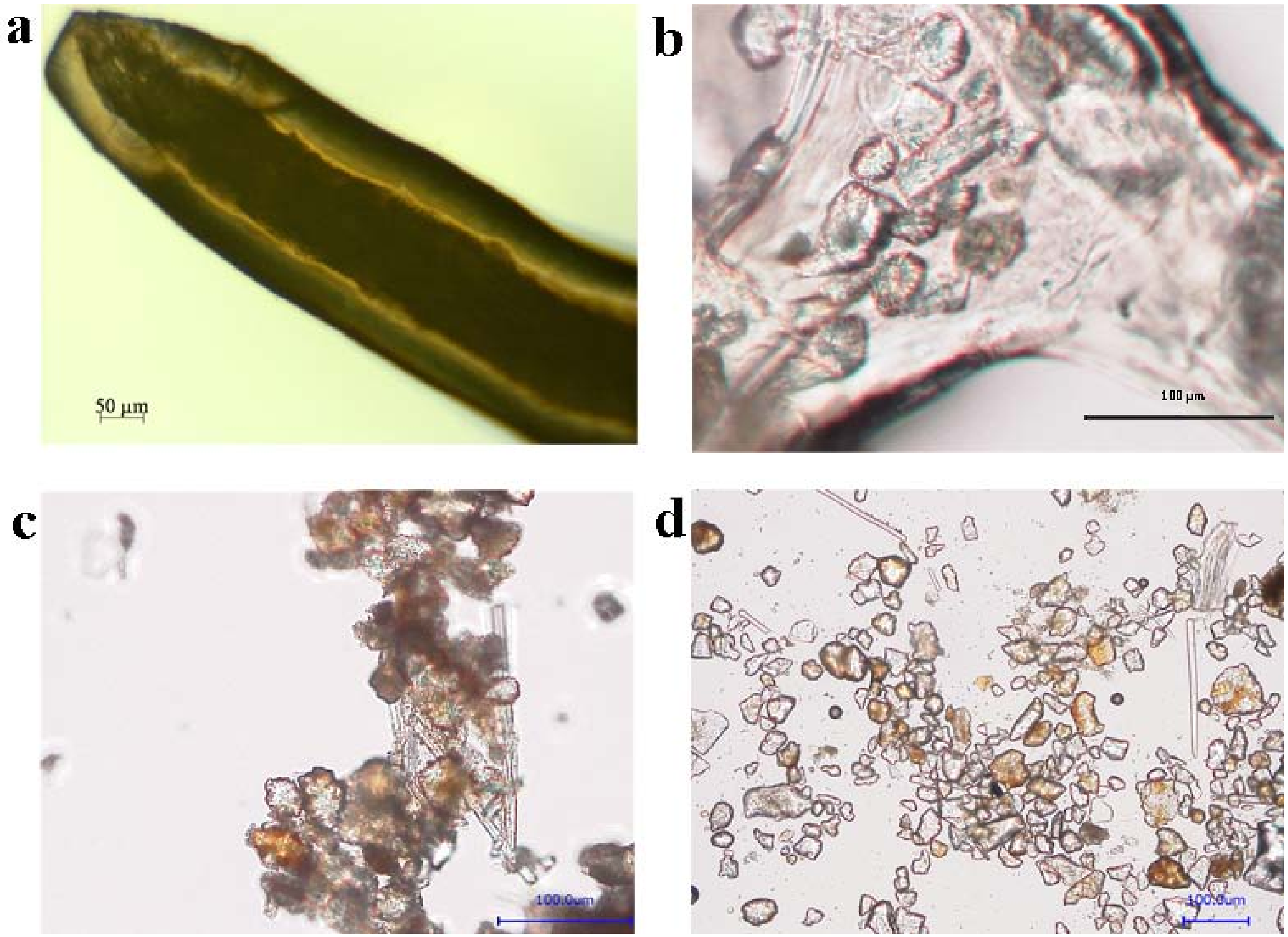

V. gigantea (**a**) show no presence of foreign particles. However, skeletal spongin-based fiber of *Dysidea avara* (**b**) shows typical accumulation of sediment particles including debris of sponge spicules. Heating of these fibers at 500°C during 5 h leads to more definitive visualization of the fiber contents after thermal damage of spongin (**c**). Image (**d**) represents results of the 1M HCl action on the particle agglomerates observed in image (**c**).

Identification of silica and $CaCO_3$

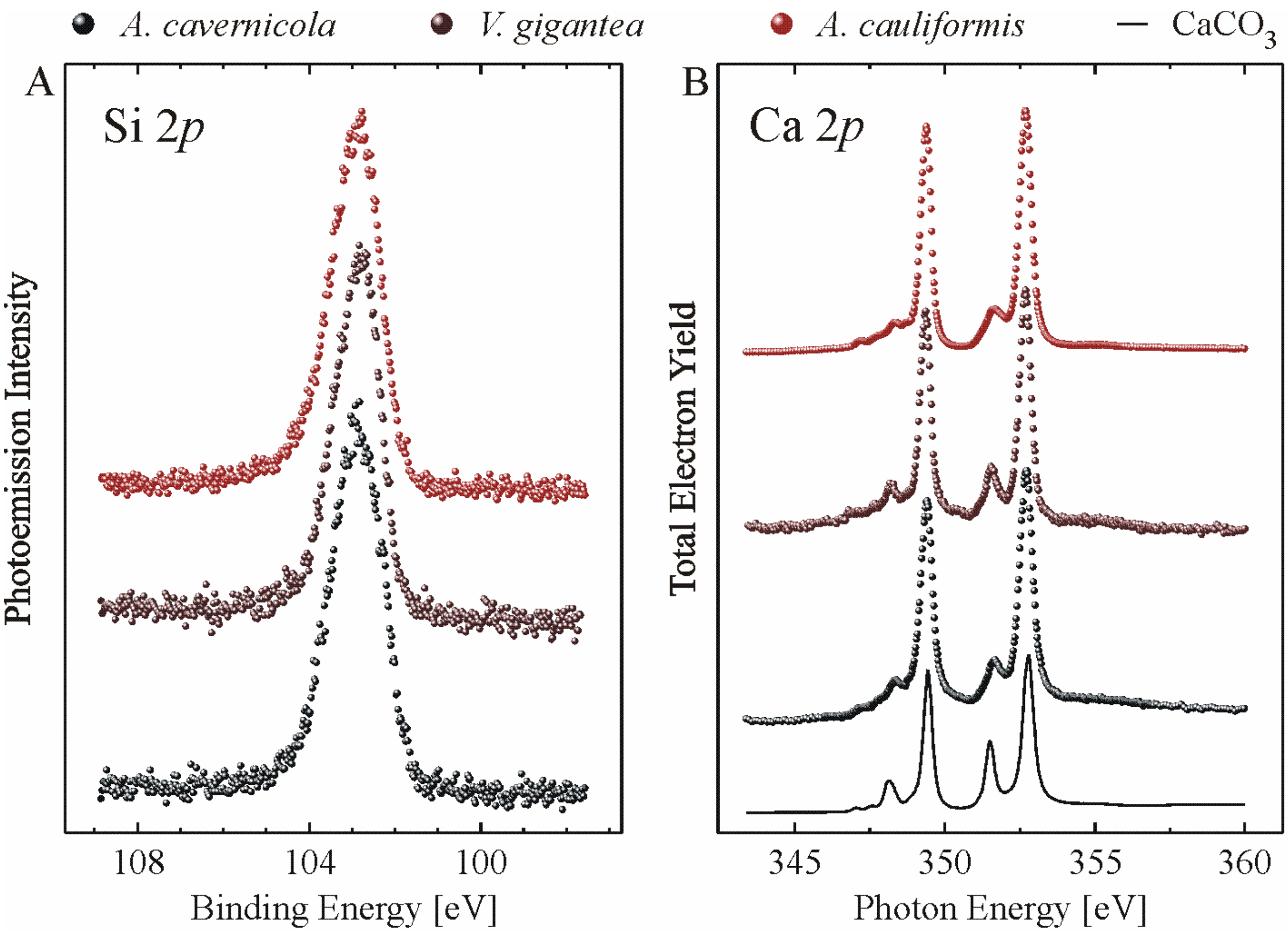

A, Photoemission spectra of natural sponge fibres showing the presence of silicon oxide bound to an organic matrix.

B, X-ray absorption spectra showing that calcium carbonate is the second mineral component present within three Verongida species of different geographical origin

Silica and calcium carbonate were additionally identified using **FTIR** and **Raman** spectroscopy

FIB cut and TEM imagery of the sponge fiber

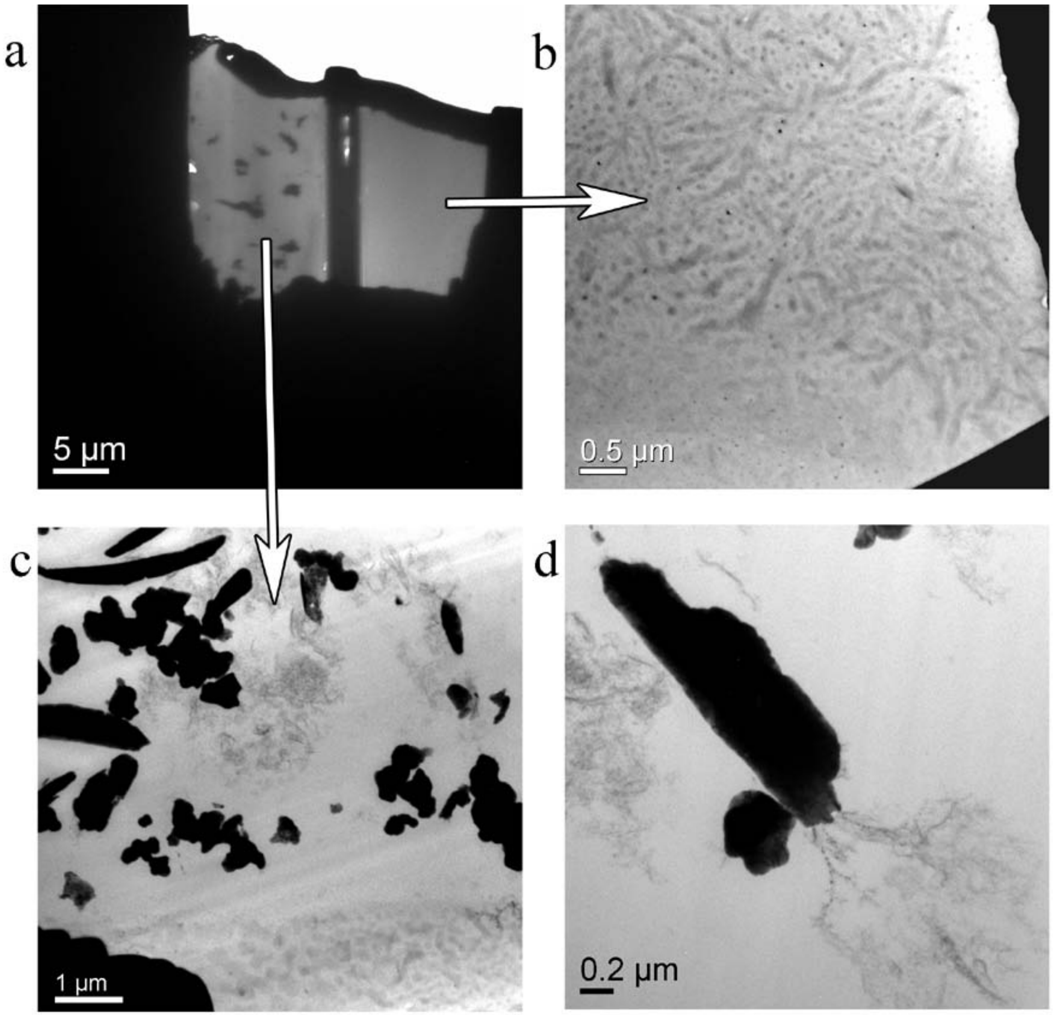

TEM images (**b** and **c**) of the FIB cut of the both fiber regions represented in (**a**) show that silica-based layers are located in the outermost region (**b**), however calcium carbonate is grown on the chitin nanofibers (**c**, **d**) which are localized near the axial channel

TEM image of the silica-chitin-aragonite biocomposite

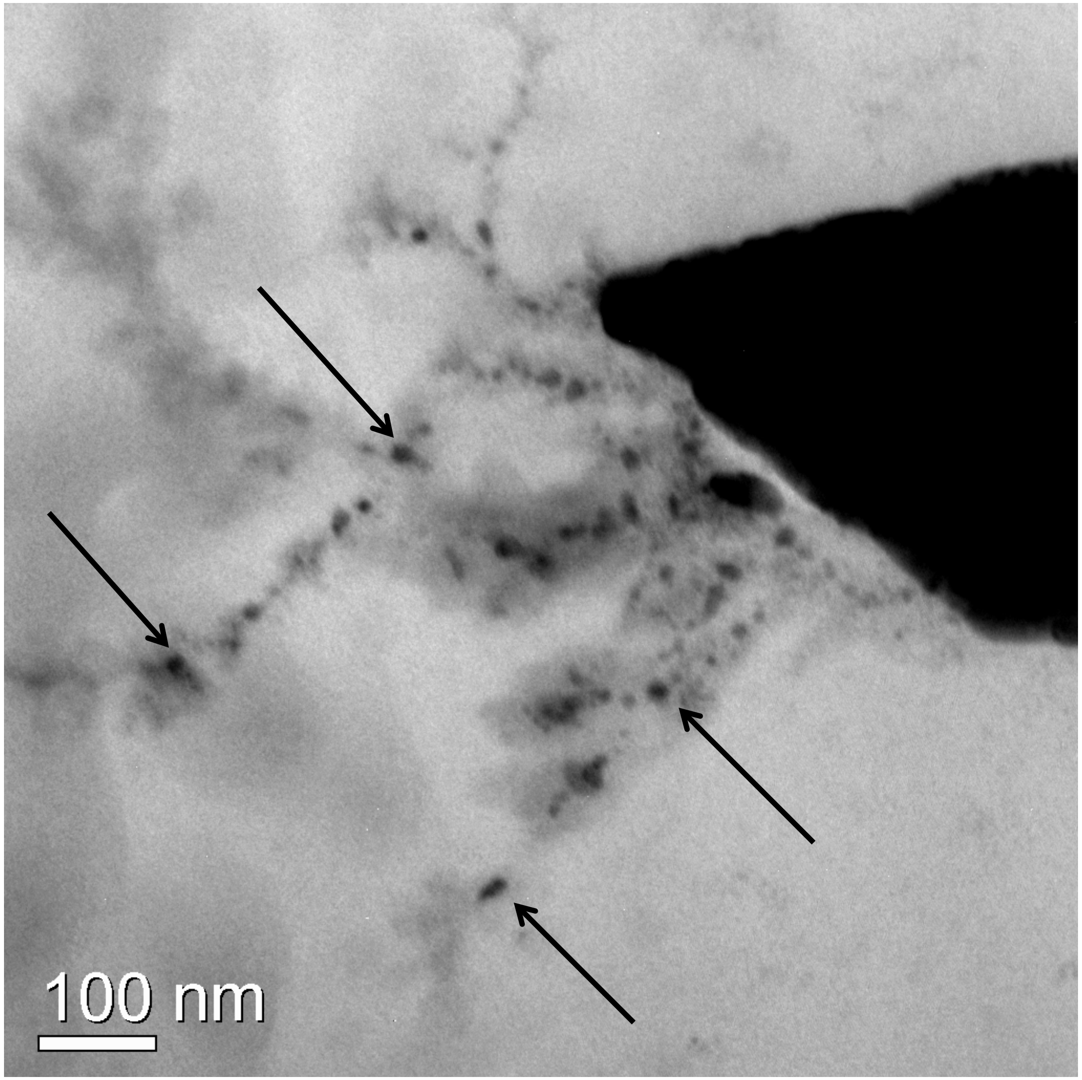

Both micro- and nanoparticles (arrows) of the mineral are tightly bound on and into organic matrix that additionally rules out any kind of foreign mineral particles.

HR-TEM and electron diffraction analysis

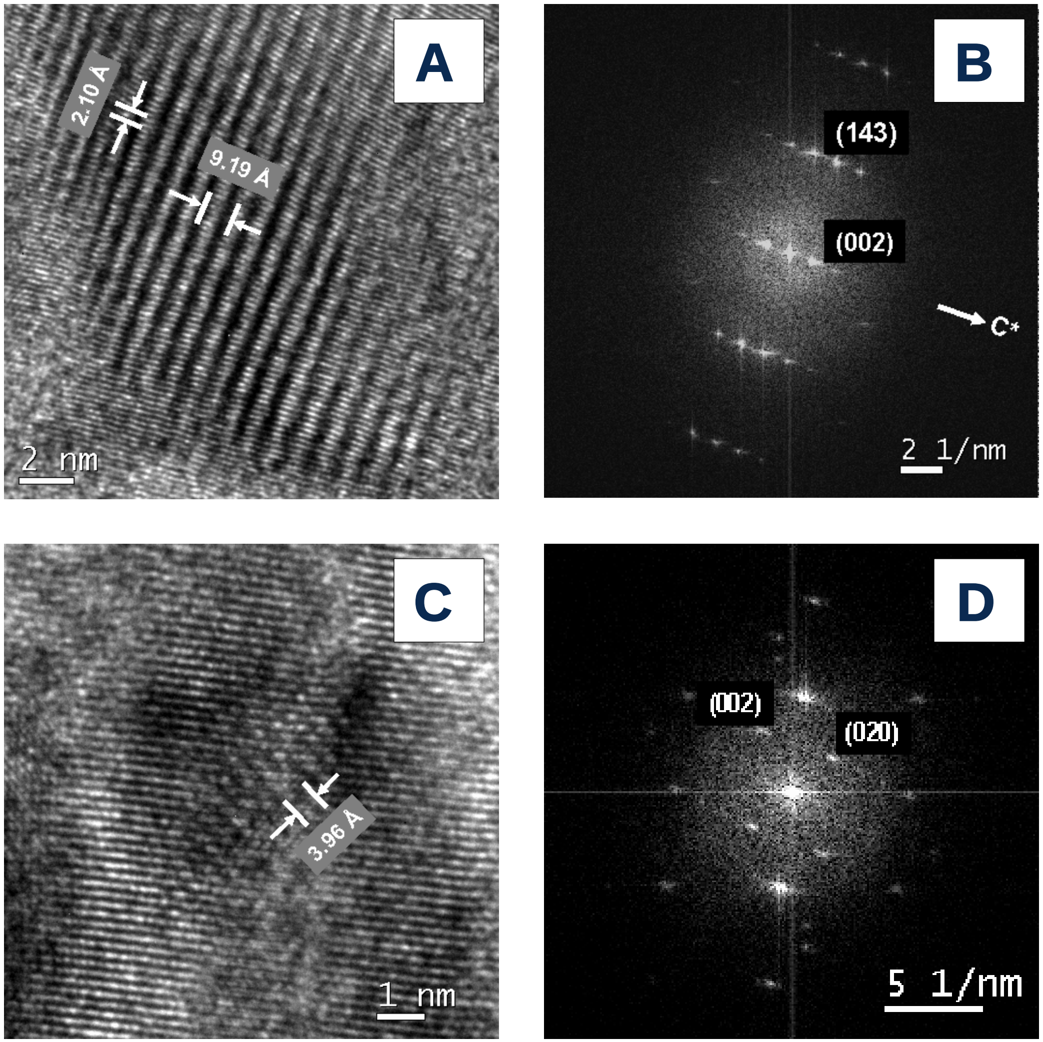

A, high resolution TEM image of the crystalline phase within this agglomerate, displaying spacings of 9.19 Å, 4.45 Å and 2.10 Å corresponding to (002), (120) and (143)/(136) lattice planes typical for **alpha-chitin** (**B**).

C, HR-TEM image showing the presence of crystalline aragonite within the same mineral agglomerate.

D, Fast Fourier transform of **C** displaying orthorhombic structure of **aragonite** with denoted spacings of 3.96 Å, 3.00 Å, 2.78 Å and 2.11 Å corresponding to (020), (002), (121) and (220) reflections.

Selective Demineralization

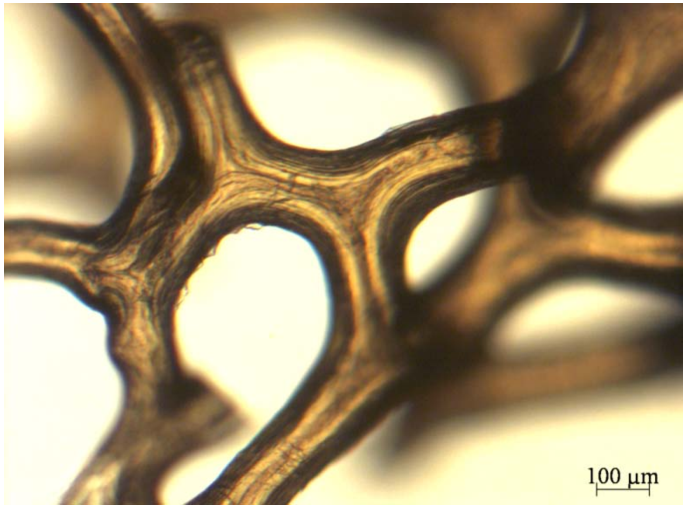

Sponge skeleton

HCl

NaOH

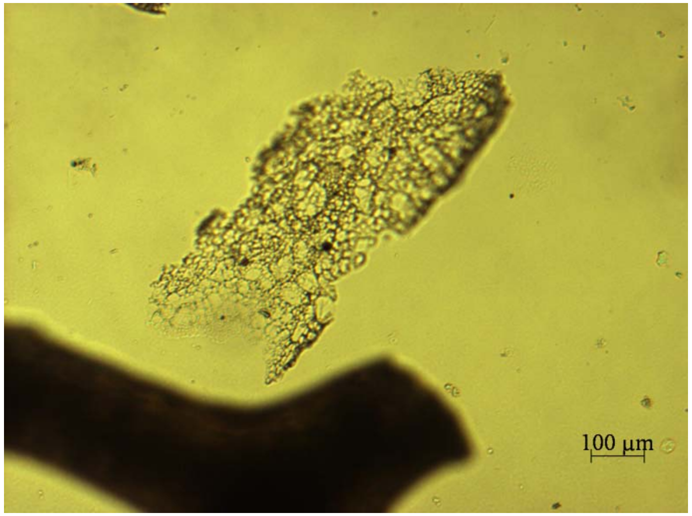

Silica layers

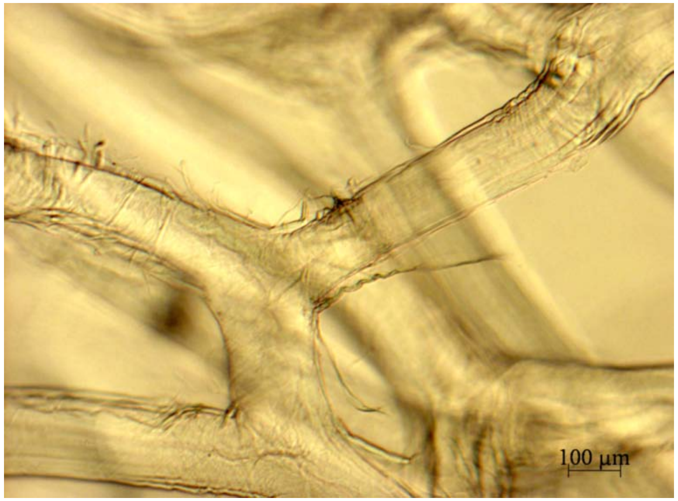

Chitin

HCl-based demineralization of the sponge skeleton

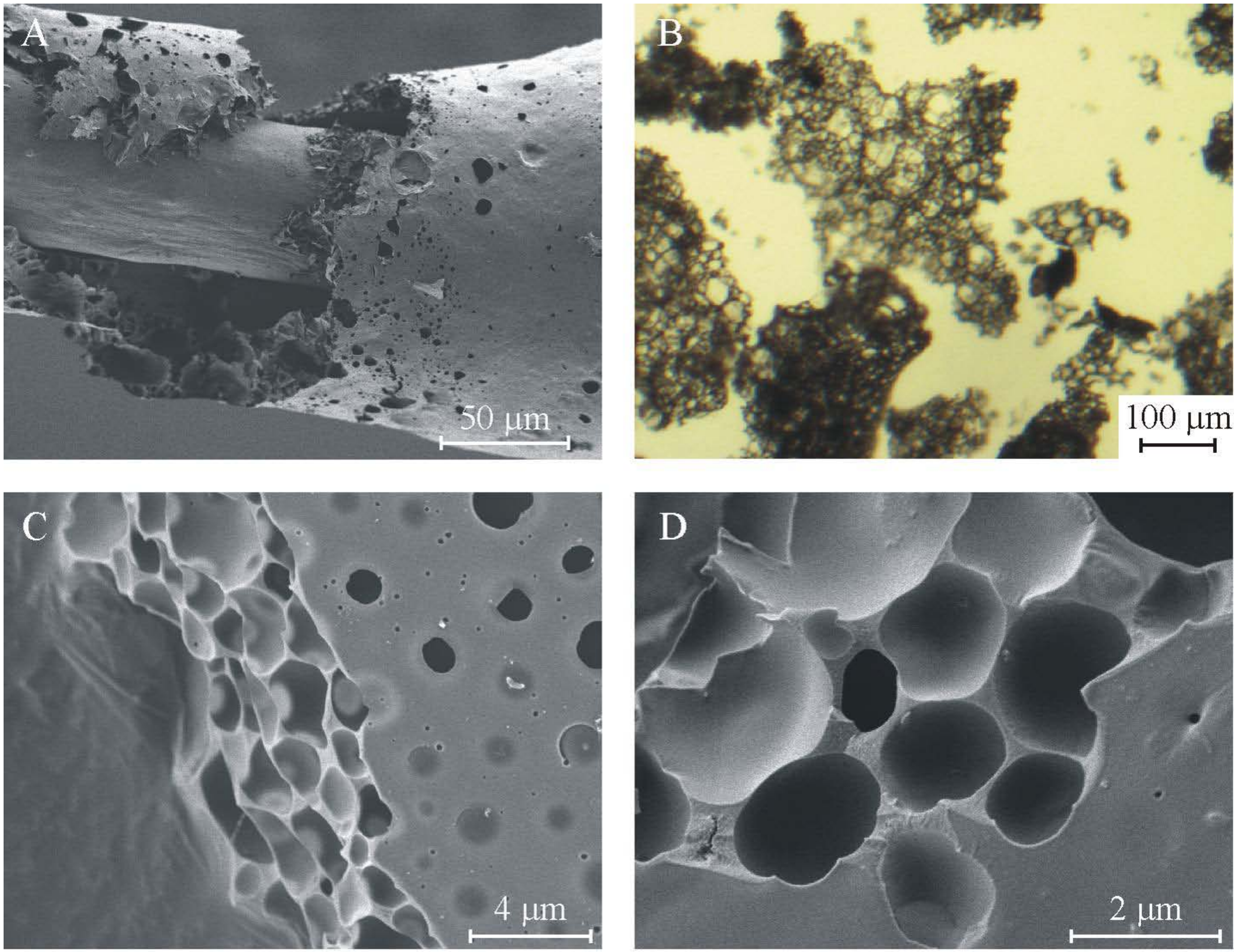

A, SEM image of skeletal fibre after treatment with 3 M HCl at 37 °C for 3 weeks, showing perforated layers that cover the pith region.
B, light microscopy micrograph of isolated layers showing their perforated structure.
C, SEM image showing three dimensional organisation of the layers. **D**, nano- and microscale apertures visible using SEM within these formations corresponding to the mineral compounds that were dissolved in HCl.

Identification of nanofibrillar chitin within silica layers

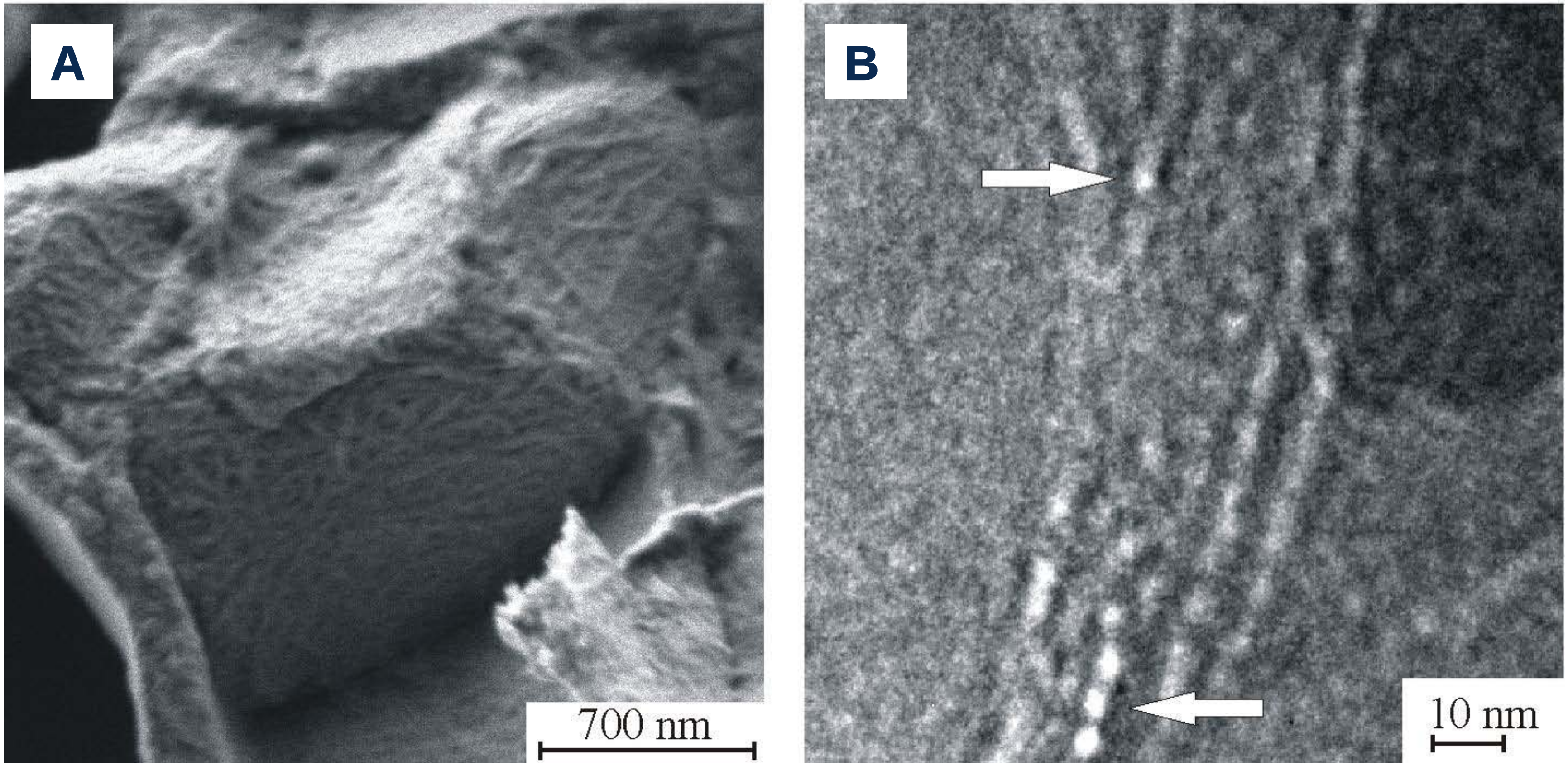

A, SEM image of the same fragment prepared at higher magnification show the presence of nanofibrillar network

B, Nanofibers in the silica matrix samples containing a nano-crystallite with diameter 2 nm (arrows), typical for α-chitin crystallites

Overview: The Model of Silica-Chitin-Aragonite Unit

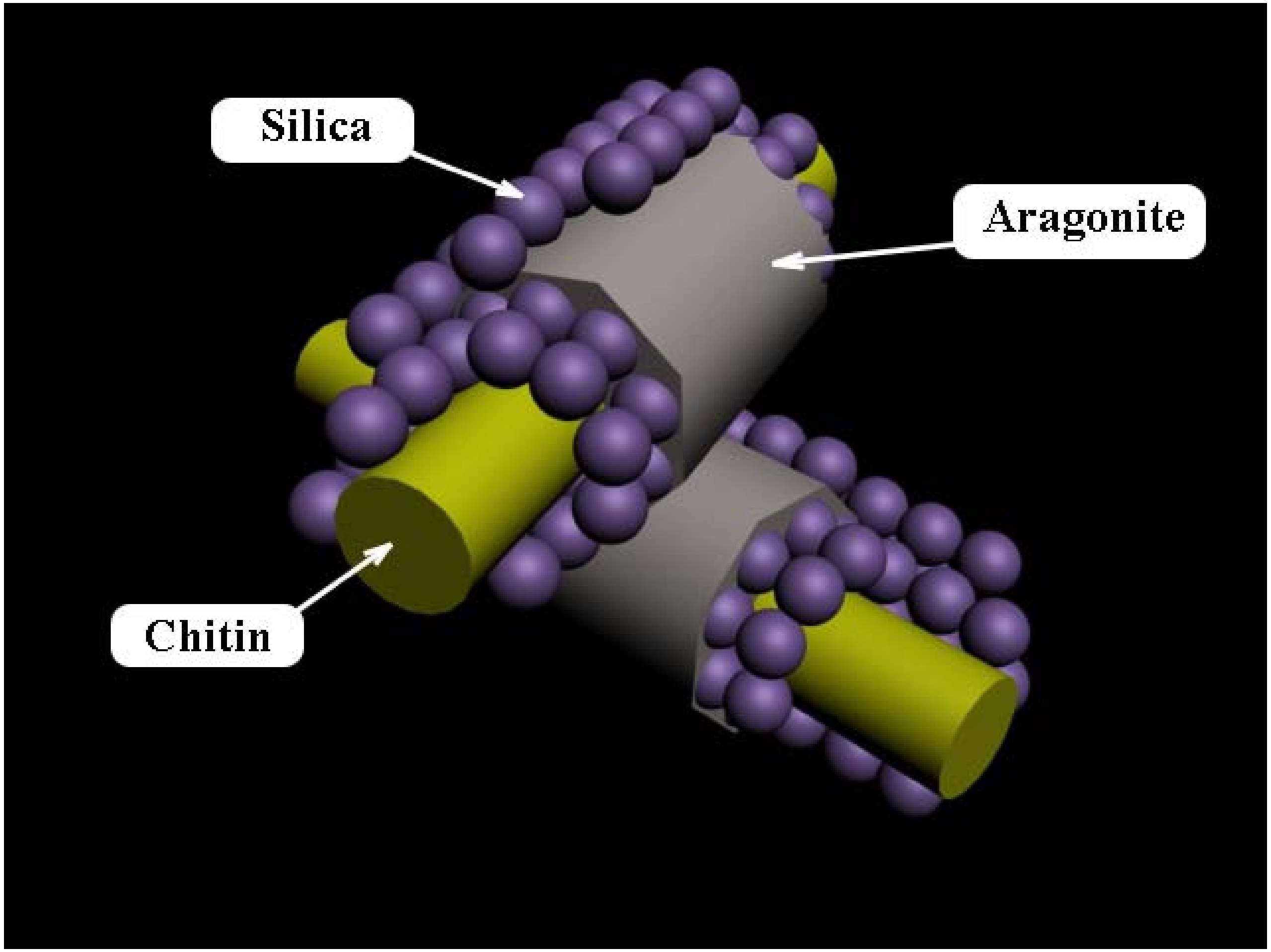

From: Ehrlich et al., *Chemistry of Materials* (2010) 22(4): 1462-1471

Examples of multiphase biomineralization

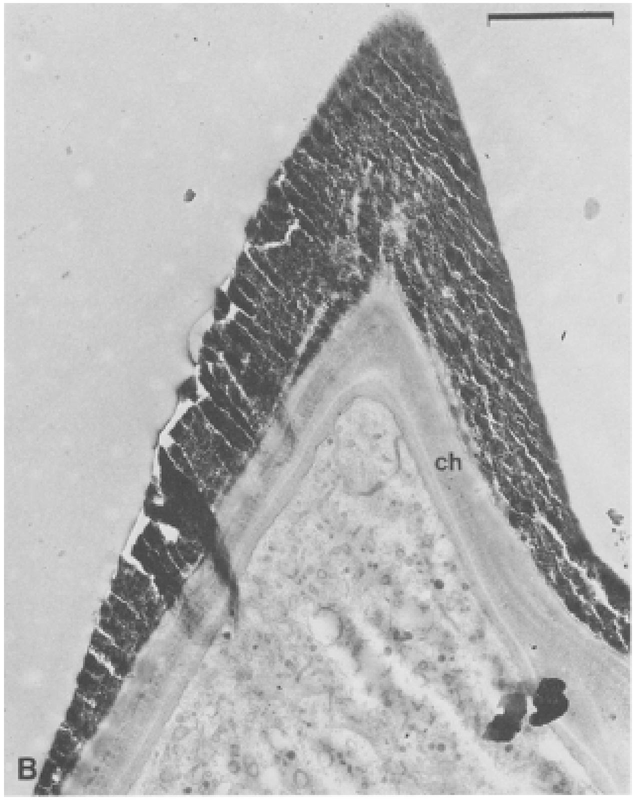

TEM image: Section of the tooth of *Calanus pacificus* made of silica, chitin and crystalline $[Zn]_2[H_4SiO_4]/[H^+]_4$ (scale bar=2.6 µm)

From Miller et all, 1990.

Miller, C.B., Nelson, D.M., Weiss, C., & Soeldner, A.H., 1990:

silica-chitin-**willemite** composite in copepoda teeth

Williams, A., Lüter, C. & Cusack, M., 2001:

silica-chitin-**apatite** composite in Brachiopoda

Sone, E. D., Weiner, S. & Addadi, L., 2007:

silica-chitin-**goethite** composite in limpet teeth

Sponges

(Porifera)

Glass sponges

(Hexactinellida)

Silica

Horn sponges

(Demospongia)

Silica or $CaCO_3$

Calcareous sponges

(Calcarea)

$CaCO_3$

Biominerals

Mushroom-like deep-sea glass sponge *Caulophacus sp.* (image courtesy NOAA).

The Eiffel tower – an example of man-made hierarchical construct (photos courtesy Vasily V. Bazhenov).

Caulophacus sp. glass sponge

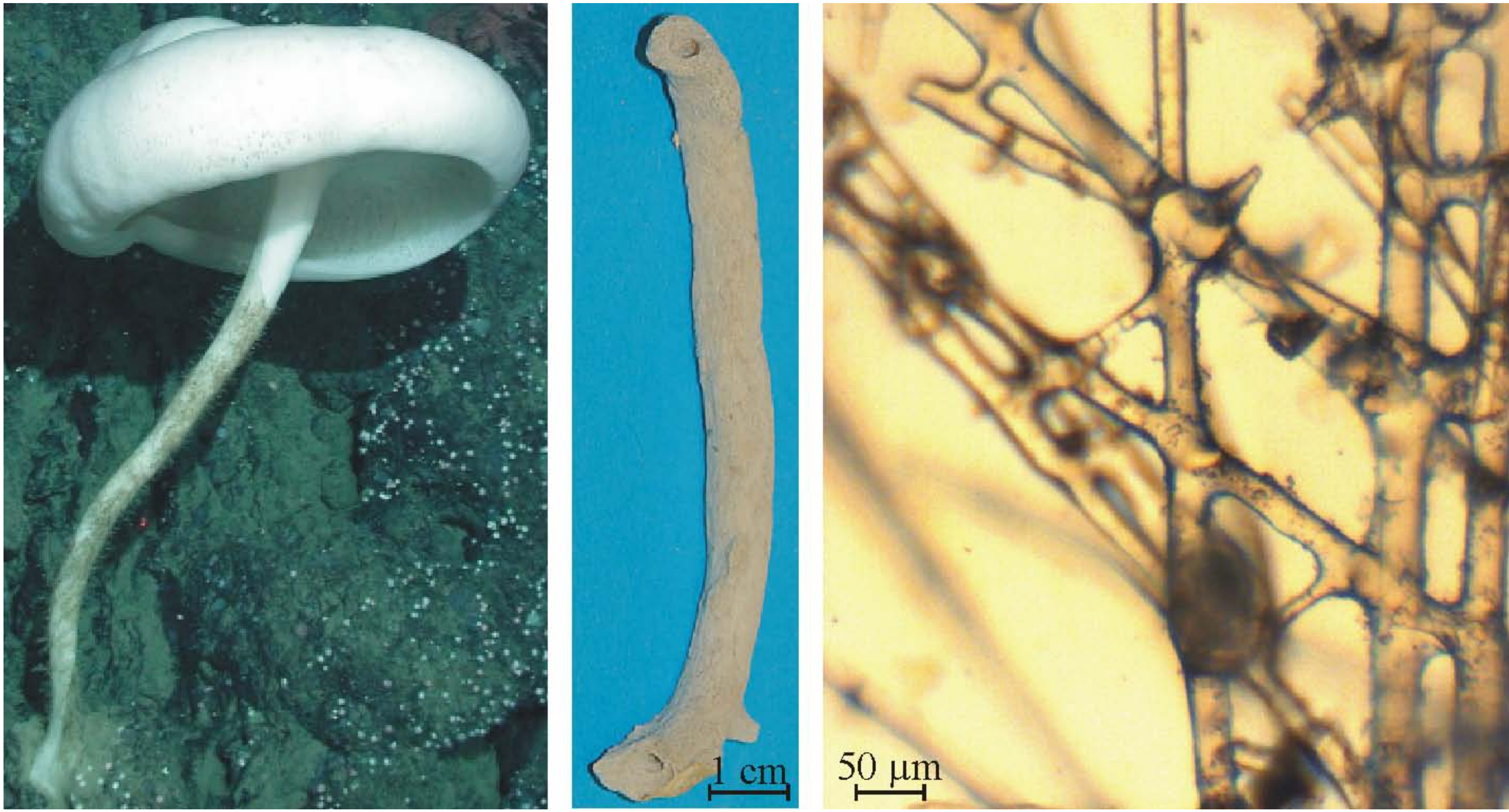

The stalks of *Caulophacus* sp. possess complex network of glassy spicules

Eiffel tower motive in glass sponges

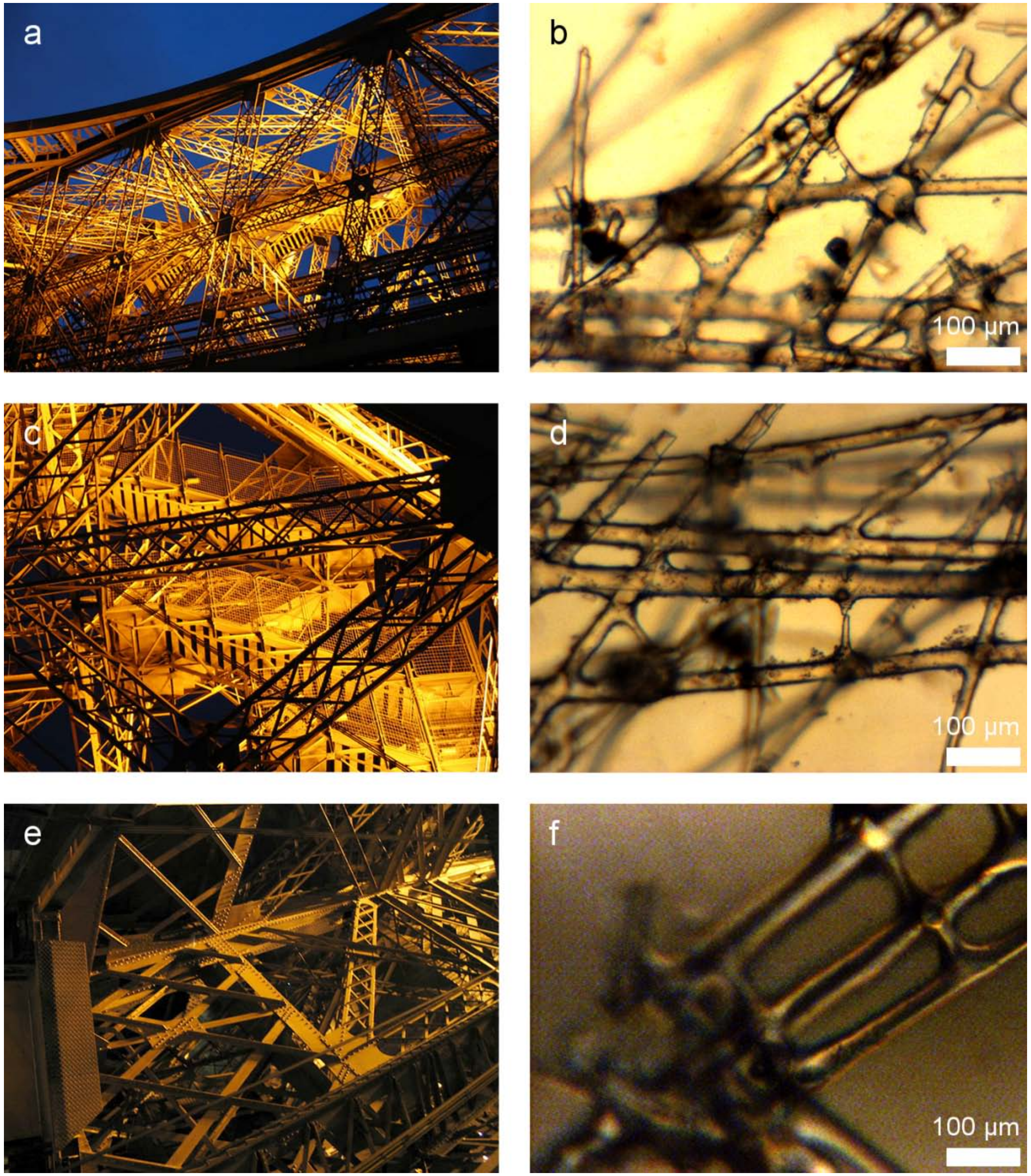

There are several similarities between structural motives in Eiffel tower (a,c,e) and within skeletal framework of *Caulophacus* sp. stalk (b,d,f) observed using light microscopy.

SEM: club-formed structures

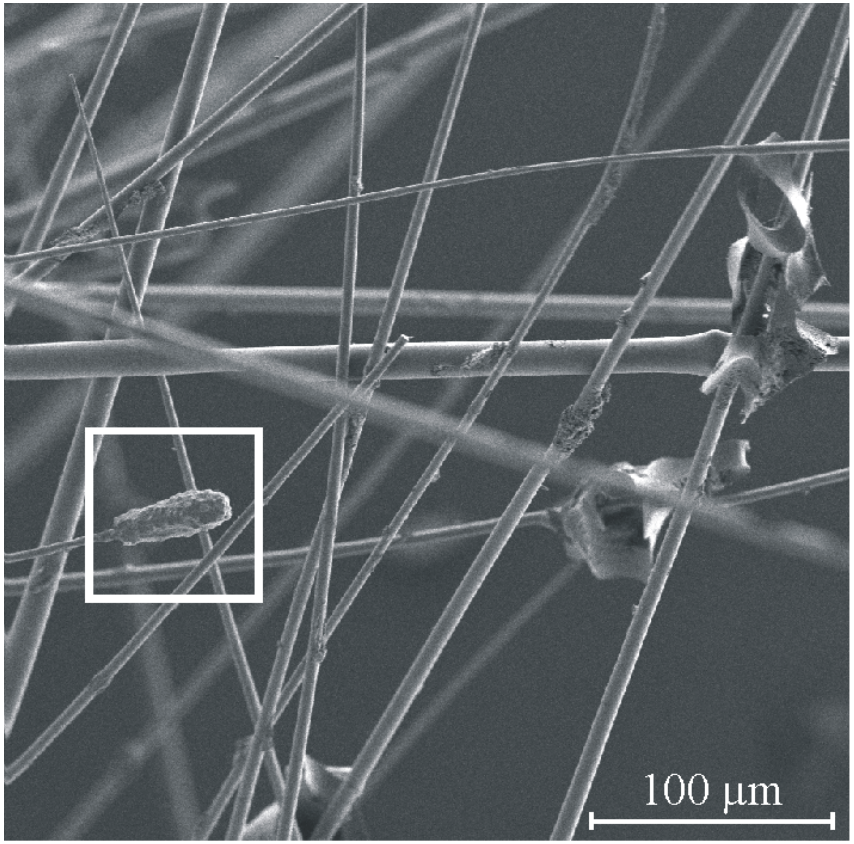

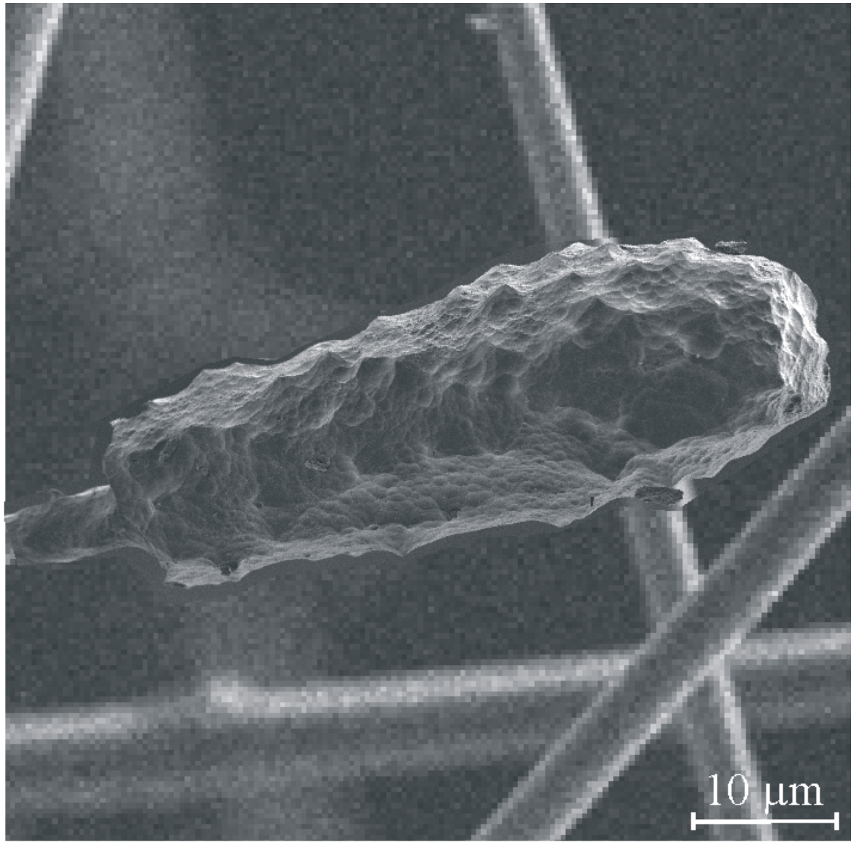

It is possible to destroy structural integrity of the stalk using pincers (left). After this procedure club-formed structures were observed (right).

Club-formed structures and their role

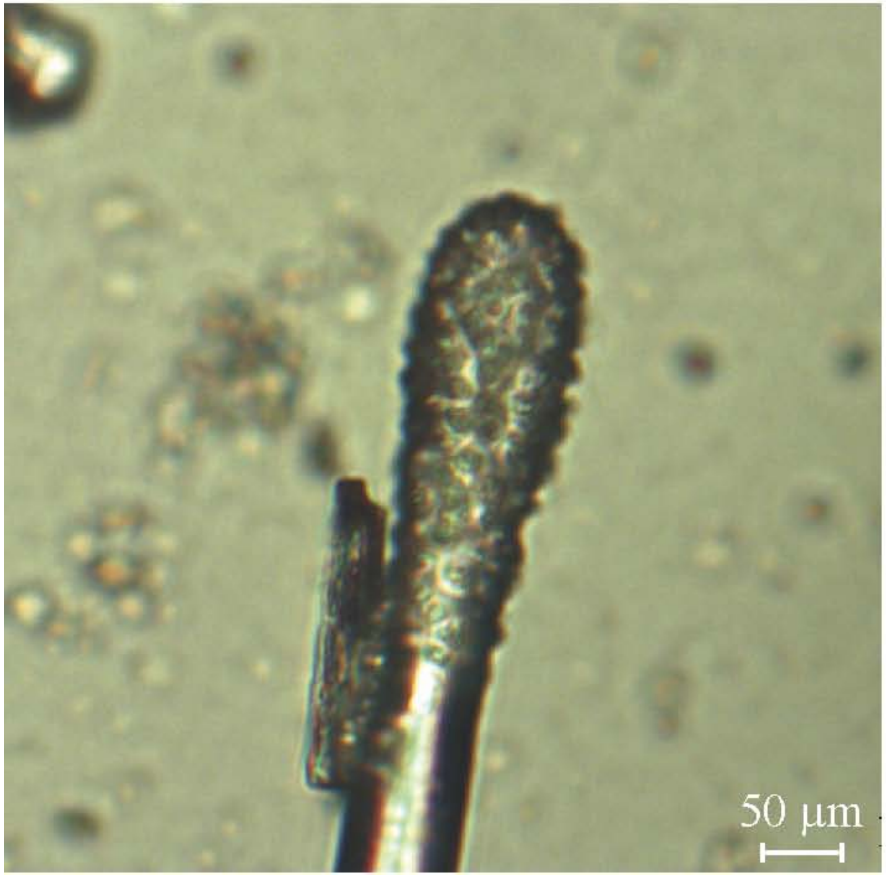

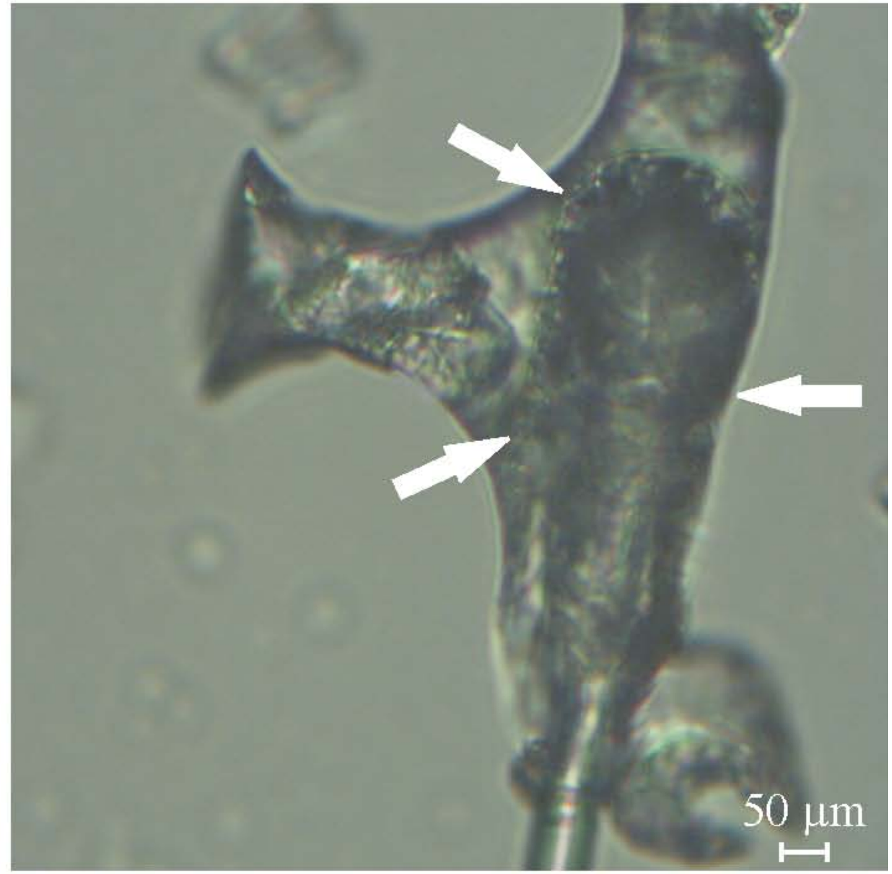

Club morphology of the spicules could be also observed using light microscopy. The stalks were incubated in alkali solution at 37°C during two weeks. After partial dissolution of silica-based articulations club-formed spicule (arrows) are well seen within articulation (right)

SEM studies on club-formed structures

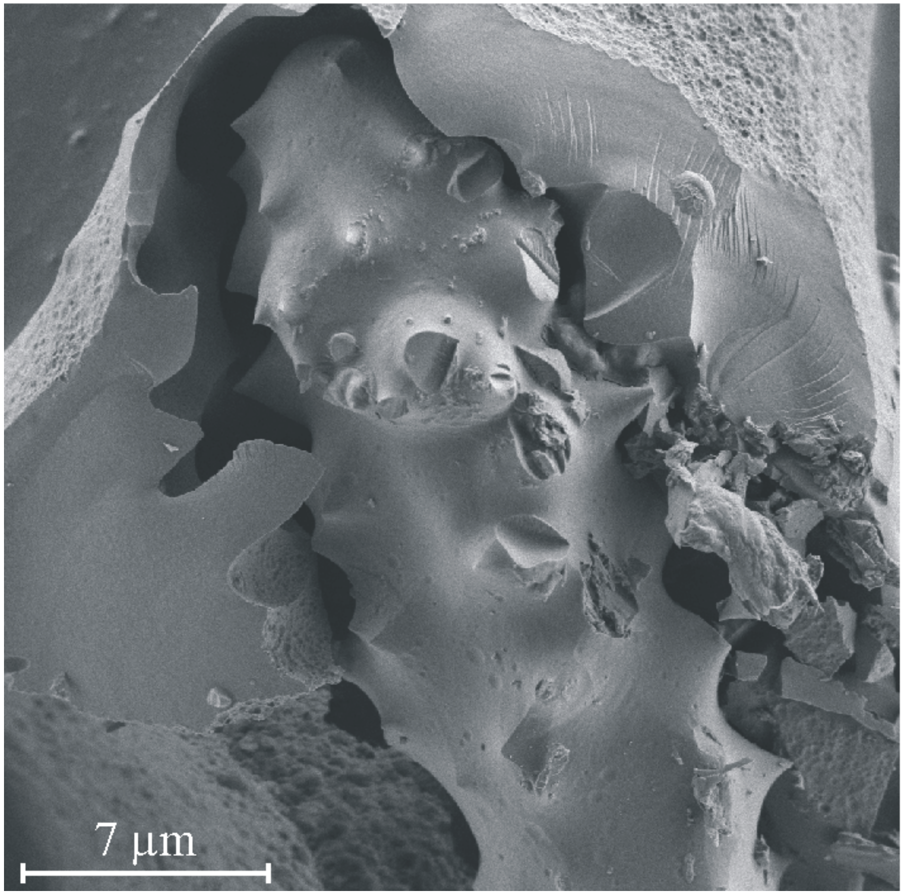

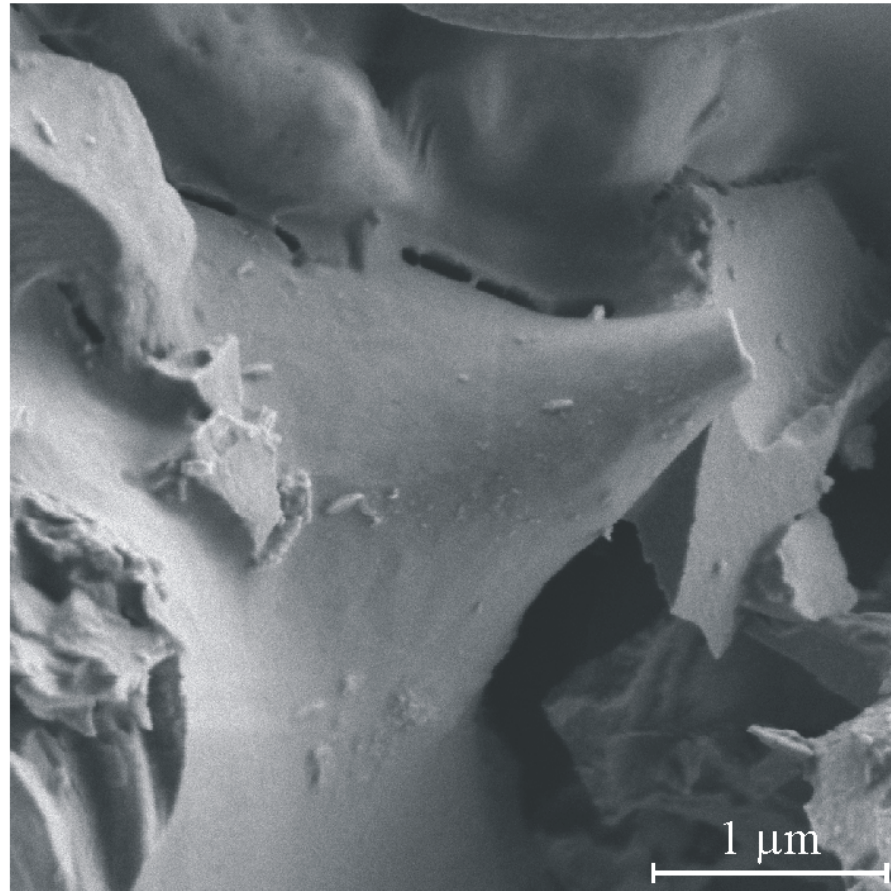

The same phenomenon could be confirmed using SEM

SEM studies on demineralized spicules

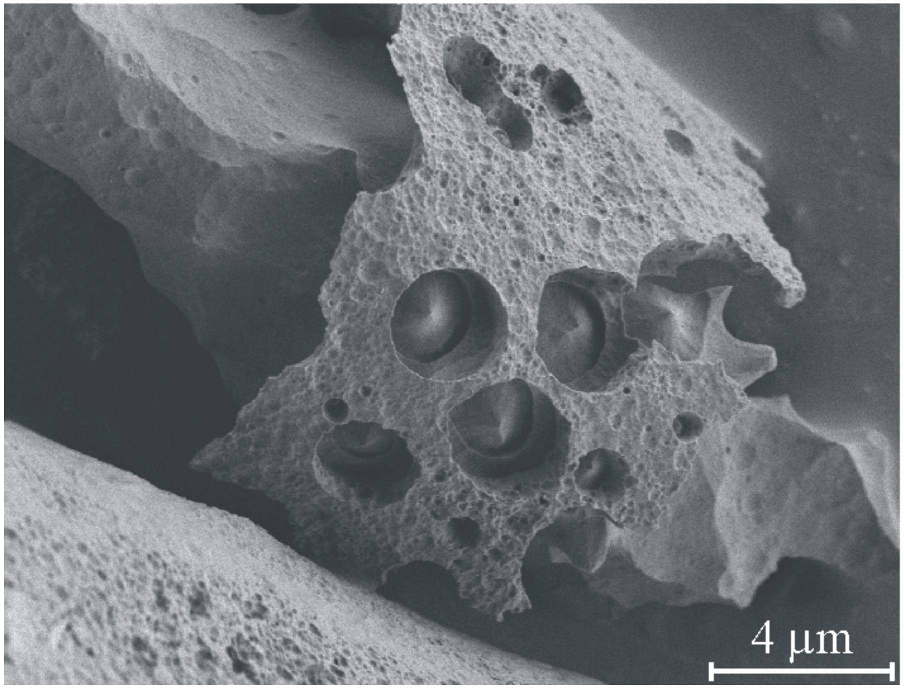

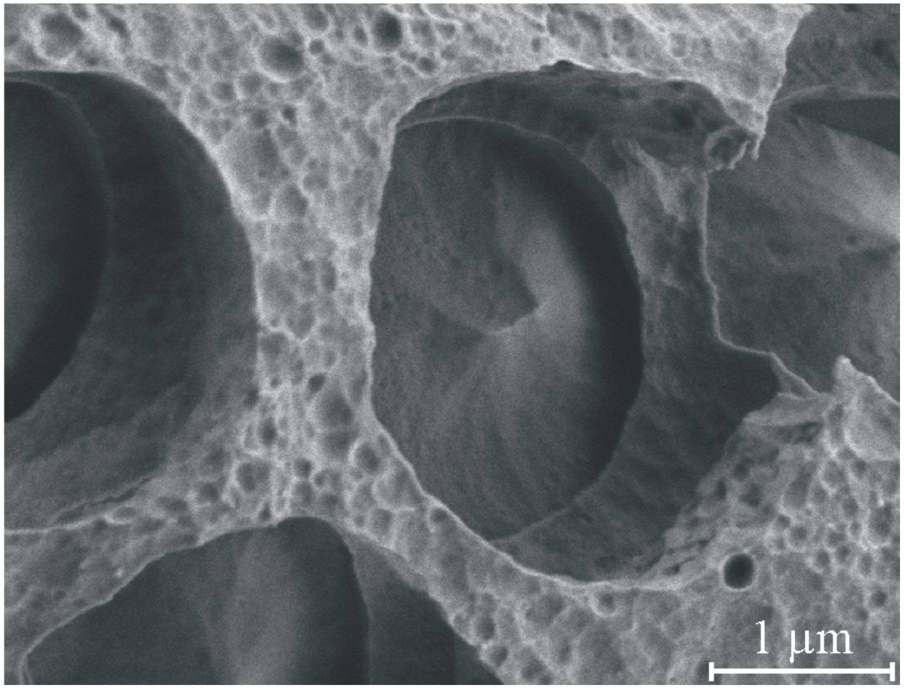

The material of articulation is corroded in alkali, however the spines of the club-formed spicule are resistant to this kind of chemical treatment.

Caulophacus sp. spicule articulations

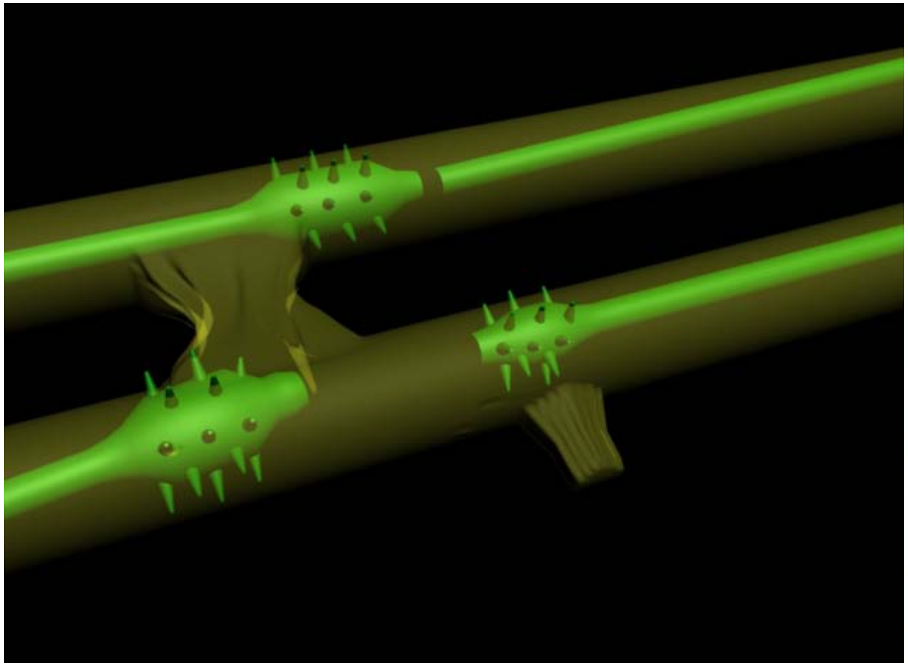

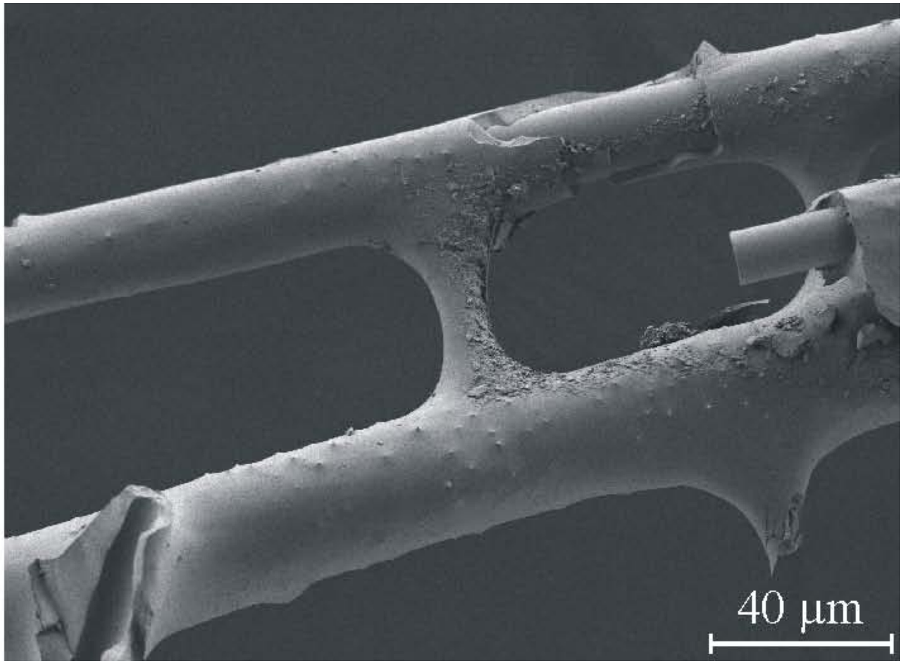

SEM image (right) show that club-formed structures are distributed within spicules.

The model view of these articulations is represented on the left image.

SEM studies on club-like structures

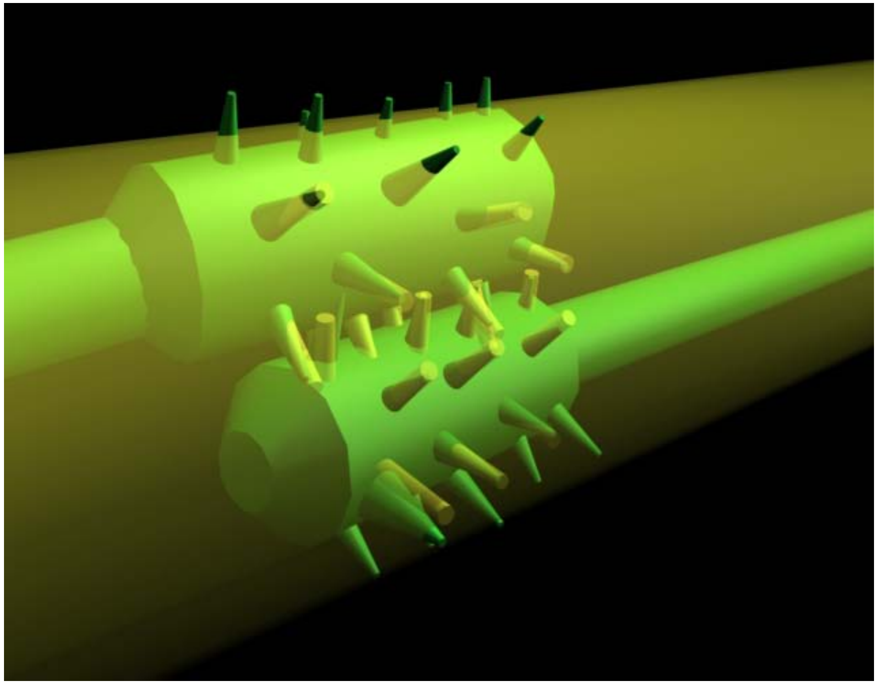

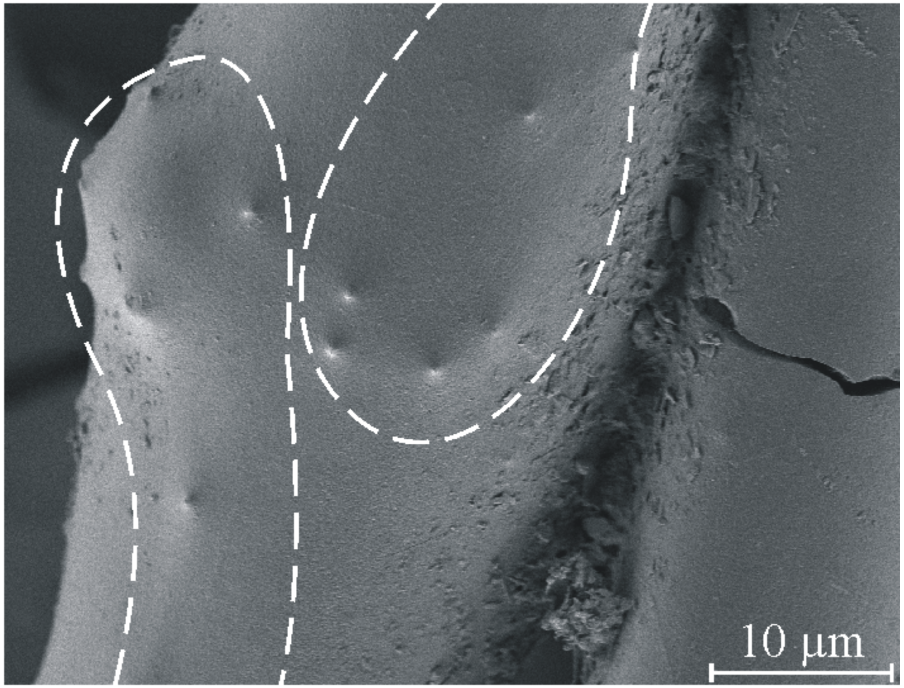

SEM image (right) show with strong evidence that club-formed structures are responsible for mechanical coupling also within one spicule.

Corresponding model of this coupling is represented on the left image.

Mother Nature vs. Human: how to connect?

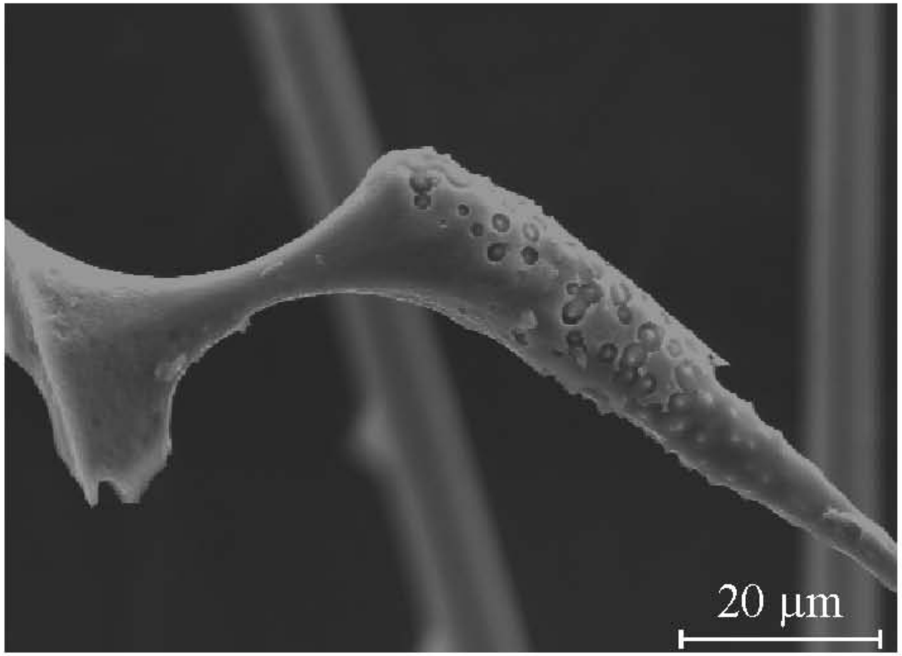

Nature - made articulation

SEM image:

club-formed spicule released from articulations after their particular dissolution using 2.5 M NaOH at 37°C on the 10th day of insertion

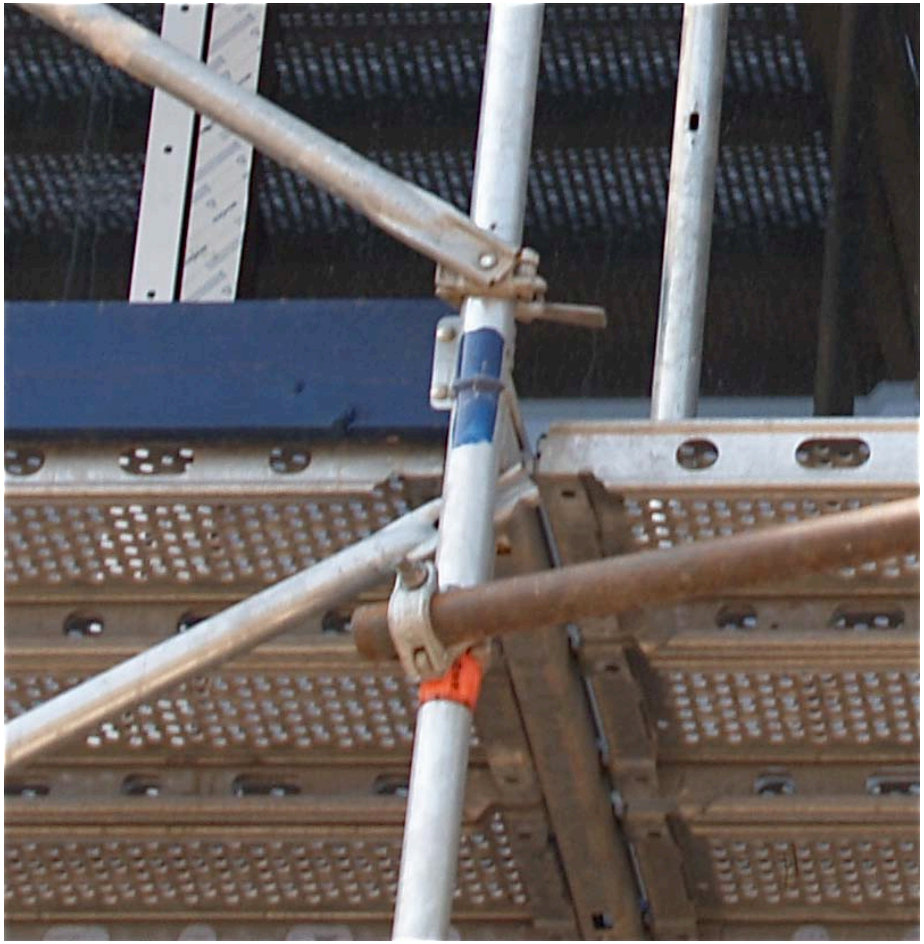

Articulation: Made in Germany

SEM studies on natural club-formed spicules

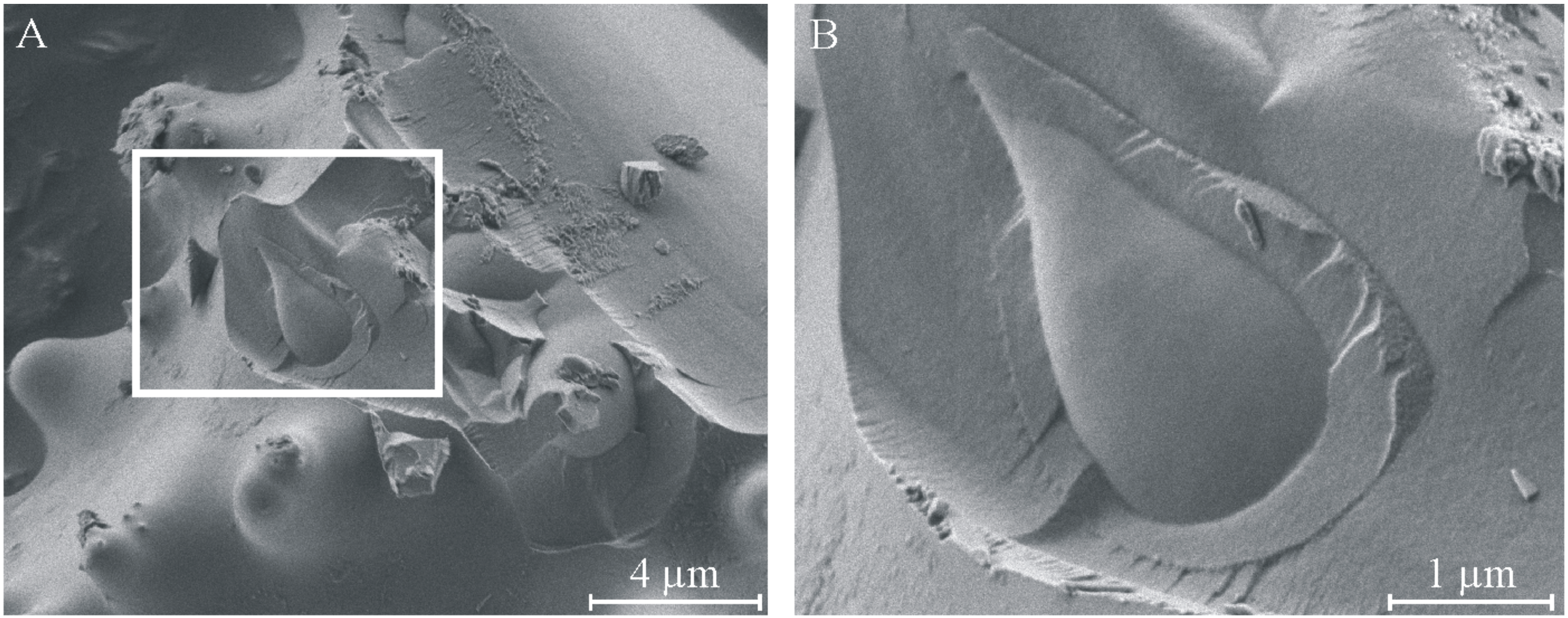

Mechanically disrupted club-formed spicule:

the spines of club-formed structures possess **seed-like** formation which is covered with silica layers

Calcium identification within club-formed structures

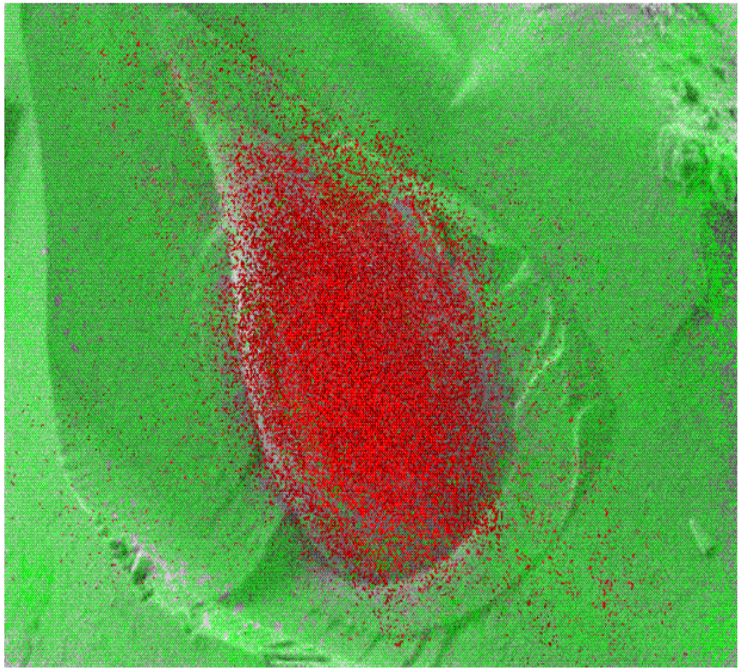

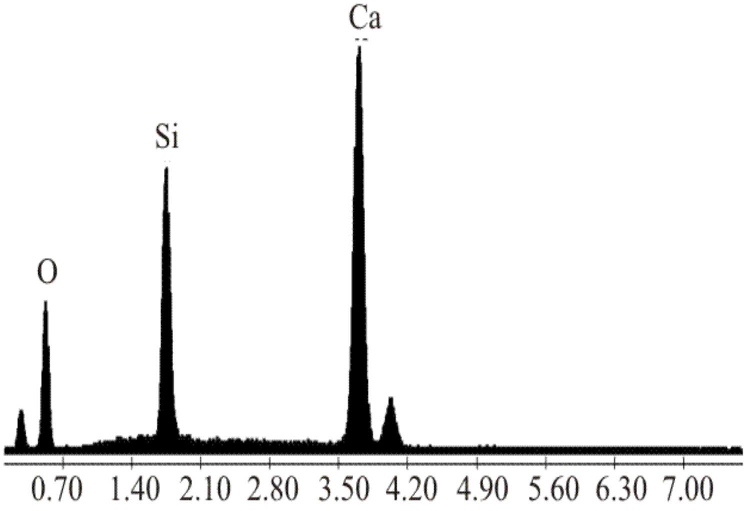

For EDX analysis air-dried samples were embedded in Epoxy resin without additional staining and cut on a Leica EM UCT ultramicrotome to obtain a flat block face. Samples were coated with carbon and analysed in an ESEM XL 30 Philips. EDX-analysis and elemental mapping was done with an EDAX detecting unit and EDAX software.

Silica and $CaCO_3$ identification

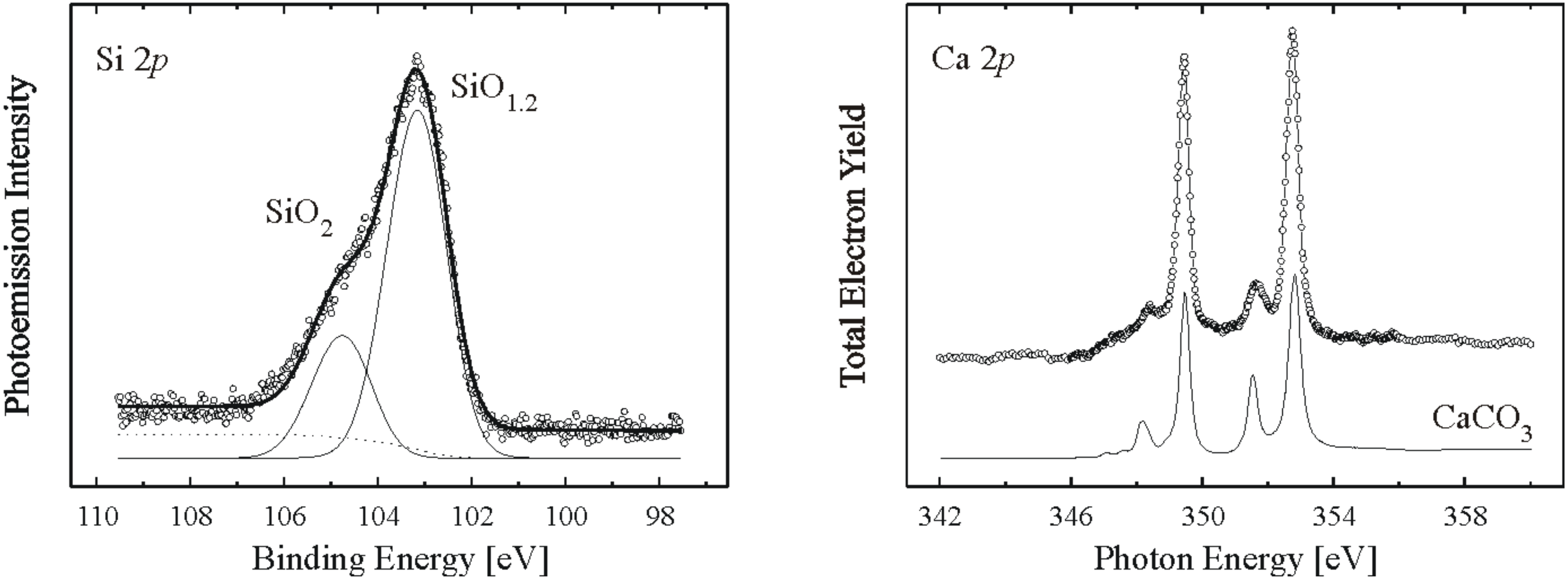

Left: Photoemission spectra of natural *Caulophacus* sp. spicules showing the presence of silicon oxide bound to an organic matrix

Right: X-ray absorption spectra showing that calcium carbonate is the second mineral component present within the same spicules

TEM and electron diffraction analysis

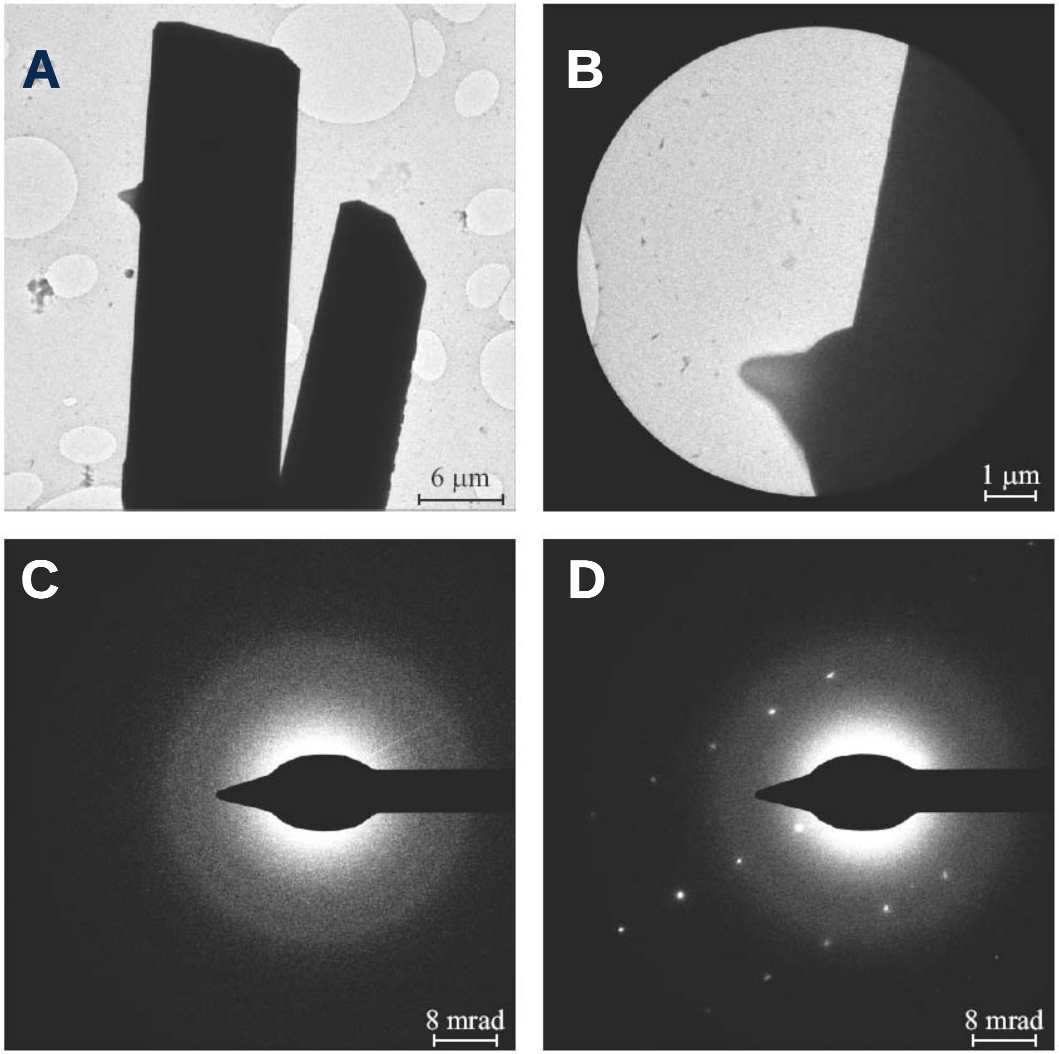

A, TEM image of the natural *Caulophacus* sp. spicule with a fragment of club-formed structure (**B**).

TEM diffraction analysis of the spicule shows the presence of two phases: amorphous (**C**) and crystalline (**D**)

Electron diffraction pattern corresponding to the spines shown as a TEM image in (**B**) corresponds to the (0001) zone axis of **calcite** with d spacings:

100 (1010) 4.32 Å
010 (0110) 4.32 Å
and
210 (2110) 2.49 Å

Results of alkali-based demineralization

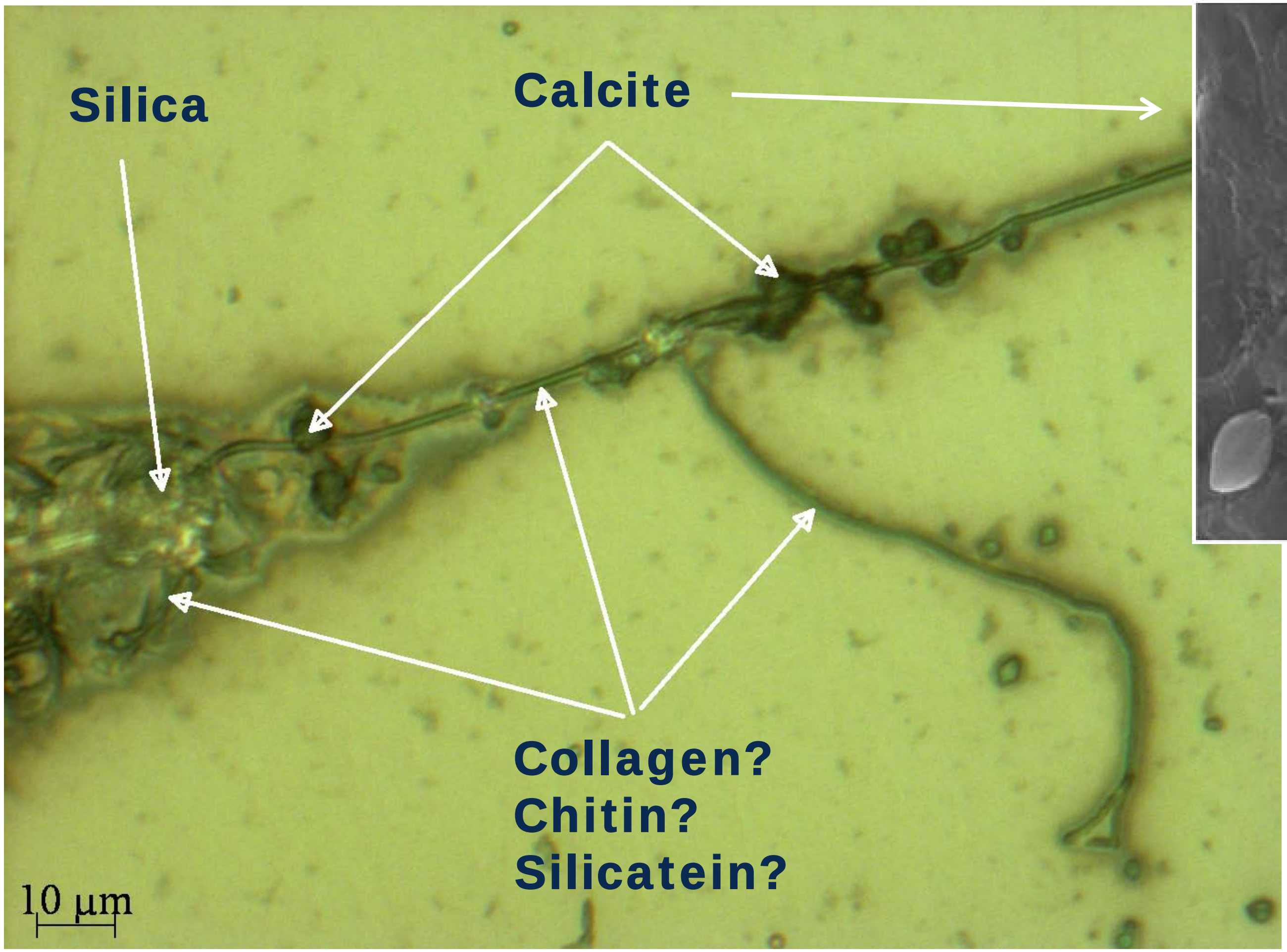

Light microscopy image

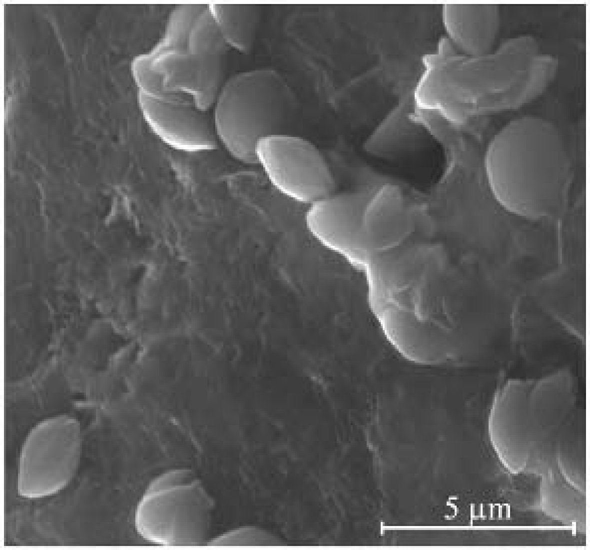

SEM image

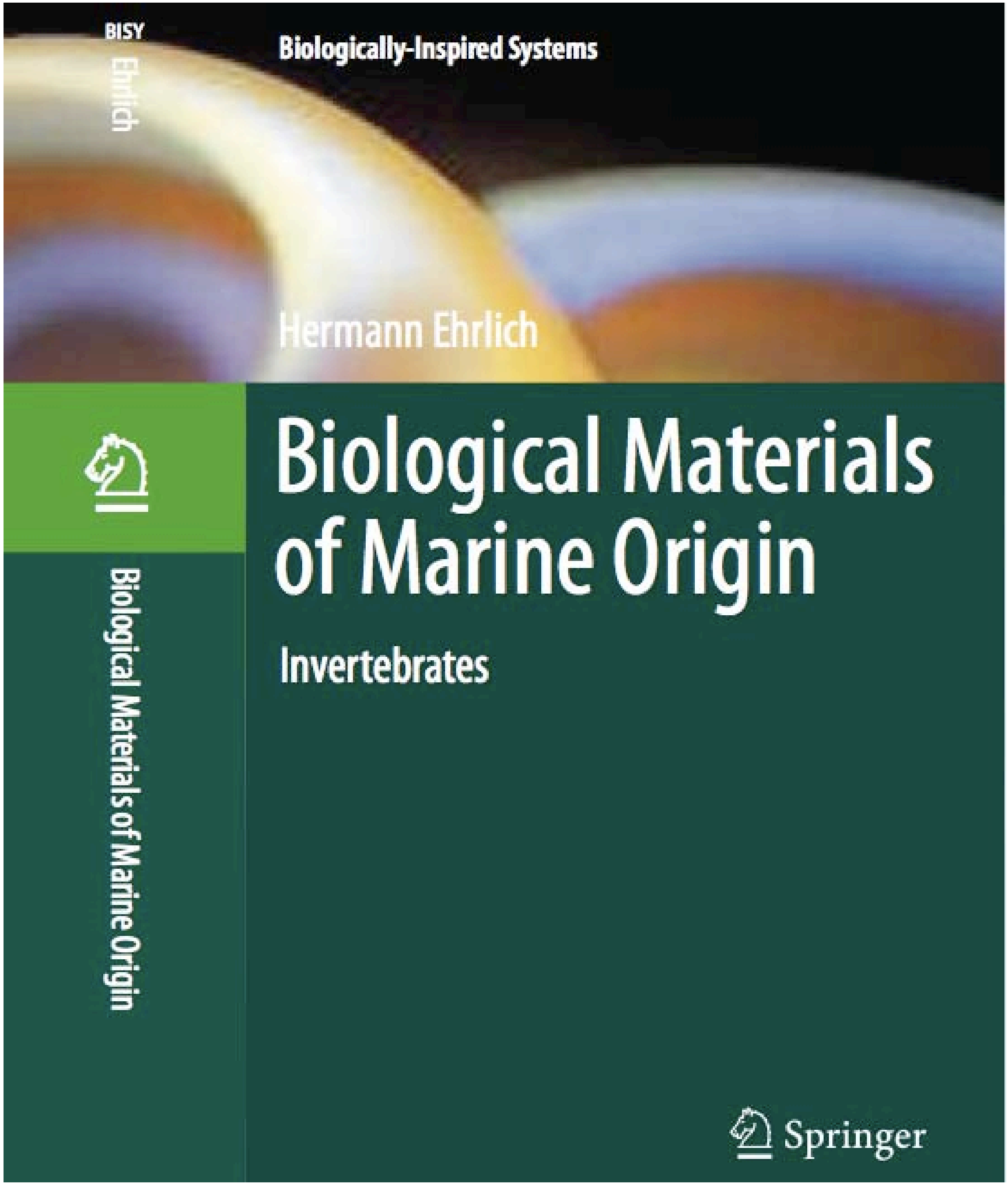
BISY
Ehrlich
Biologically-Inspired Systems
Hermann Ehrlich
Biological Materials of Marine Origin
Invertebrates
Biological Materials of Marine Origin
Springer

Content

- **Part One: *Biomaterials***
- **Part Two: *Biominerals and Biomineralization***
- **Part Three: *Biomineralized Structures and Biocomposites***
- **Part Four: *Non-mineralized Structures***
- **Part Five: *Suction-based Adhesion in Marine Invertebrates***
- **Part Six: *Macromolecular Biopolymers***
- **Part Seven: *Self Made Biological Materials***
- **Part Eight: *Extreme Biomimetics***
- **Addendum**

http://www.springer.com/life+sciences/animal+sciences/book/978-90-481-9129-1

Temperature diapasons of biosilicification

Organisms		**Temperature, ^{o}C**	**Organisms**		**Temperature, ^{o}C**
Bacteria, Cyanobacteria	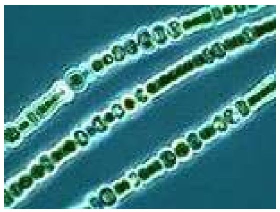	45-90	Sponges (Porifera): Hexactinellida Demospongiae		**-1.5 -10**
Protista: Silica plankton	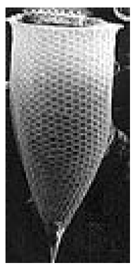	0-10	Plants: bamboo		10-18
Diatoms (Algae)		**-1.5 - 80**	Brachiopoda	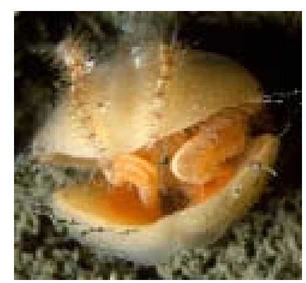	2-10

Adapted from: Ehrlich H., *Biological materials of marine origin*. Springer. 2010

Biosilicification at -1.9°C

Scolymastra joubini glass sponge:
-Up to **2 m** tall
-Up to **1.4 m** in diameter
-Up to **600 kg** wet weight
-Up to **50 kg** biosilica

Deep sea glass sponges and „cold biomineralization“

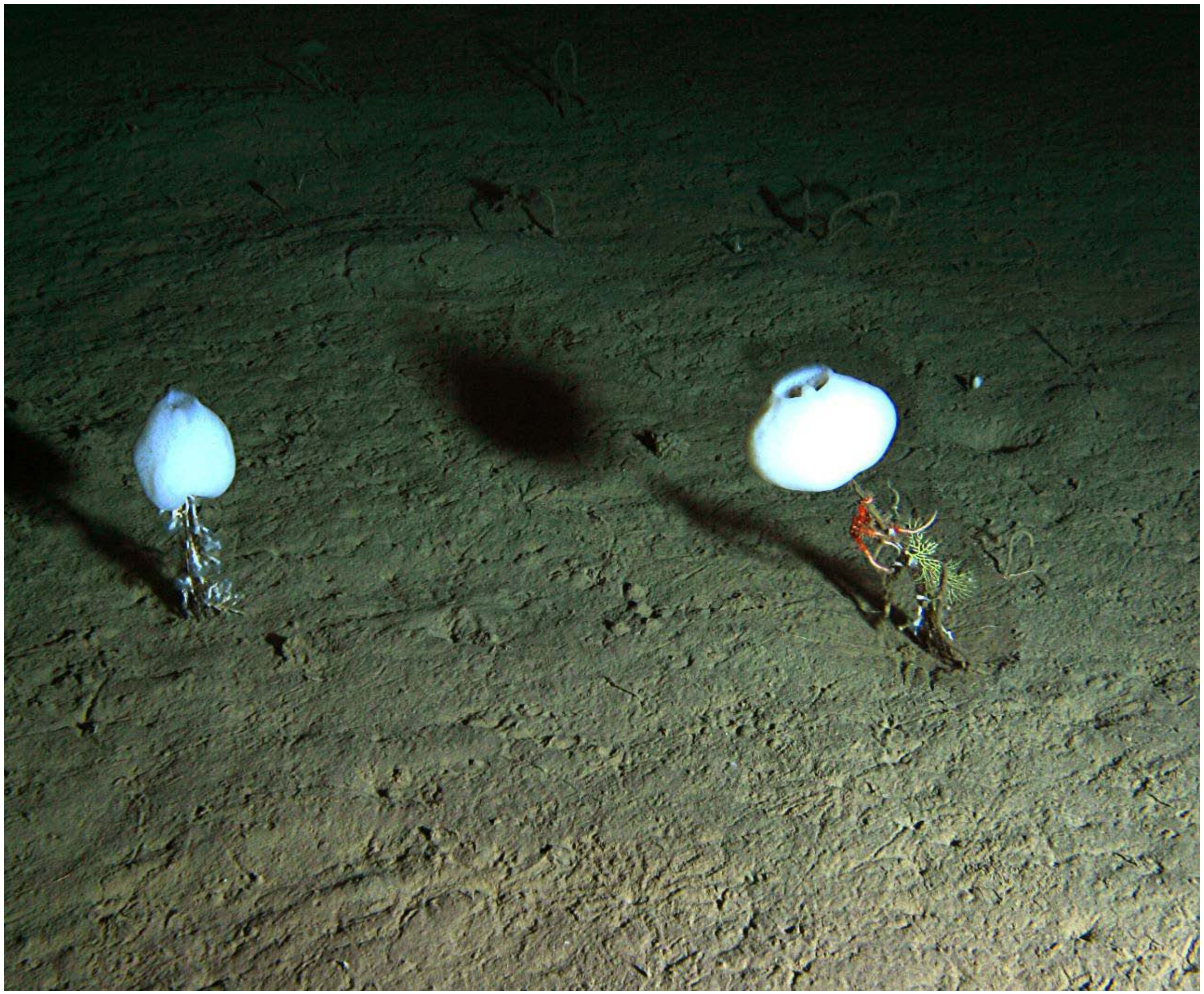

Glass sponges are the most ancient multicellular organisms:
the oldest hexactinellid spicules date from Edicarian (630 to 542 Myr)

Does *Hyalonema sieboldi* spicules contain collagen?

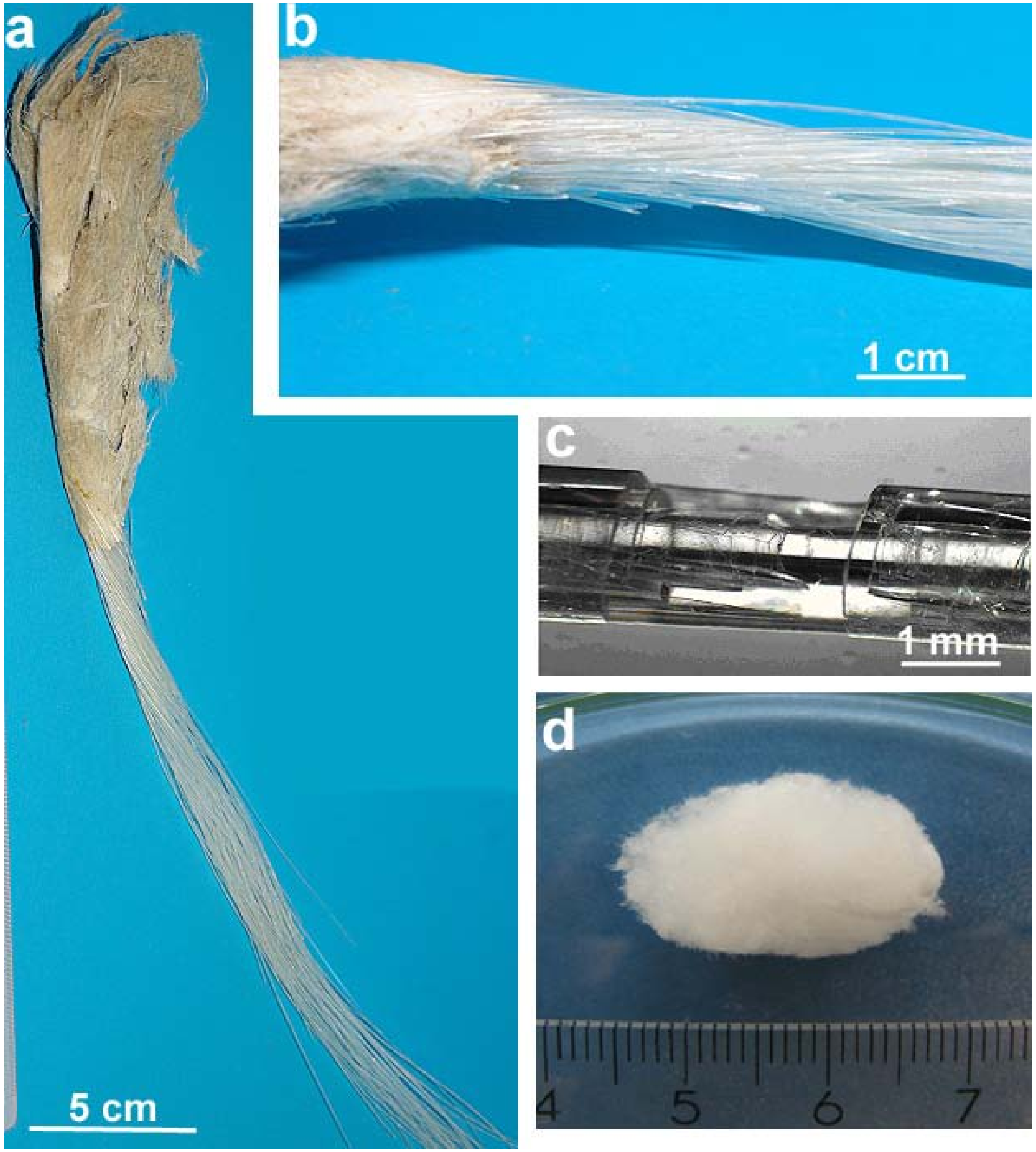

Unique flexibility of anchoring spicules of *H. sieboldi*

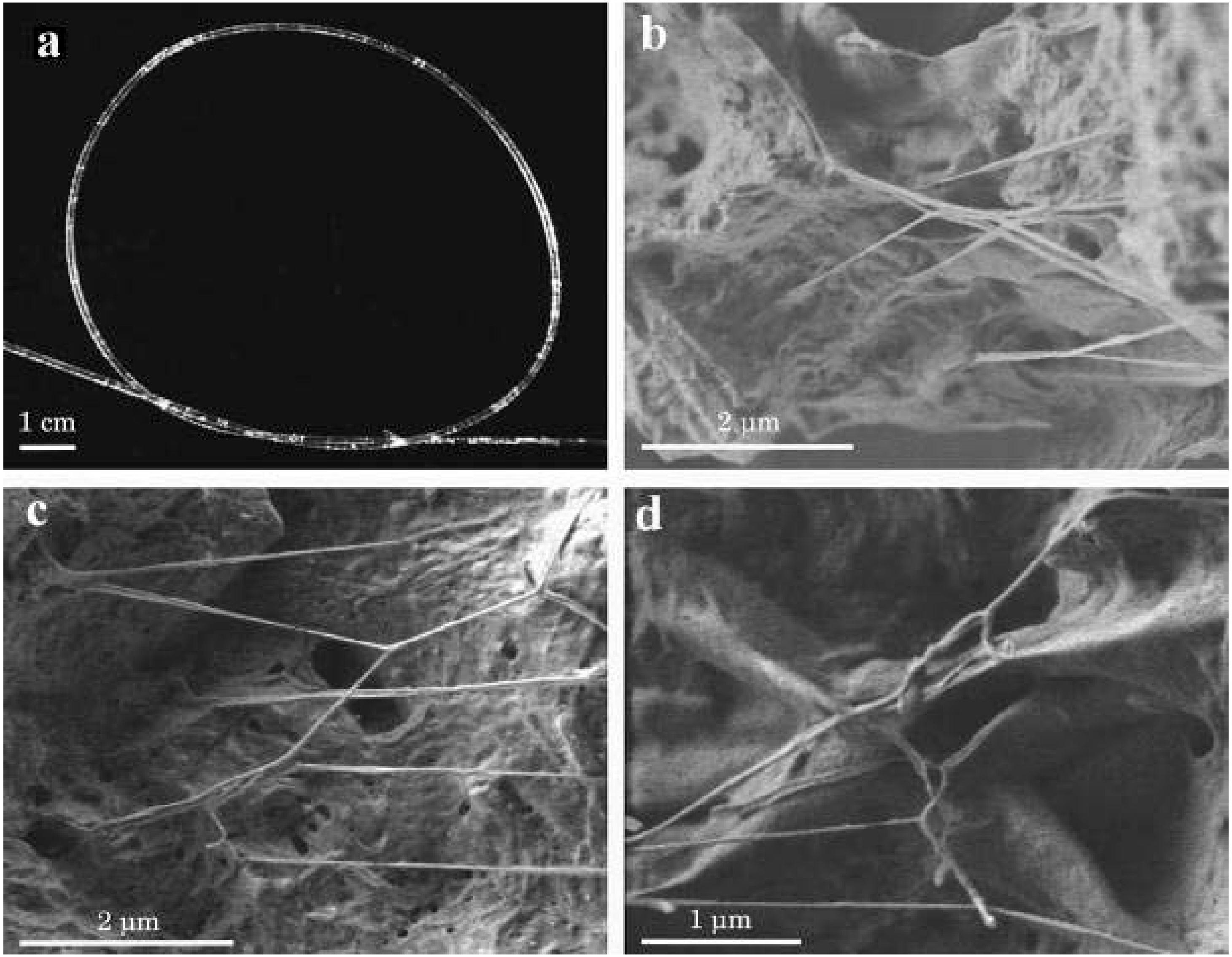

Amino acid sequencing of *H. sieboldi* collagen

List of peptides:

G A Q G (P) L G P
G G F G L 4Hyp G R
G (V) D G N 4Hyp G I X G A T G S
G S V G 3Hyp 4Hyp G N 4Hyp G V Q G V S G 3Hyp
I G P D E P L K G K I
G I 4Hyp G P Q G F T G A I G V T G S 4Hyp G E I G A 4Hyp G
V G D 4Hyp G L V G D L G A Q G P Q G S Q G L V G
G A T G 3Hyp 4Hyp G I S G 3Hyp 4Hyp G P Q G Q 4Hyp G T 4Hyp G I
I G P A G P Q G Q 4Hyp G 3Hyp 4Hyp G P G G P X G 3Hyp 4Hyp
G G S G A 4Hyp G L 4Hyp G A I G N Q G A 4Hyp

Possible role of Gly-3-Hyp-4-Hyp in Silicification

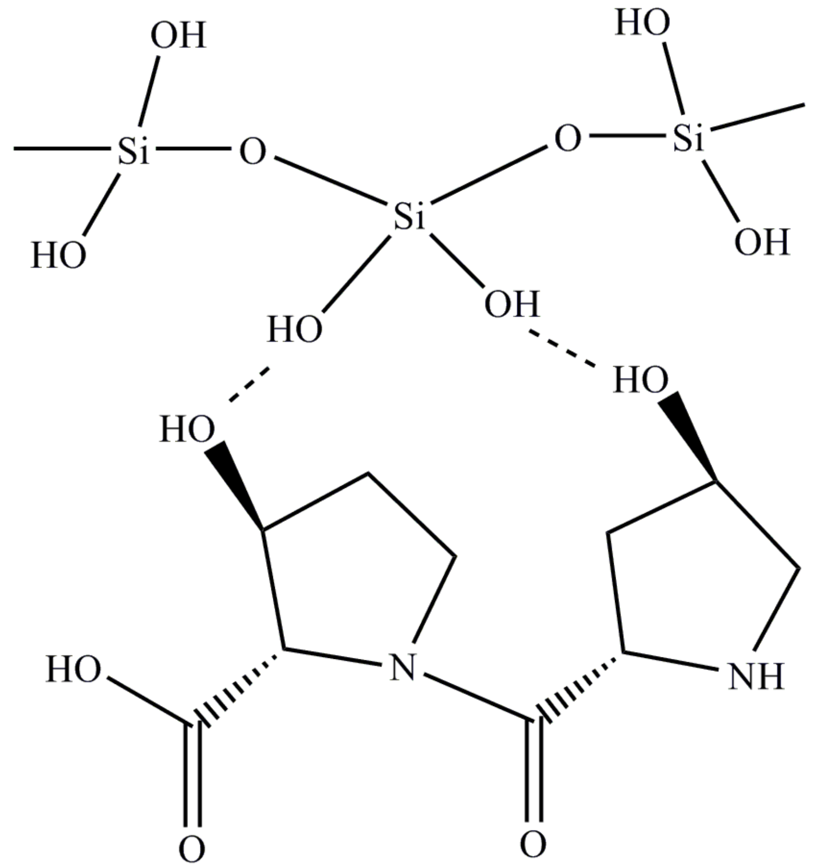

trans-3-hydroxyproline   trans-4-hydroxyproline

Unique feature of *H. sieboldi* collagen

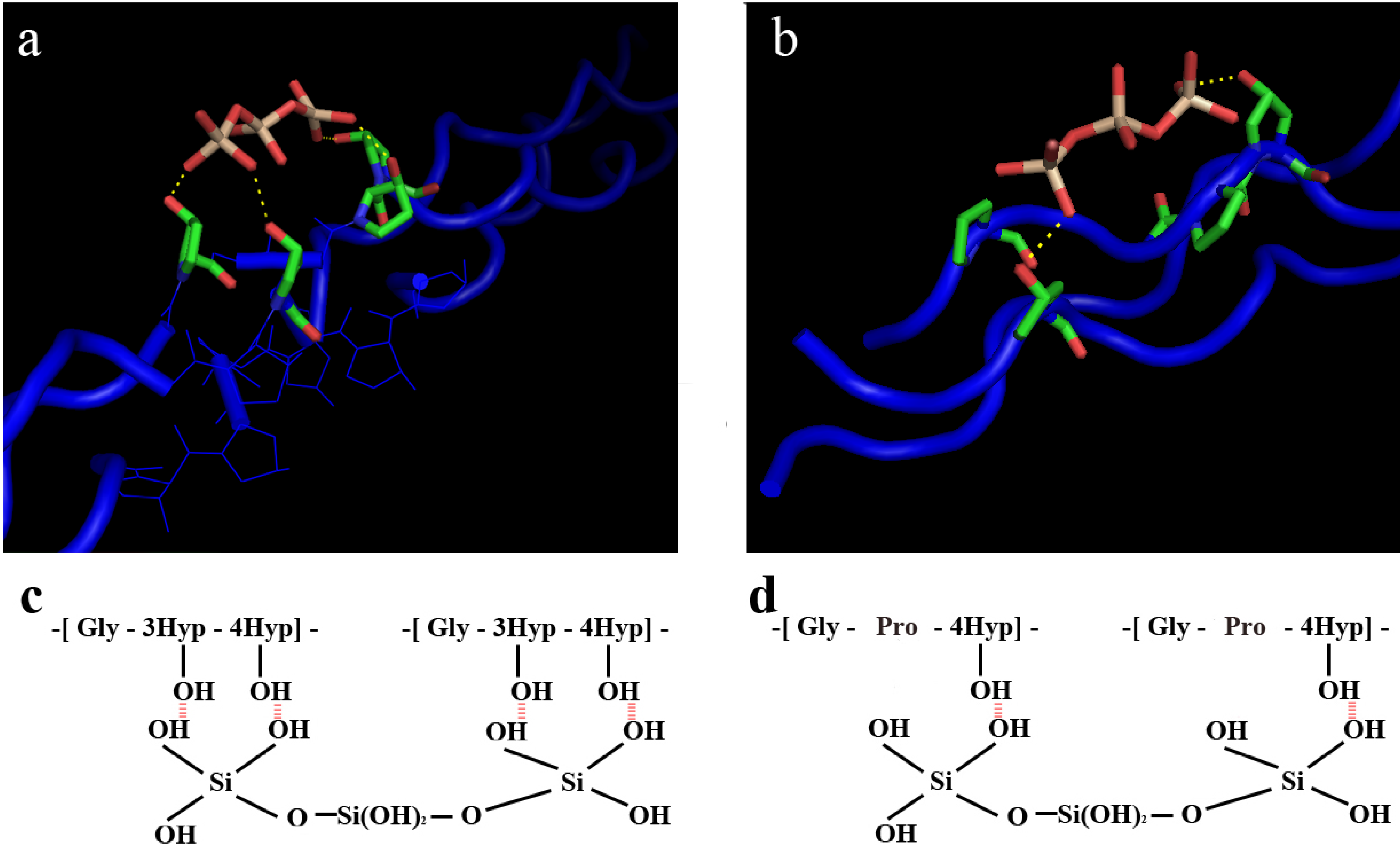

H. Ehrlich et al. Nature Chemistry (2010) (in press)

Some doubts about stability?

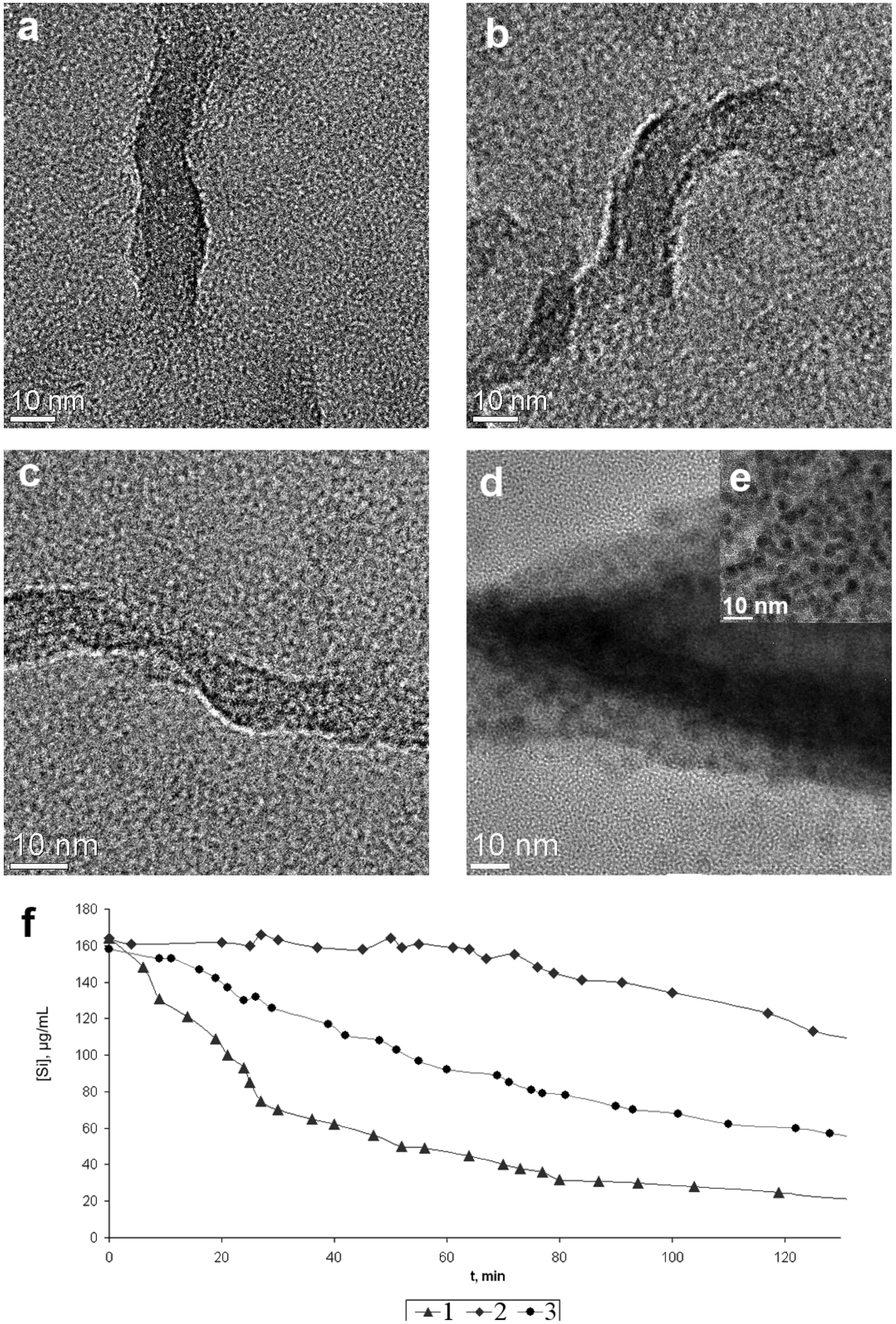

HR-TEM images of silicification on *H. sieboldii* collagen. Silicification is apparent as nano particles after exposure of nanofibrillar *H. sieboldii* spicular collagen to a solution of sodium methasilicate solution for 30 minutes (a). However after protection of 3- and 4-hydroxyproline residues by ketal groups there is no visible silica deposition (b). Cleavage of the ketal protecting groups from collagen leads to a functional recovery with respect to silicification (c). The layer of silica nanoparticles is formed around the nanofibril of native spicular collagen (d, e) during the first 30 minutes of silicification as seen in the native collagen fibre The results are in good agreement with measurements of activity (f) of nonprotected collagen (▲), which is lost following protection (◆) and partially restored when this protection is removed (●).

“Collagen, isolated from meter-long silica spicules of a primitive glass sponge, contains an unusual [Gly-3Hyp-4Hyp] motif which is shown to structure the spicule and provide a site for silica deposition. This is central to understanding the role of this unusual collagen as a novel and specific template for biosilicification in nature.”

Ehlich H., Deutzmann R., Brunner E., Cappellini E., Koon H., Solazzo C., Yang Y., Ashford D., Thomas-Oats J., Lubeck M., Baessmann C., Langrock T., Hoffmann R., Woerheide G., Reitner J., Simon P., Tsurkan M., Ereskovsky A., Kurek D., Bazhenov V., Hunoldt S., Mertig M., Vyalikh D., Molodtsov S., Kummer K., Worch H., Smetacek V. & Collins M.

Mineralization of the meter-long silica structures of glass sponges is templated on hydroxylated collagen

Nature Chemistry *(2010)* ***(in press)***

Biosilicification in Glass Sponges (Hexactinellida)

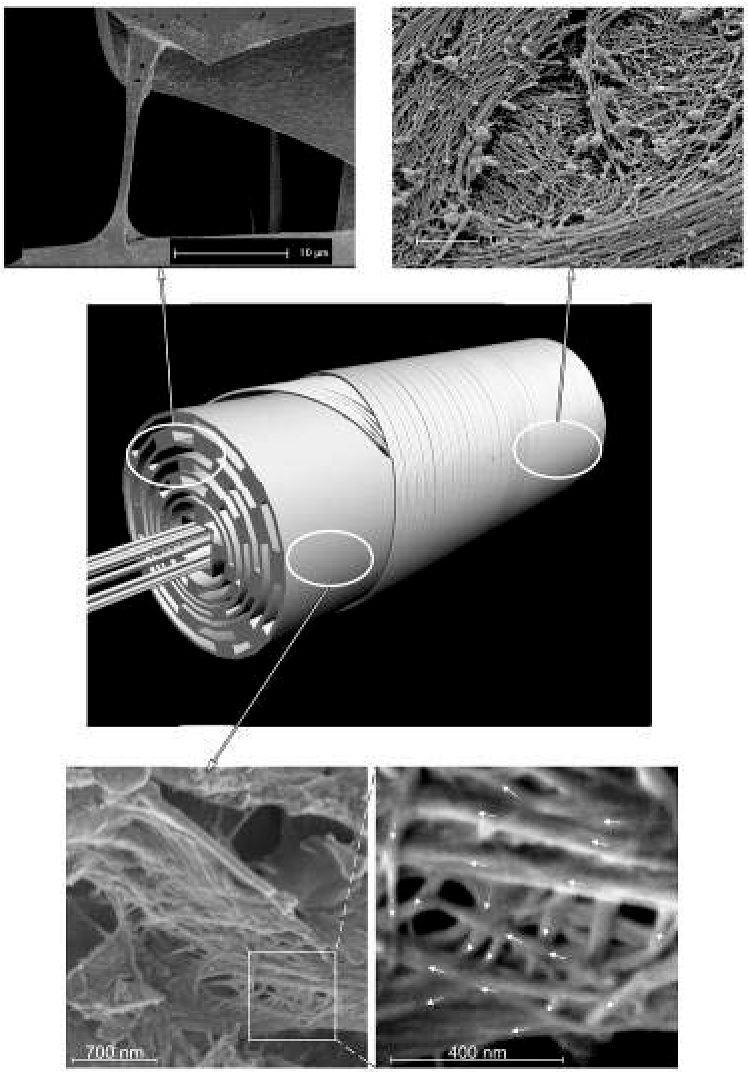

•Brunner E., Ehrlich H., Kammer M. (2010) Biomimetic Synthesis of Nanostructures Inspired by Biomineralization. *Handbook of Nanophysics: Nanomedicine and Nanorobotics* , v.7, p. 6-1…..6-14.

•Ehrlich et al. *Chemical Reviews* (2010) 110: 4656 - 4689

•Ehrlich H. (2011)
Silica biomineralization in Sponges. In:
Encyclopedia of Geobiology
Ed. by J. Reitner and V. Thiel
Springer Verlag (*in press*)

Creatures from the deep freeze: ice fish

Principles of calcification at minus 1.9 °C are unknown.

What are the nature and origin of skeleton, teeth and otoliths(otoconia) of ice fish species?

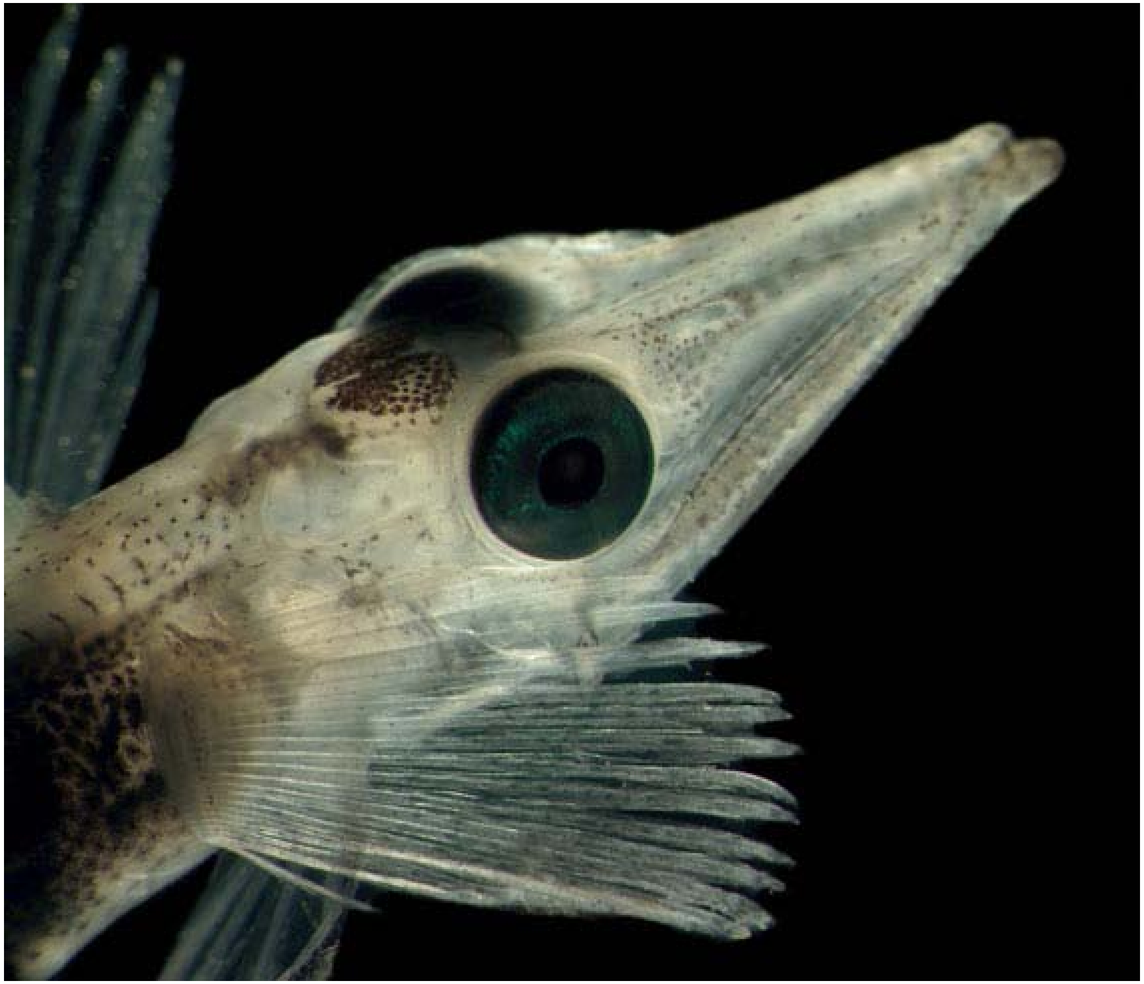

Chionodraco hamatus, one of the Antartic's ice fish, can withstand temperatures (-1.9°C) that freeze the blood of all other types of fish.

Through the replacement of bone by connective tissue and **decreased mineralization of the skeleton** as a whole, many Antarctic fish species have evolved reduced bone density. This adaptation increases their buoyancy in water, a characteristic that enables them to move easily in the water column for feeding. This adaptive trait **clearly mimics the detrimental human condition osteopenia,** a reduction in bone mineral density.

Open question: if the skeleton of this fish is really non-mineralized, what is about their teeth and otoliths ?

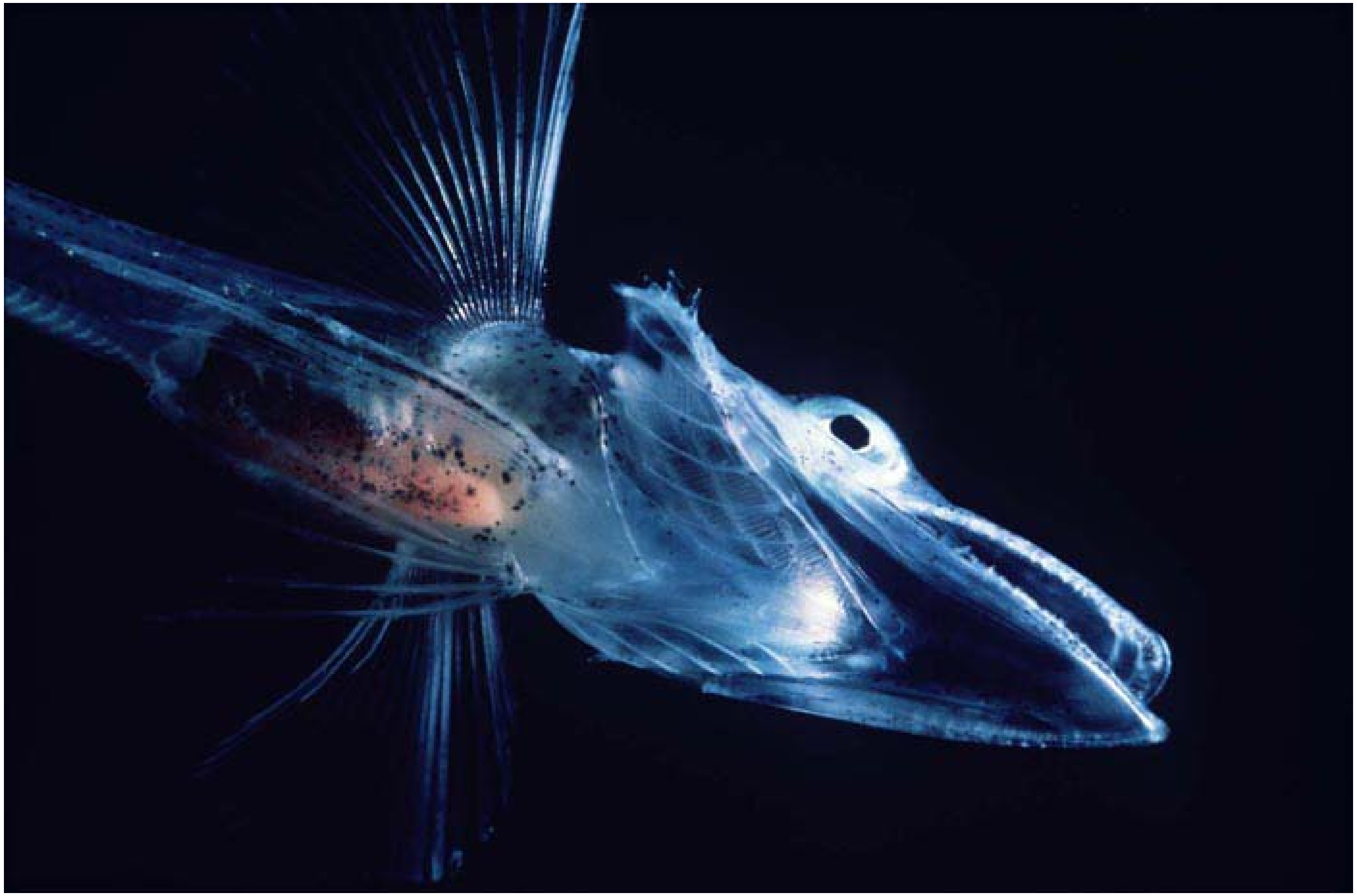

Ice fish have long snouts, wide mouths, and large teeth (!)
Open question: What is the mineral composition and nanostructure of these teeth?

Extreme Biomimetics: life between 50°C and 400 °C

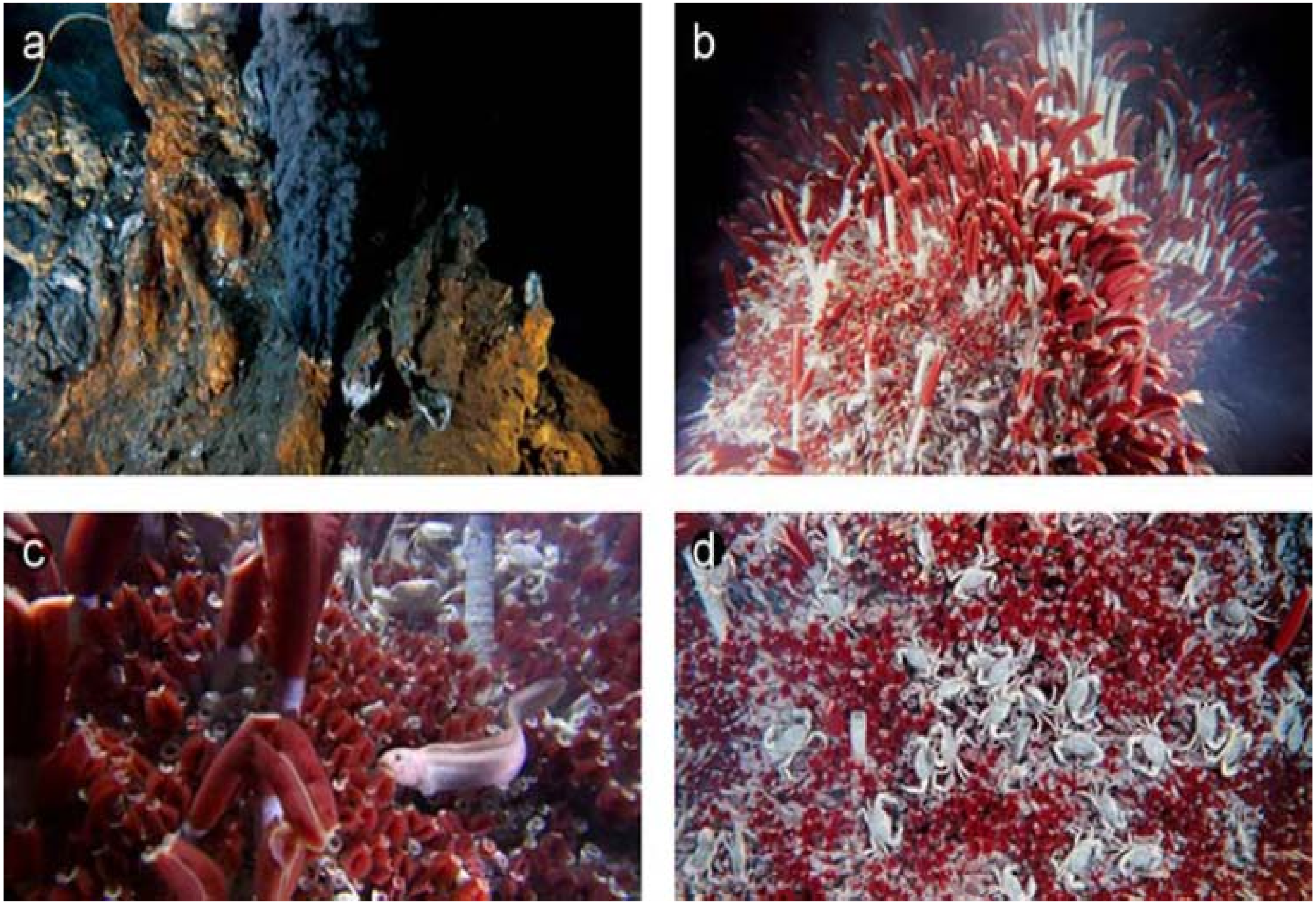

Deep-sea images of hydrothermal vent (a) as well as of vestimentiferan fauna (b, c, d), which is well adapted to these extreme environment. (Images from the IMAX film "Volcanoes of the Deep Sea", courtesy Rutgers University and The Stephen Law Company).

Extreme Biomimetics: Biosilicification at 90°C

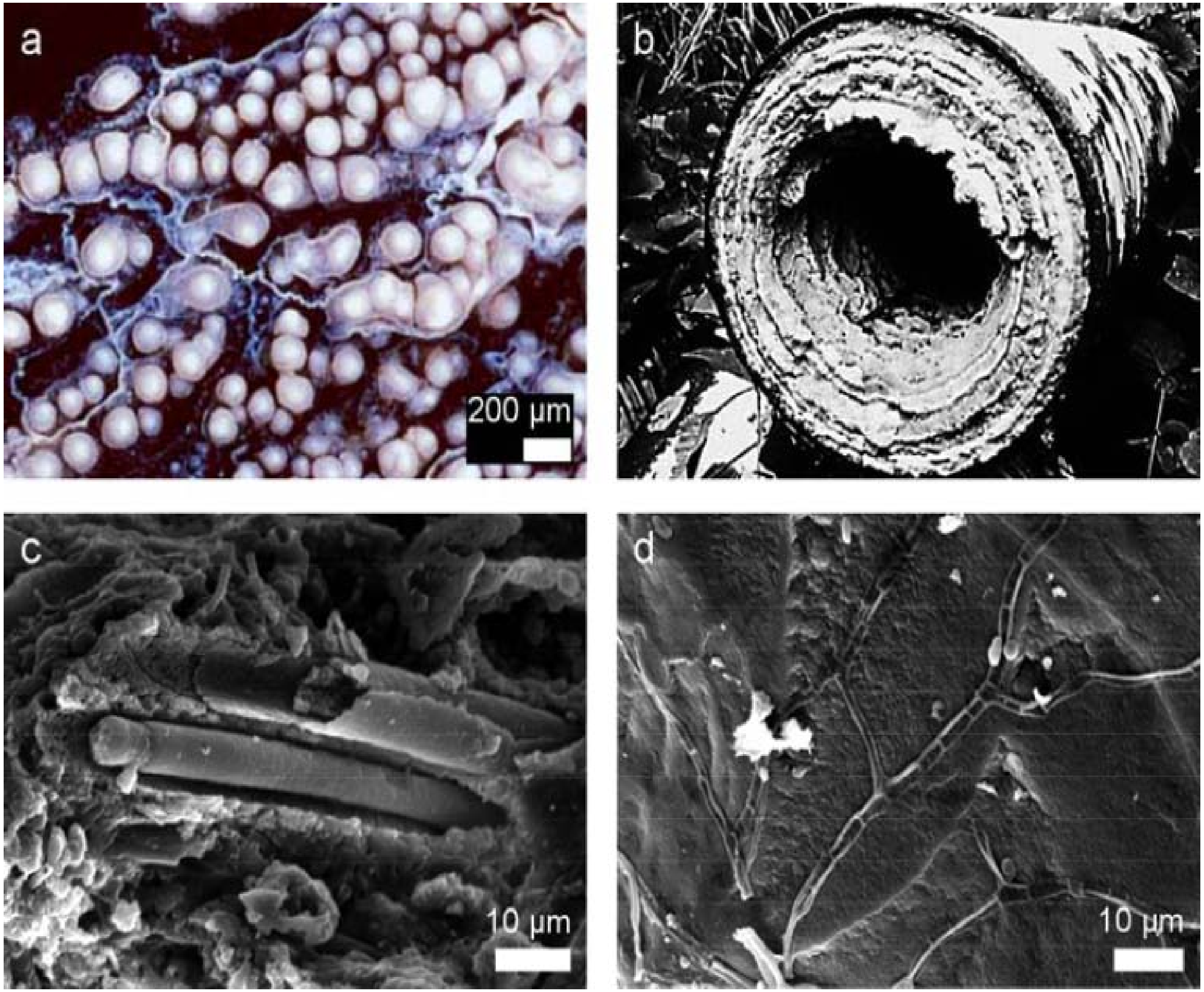

Examples of inspiration for “extreme biomimetics”: (a) silica microparticles of geyserites from Kamchatka surrounding by organic matter; (c and d) different kind of silicified microorganisms observed using SEM within these formations (images courtesy Gennady Karpov); (b) *Thermus* and *Hydrogenobacter* are predominant components among the indigenous microbial community in huge siliceous deposits formed within the pipes and equipment of Japanese geothermal power plants.

Thermotolerant Diatom

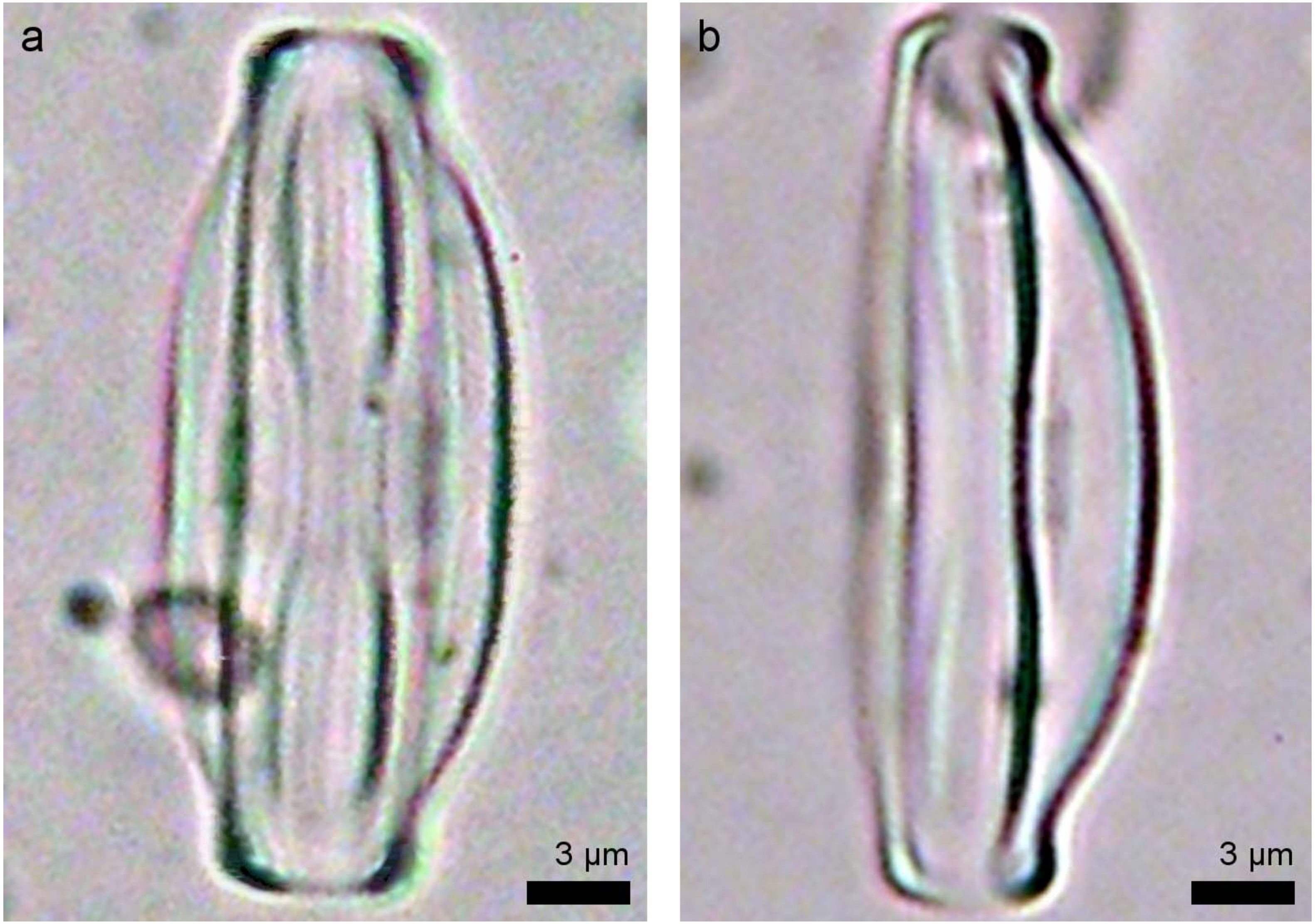

Light microscopy images (a, b) of *Amphora veneta* isolated from hot spring (**80°C**) in Kamchatka region (images courtesy Philipp Sapozhnikov).

Chitin Scaffold as Integral Part of the Diatom Cell Wall

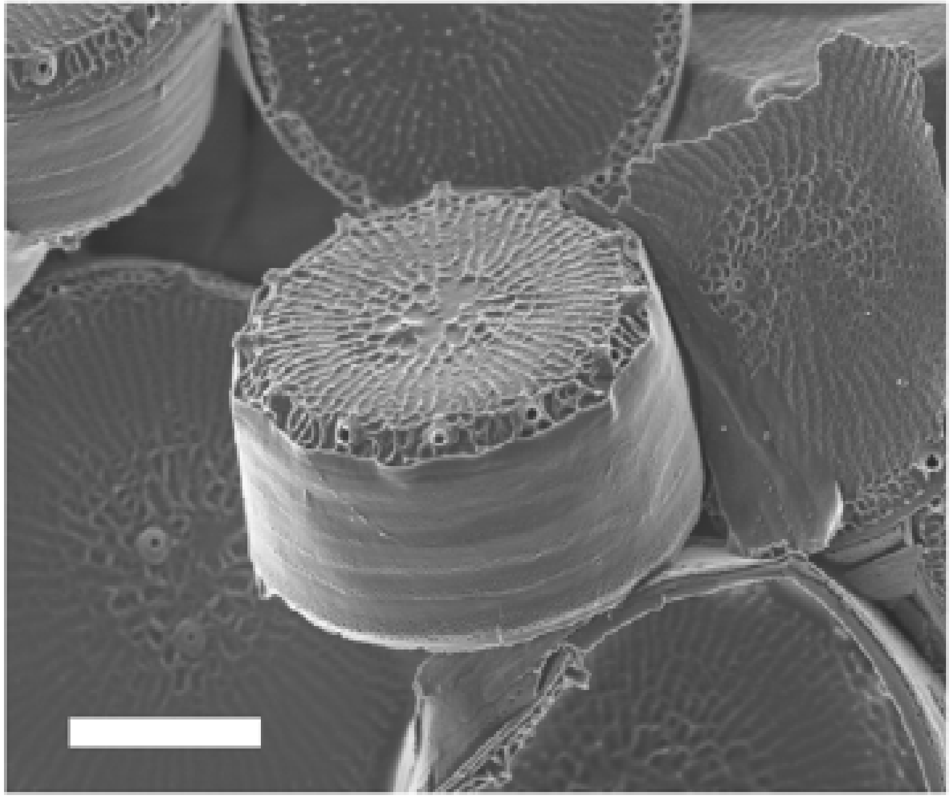

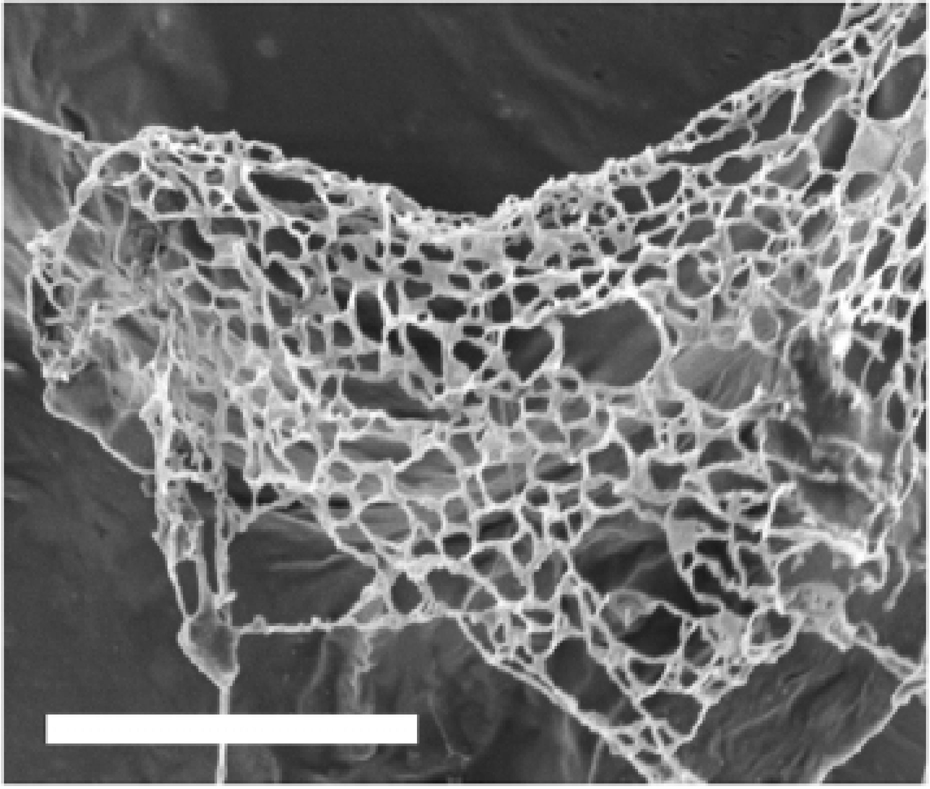

SEM images of SDS/EDTA treated *T. pseudonana* samples harvested using a flow centrifuge (left). The right image shows an organic scaffold extracted by NH_4F treatment. Scale bar: 2 µm.

From: Brunner E., Richthammer P., Ehrlich H. *et.al., Angew. Chem. Int. Ed.* 2009, 48: 9724-9727

TEM imagery: Chitinous scaffold of *T. pseudonana*

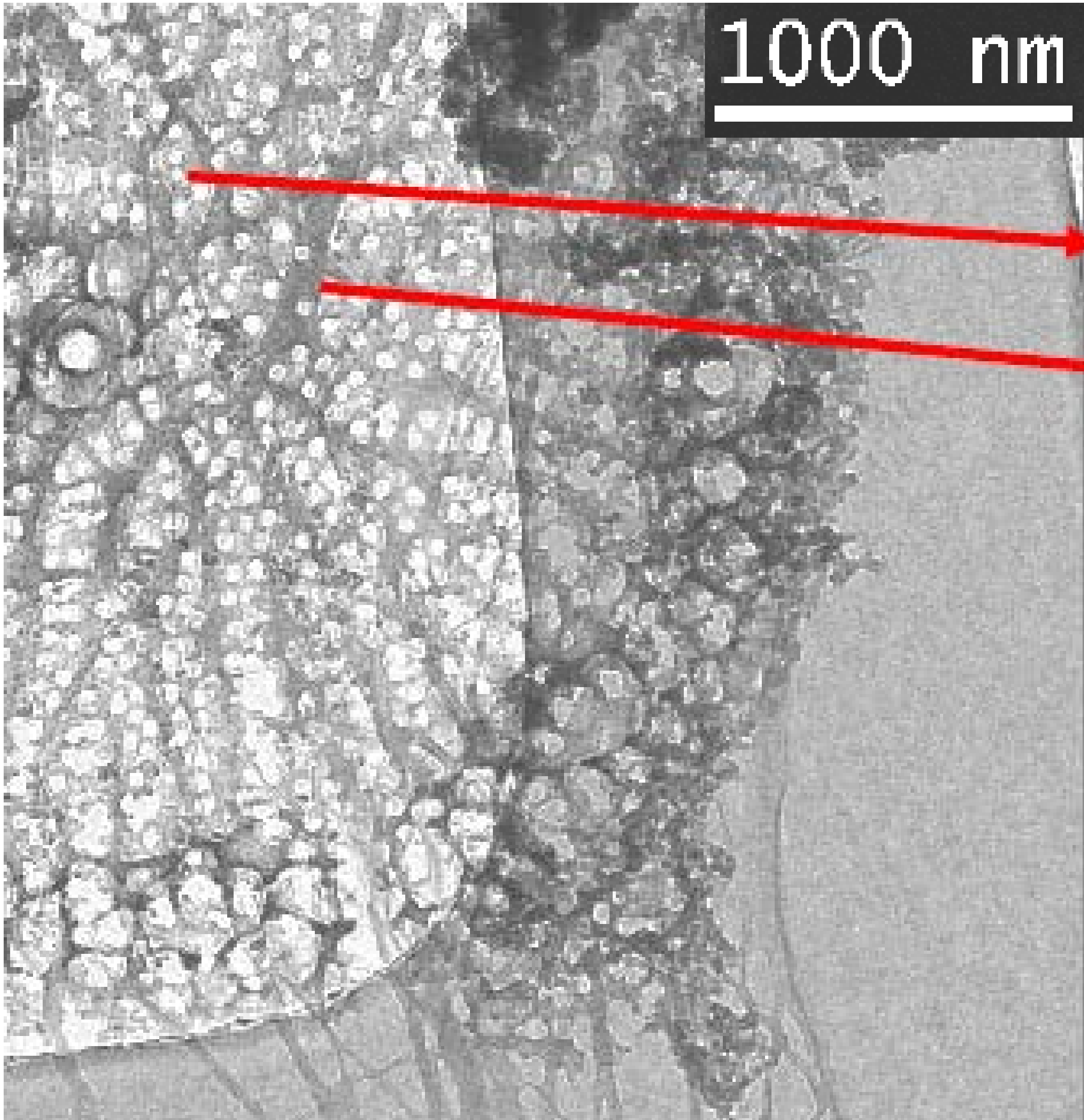

Chitin fibril ∅ 20 nm

Chitin fibril ∅ 85 nm

phytoplankton – bacillariophyceae

Thalassiosira rotula

abundance: permanent abundant
life-form: in chains
diameter: 30 - 60µm

INSTITUT FÜR OSTSEEFORSCHUNG WARNEMÜNDE
IOW

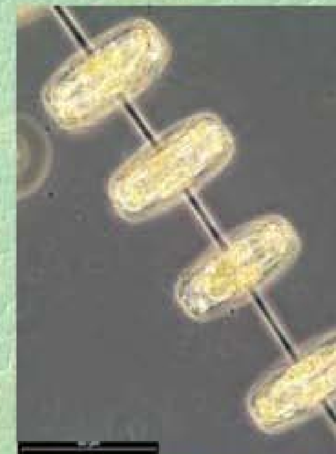

LM (North Sea, German Bight)

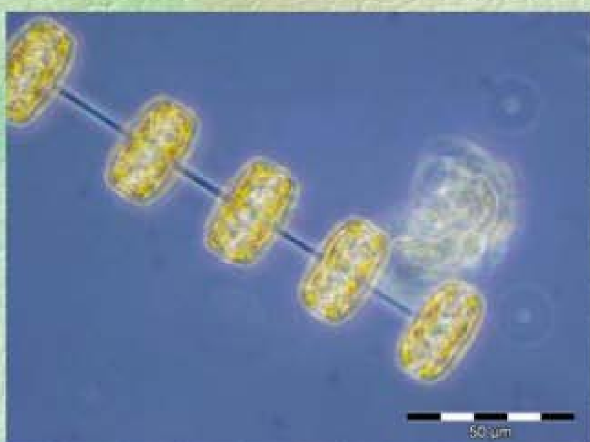

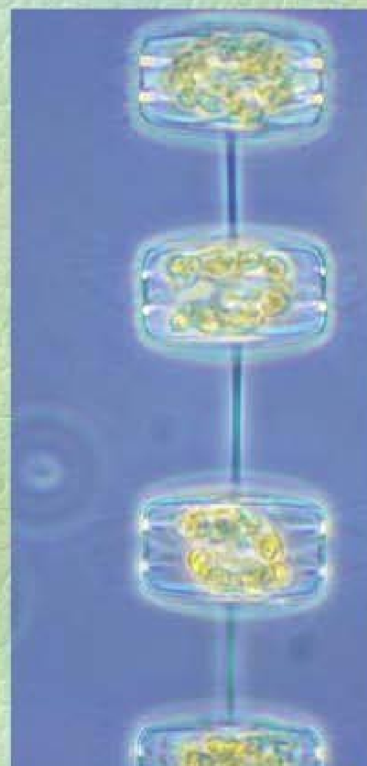

LM (coastal station Heiligendamm)

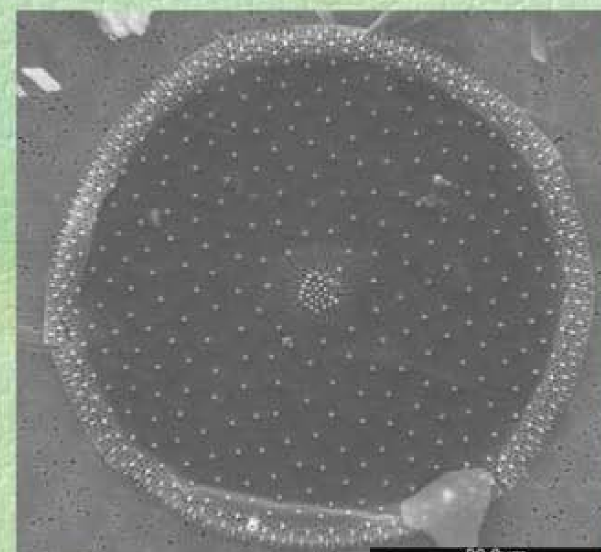

REM (North Sea, SWWBA)

Thalassiosira rotula: alkali-based desilicification

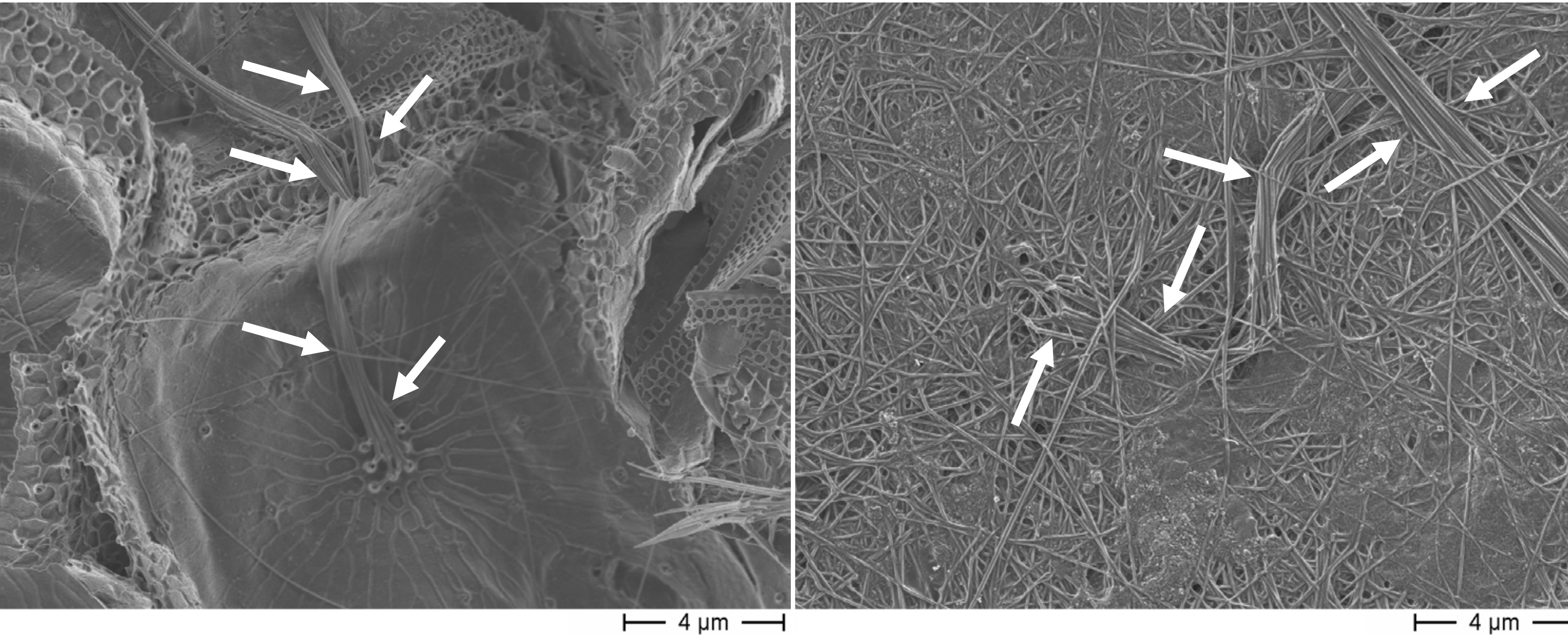

SEM images: lyophilized cells (left) and cells after treatment using 2.5 M NaOH (16 h at 37°C) (right)

Samples courtesy: Karen Wiltshire & Alex Kraberg, AWI Helgoland

Thalassiosira rotula: alkali-based desilicification

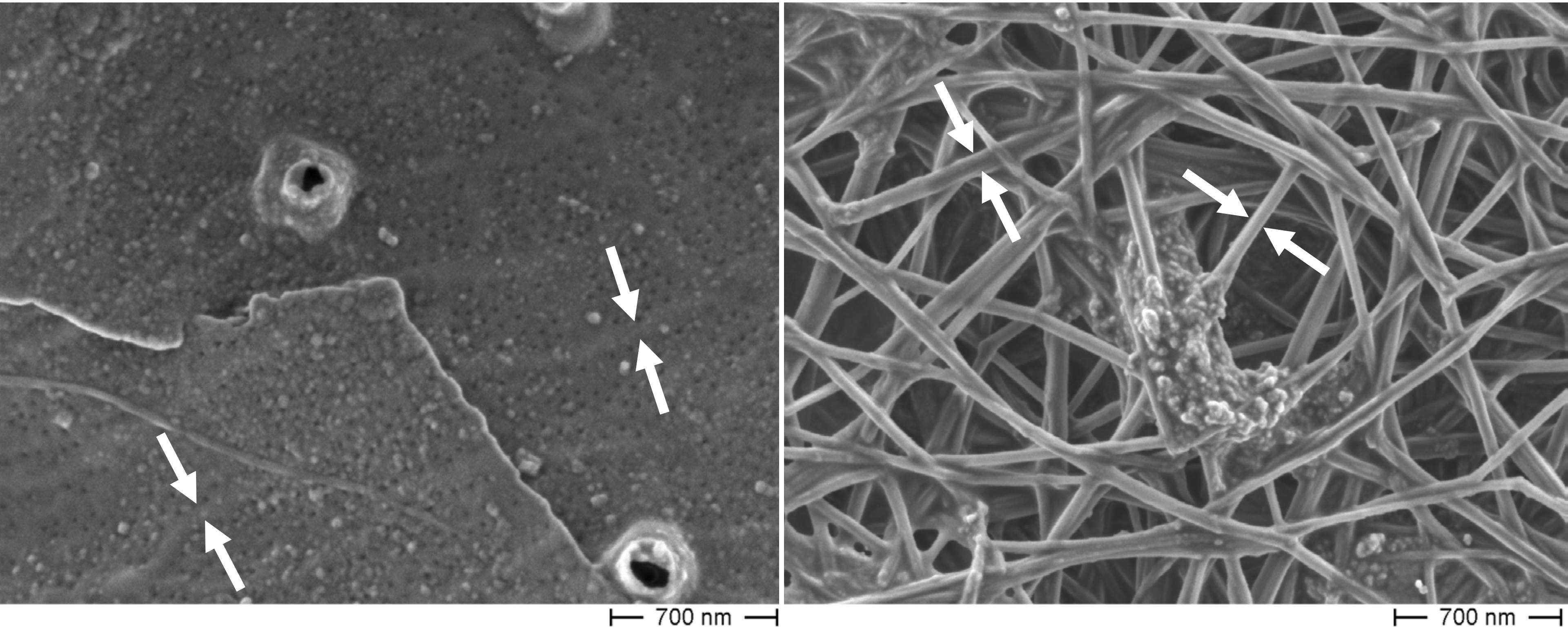

SEM images: lyophilized cells (left) and cells after treatment using 2.5 M NaOH (16 h at 37°C) (right)

Thalassiosira rotula: alkali-based desilicification

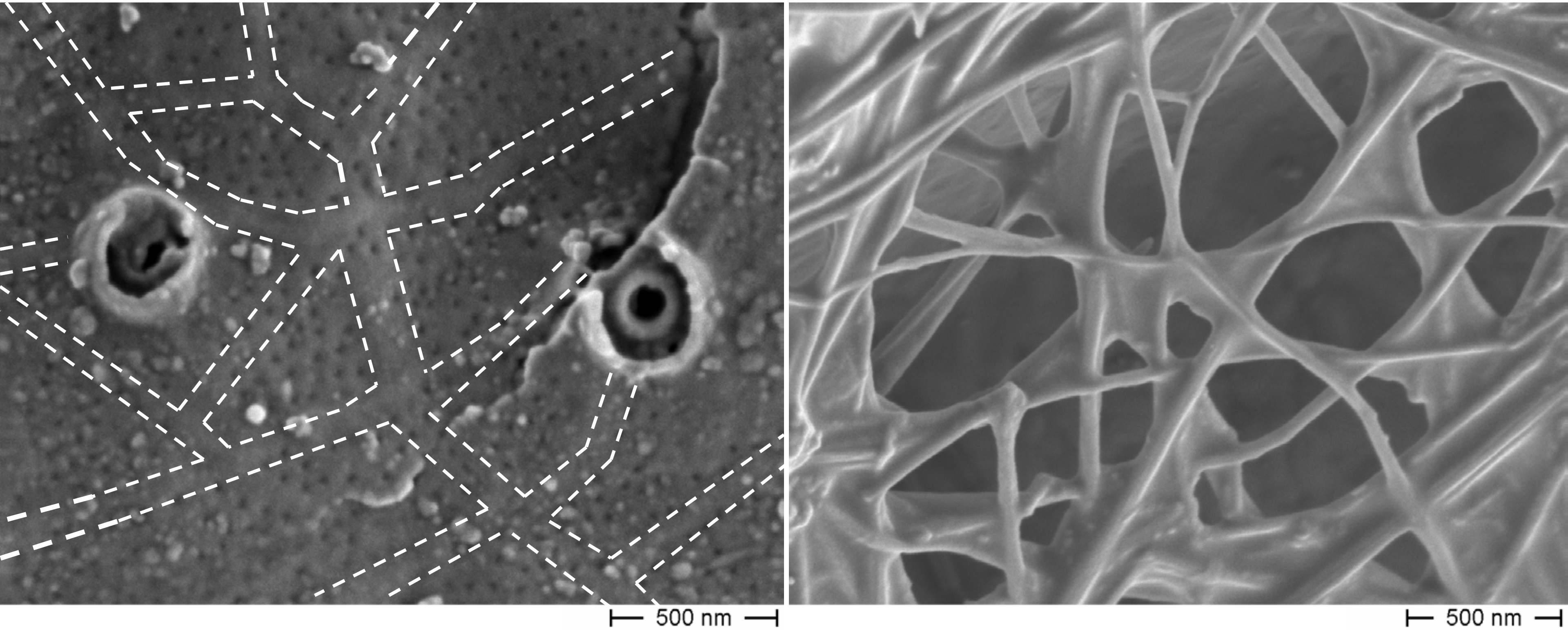

SEM images: lyophilized cells (left) and cells after treatment using 2.5 M NaOH (16 h at 37°C) (right)

Thalassiosira rotula: Nanoimagery of alkali-based desilicification

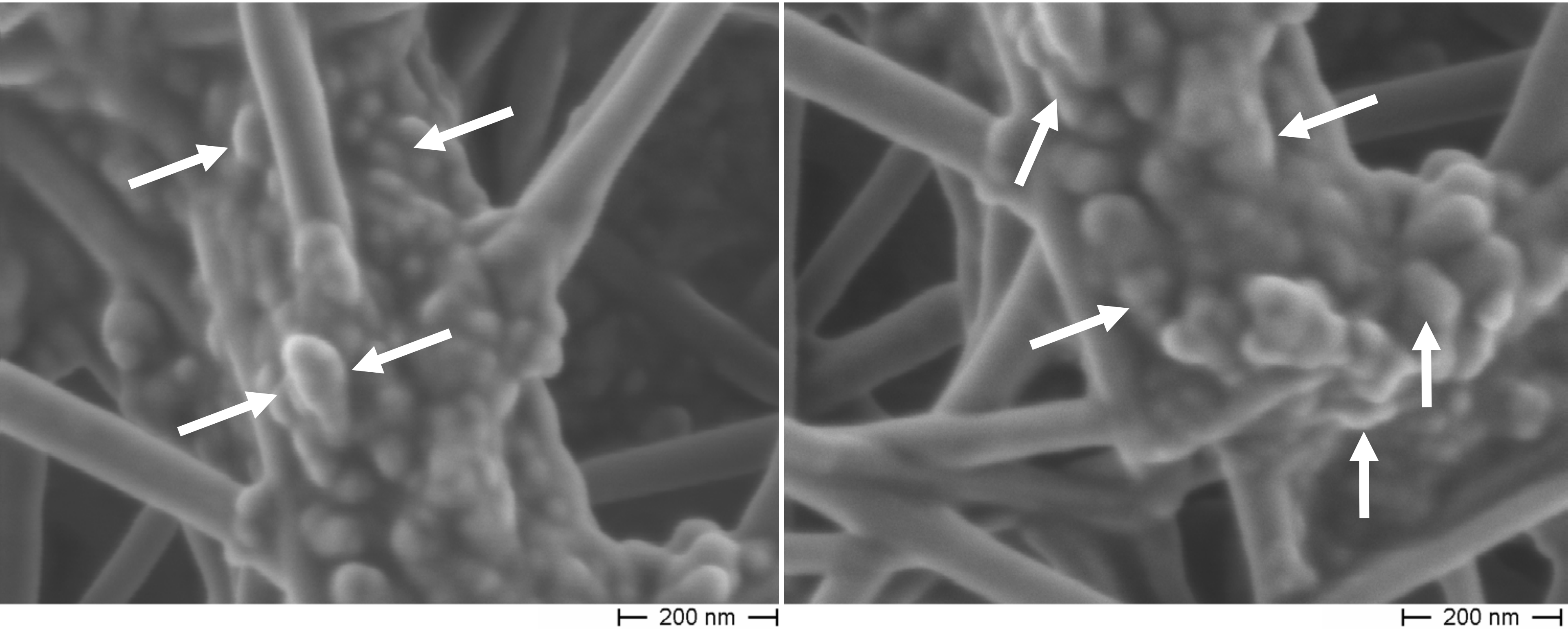

SEM images: residual silica nanoparticles (arrows) on the partially demineralized chitinous scaffold

Nanostructural organization of the naturally occuring silica-chitin composite unit

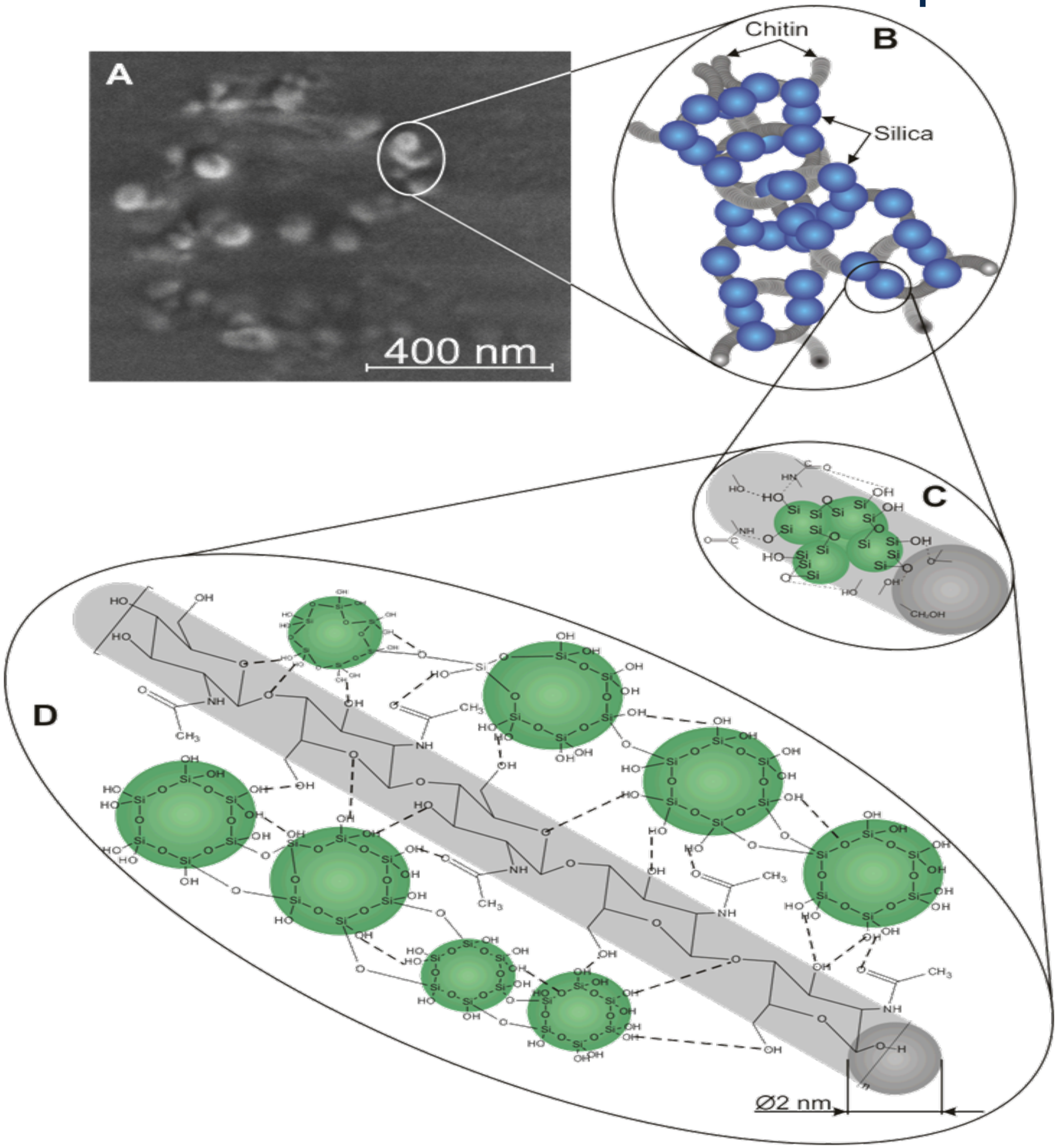

From:
Ehrlich et al.,
J. Nanomat., 2008

Possible silica-chitin interactions

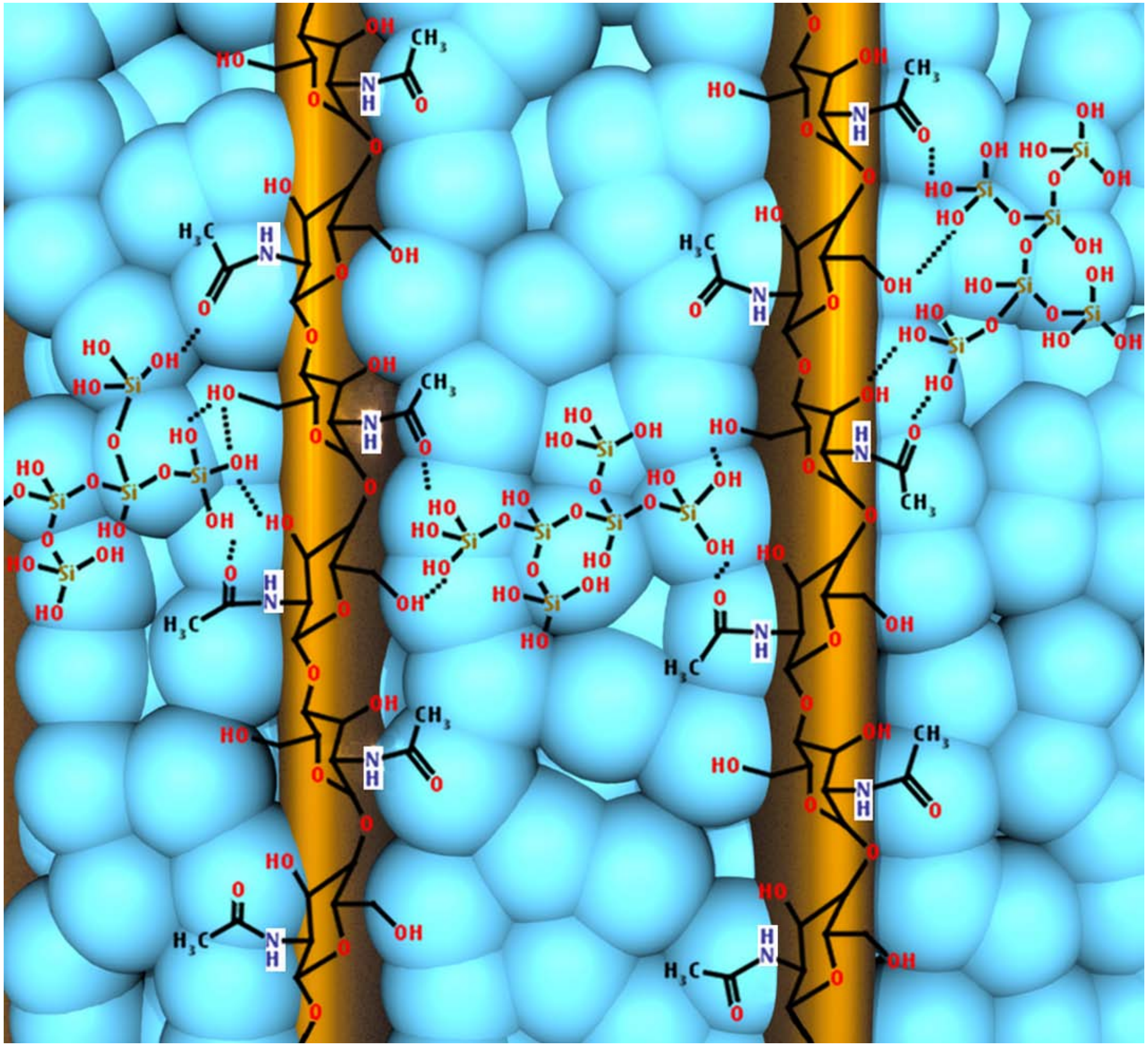

Schematic view shows a possible distribution of silica between chitin nanolamelles within silica-chitin-based outermost layer of *S. hawaiicus* spicule.

We suggest that silicate ions and silica oligomers preferentially interact with glycopyranose rings exposed at the chitin surface, presumably by polar and H-bonding interactions.

Vauxia gracilenta a 505 Myr old Chitin-based Sponge

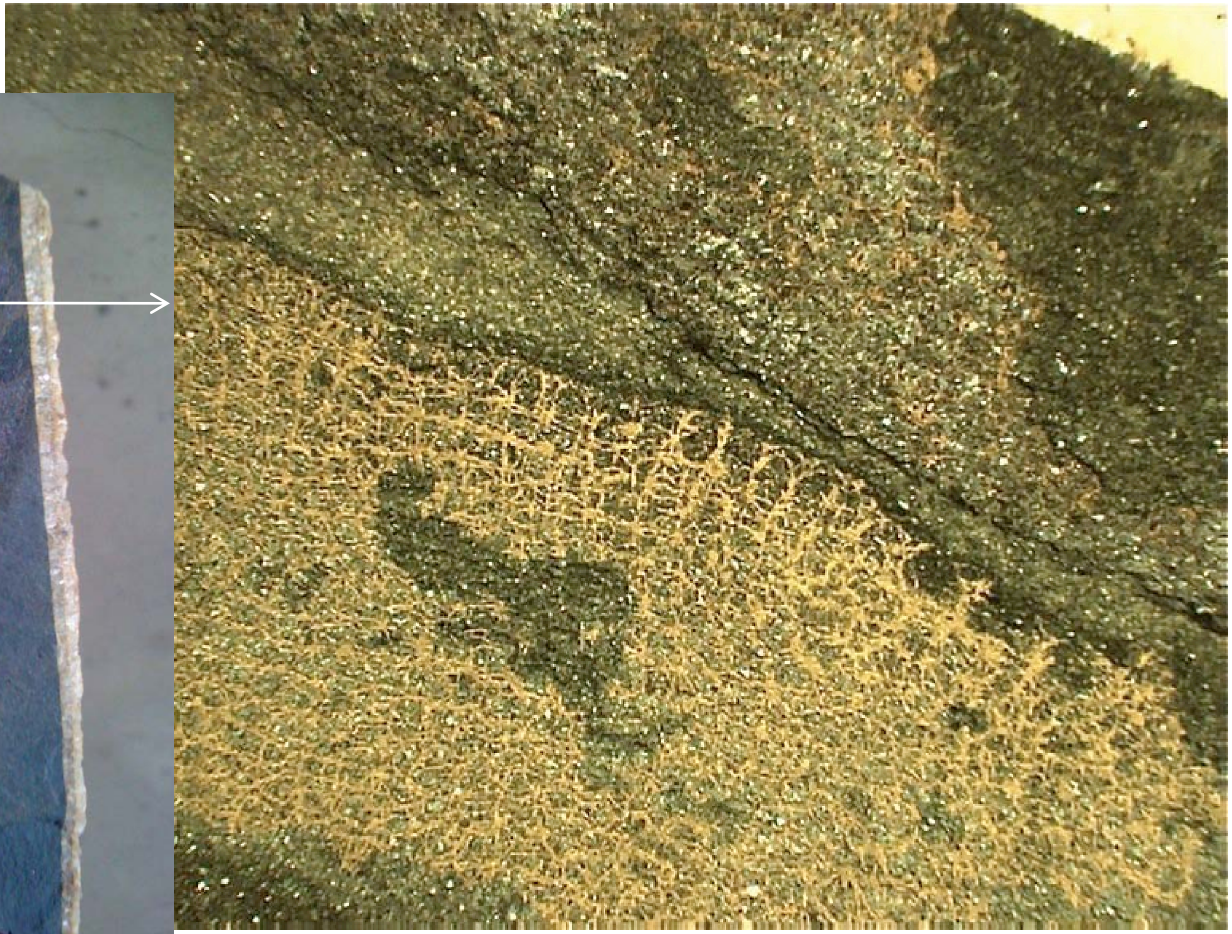

Exceptional preservation because of low grade metamorphism (**260°C**).
Sample courtesy Ontario Royal Museum, Canada

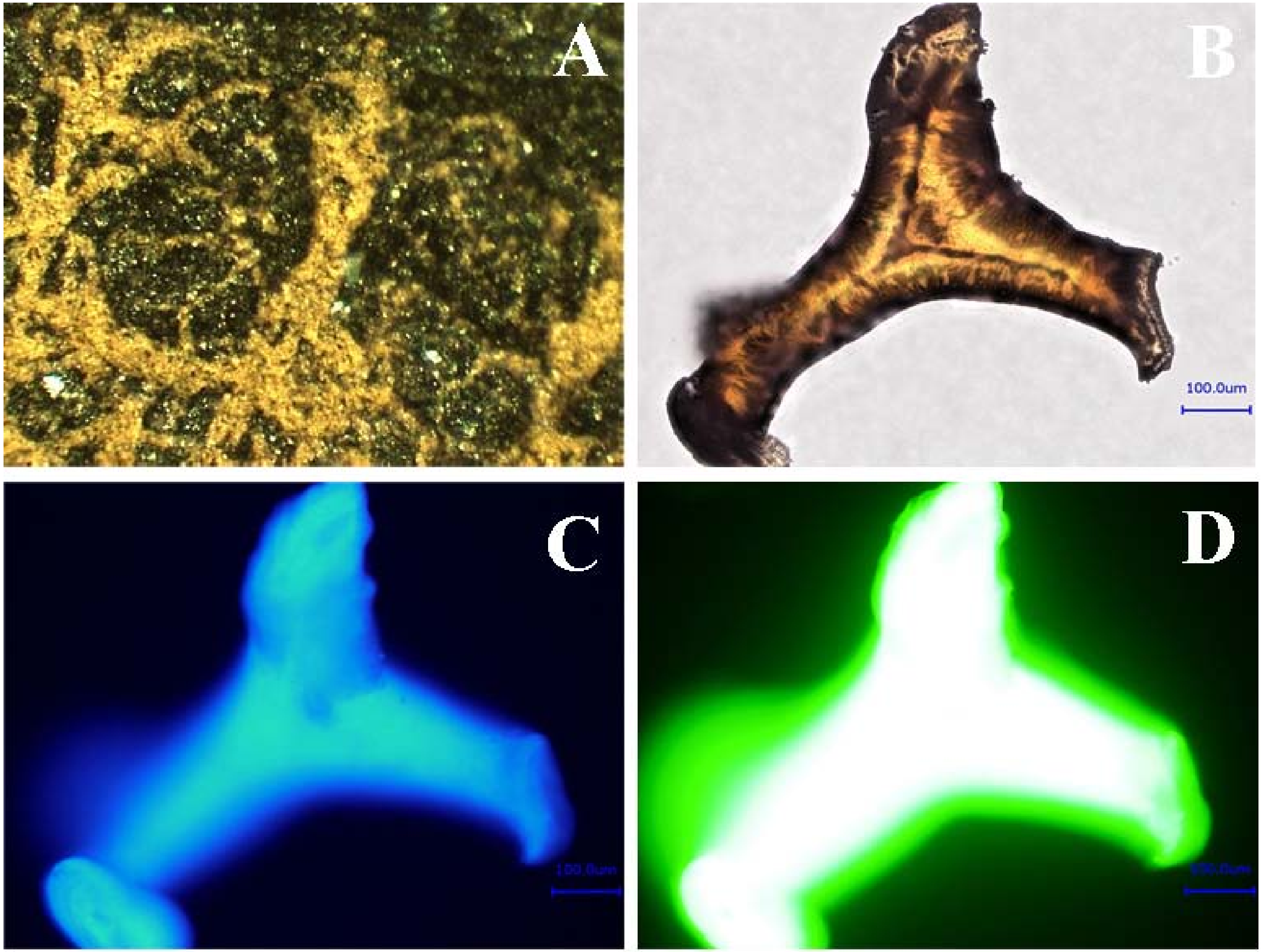

A Stereo microscopy view of the Vauxia (Verongida: Porifera) sponge skeleton fragment

B Light microscopy image of the skeletal fibre isolated from Vauxia skeleton

C and D: fluorescence microscopy images of the same fibre show autofluorescence typical for chitin and observed in studies on recent Verongida sponges

Thermostability of Chitin

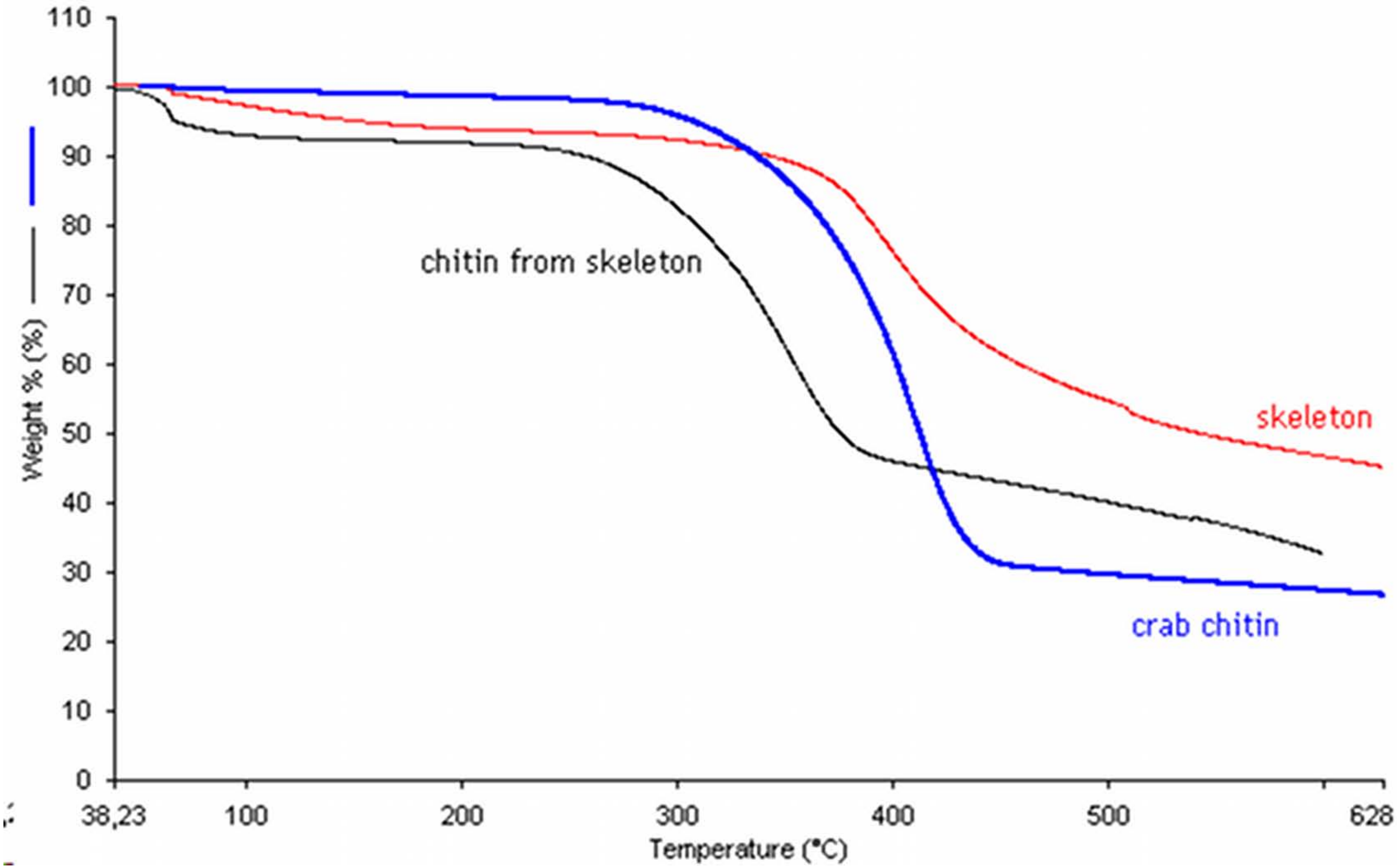

The representative thermogravimetric curve of the crab chitin, Verongida sponge chitin and Verongida chitinous sponge skeleton (courtesy Dawid Stawski).

Extreme Biomimetics *in vitro*

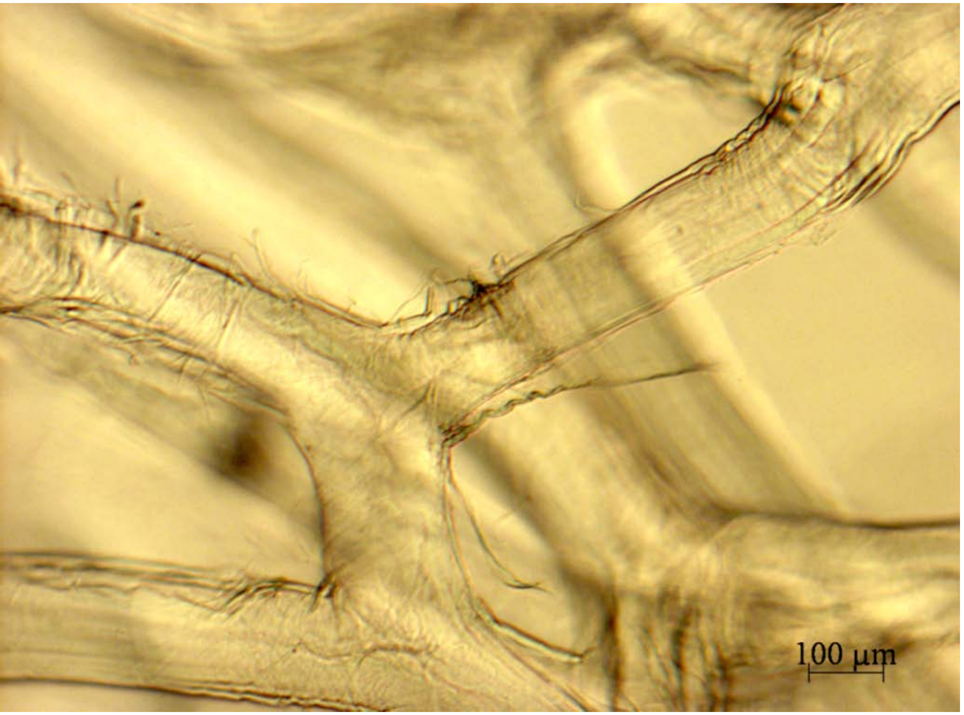

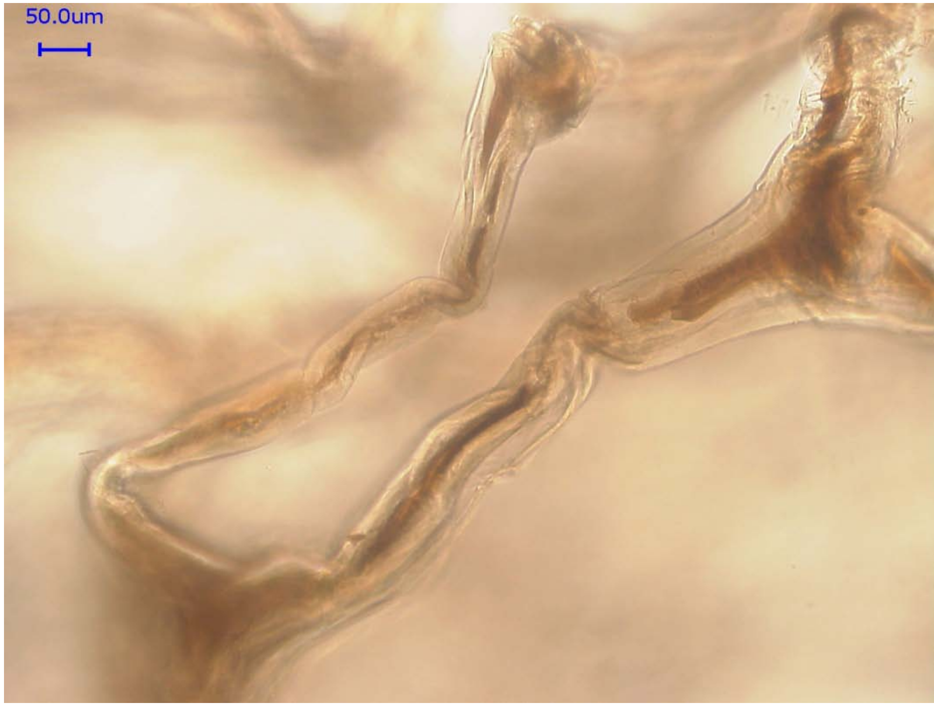

Light microscopy images of ZrO_2 crystalline phase (right) obtained within sponge chitinous matrix (left).
Precursor: Ammonium Zirconium (IV) Carbonate
Temperature: 150 °C
Reaction time: 24 h

Extreme Biomimetics *in vitro*

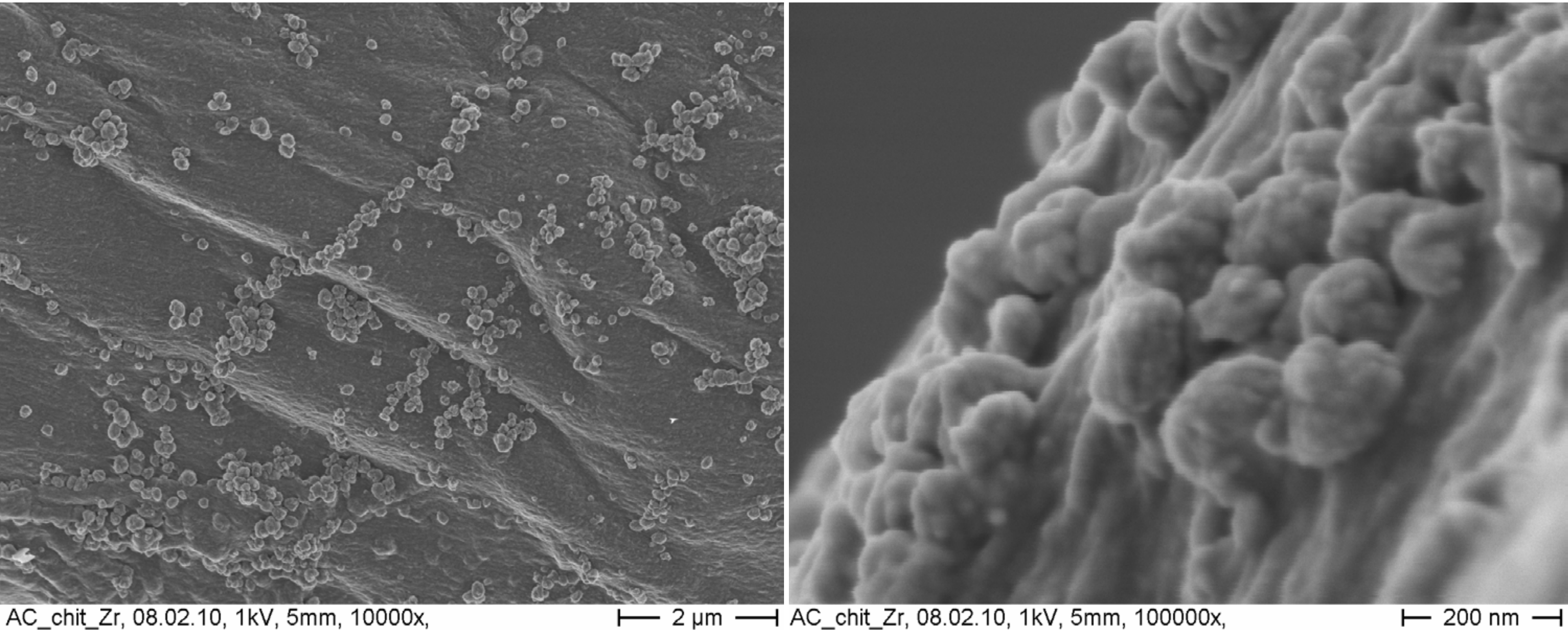

SEM images of ZrO_2 nanocrystals obtained on the surface of sponge chitinous matrix.
Precursor: Ammonium Zirconium (IV) Carbonate
Temperature: 150 °C
Reaction time: 24 h

Extreme Biomimetics: TEM and X-ray pattern of ZrO2 - chitin

ZrO_2: 3.73 Å (01-1) 2.88 Å (111),
3.17 Å (11-1) ZrO_2 1.83 Å (21-2) v (02-2) v (220)

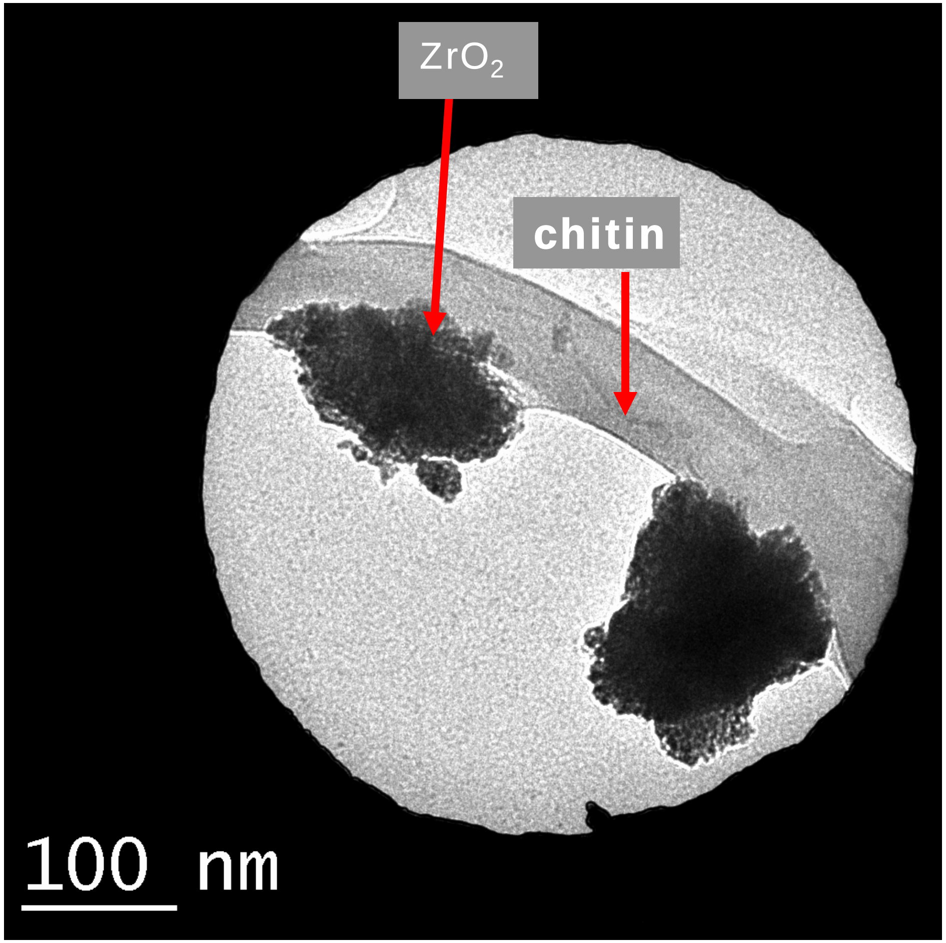

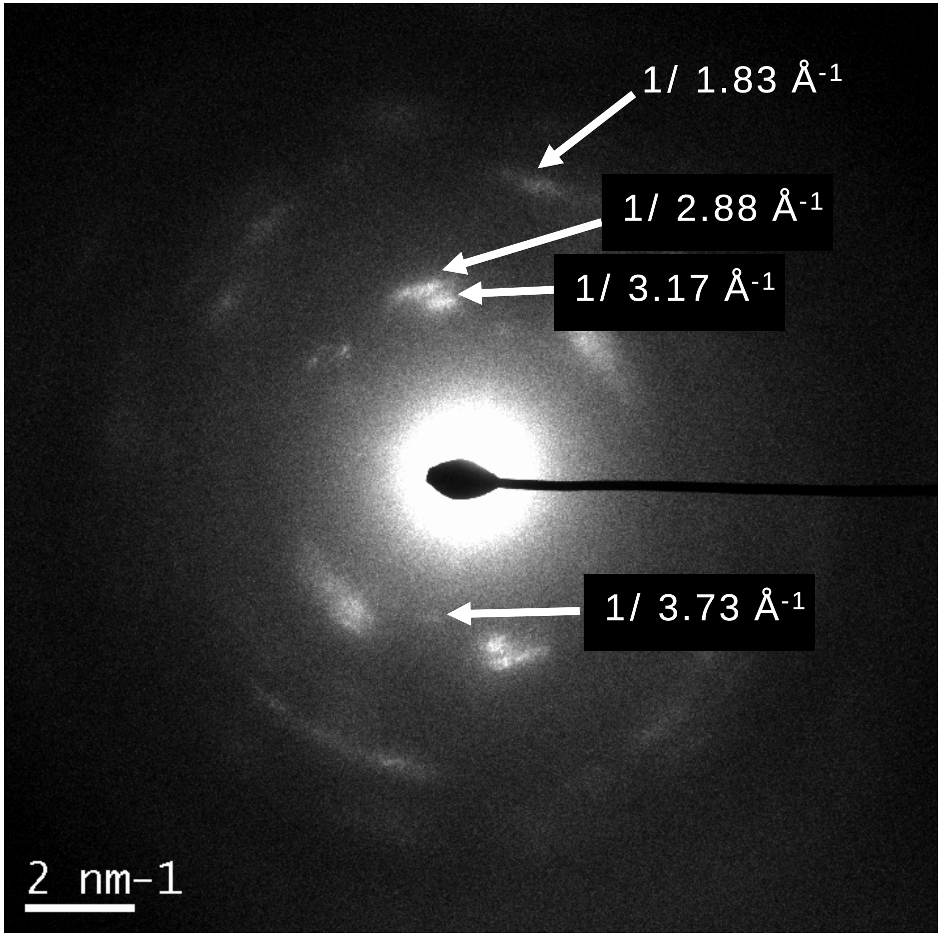

Conclusions

- Nanoorganized silica-aragonite-chitin biocomposite in demosponges as well as silica-calcite biocomposite in glass sponges are the additional evidence regarding to the presence of more complex multiphase biomineralization in nature.

- These findings motivate us to develope novel strategies to design nanostructured hybride biocomposites *in vitro*.

- *Extreme Biomimetics* is proposed as a challenging strategy to develope of new generation of biomaterials.

Outlook

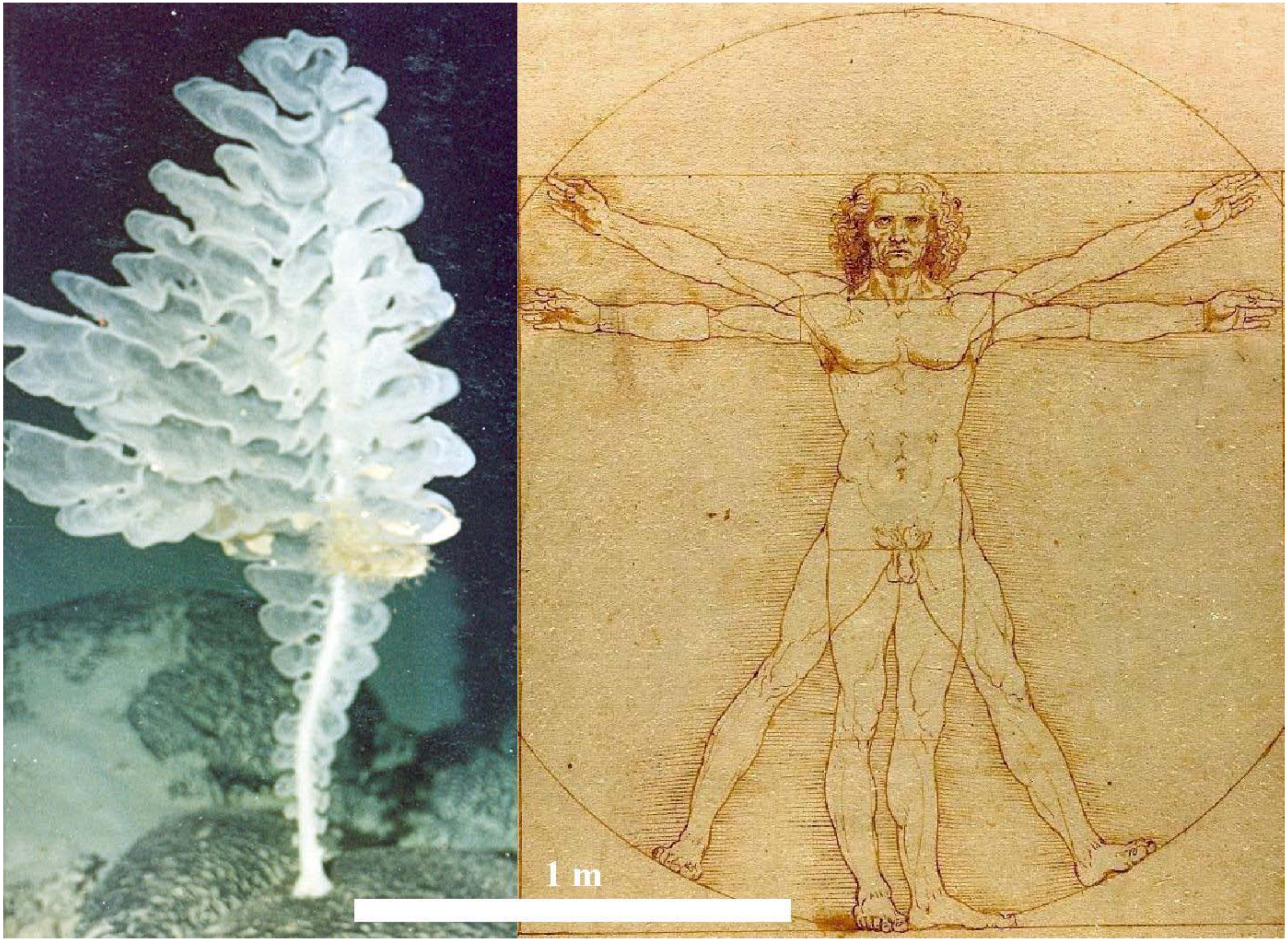

Unique hierarchically structured skeletons of up to 2 m high and 70 cm wide *Aspidoscopulia* sp. deep-sea glass sponges are present in our collection.

From: H. Ehrlich, Silica Biomineralization, In: *Encyclopedia of Geobiology*, Springer, 2011, (in press)

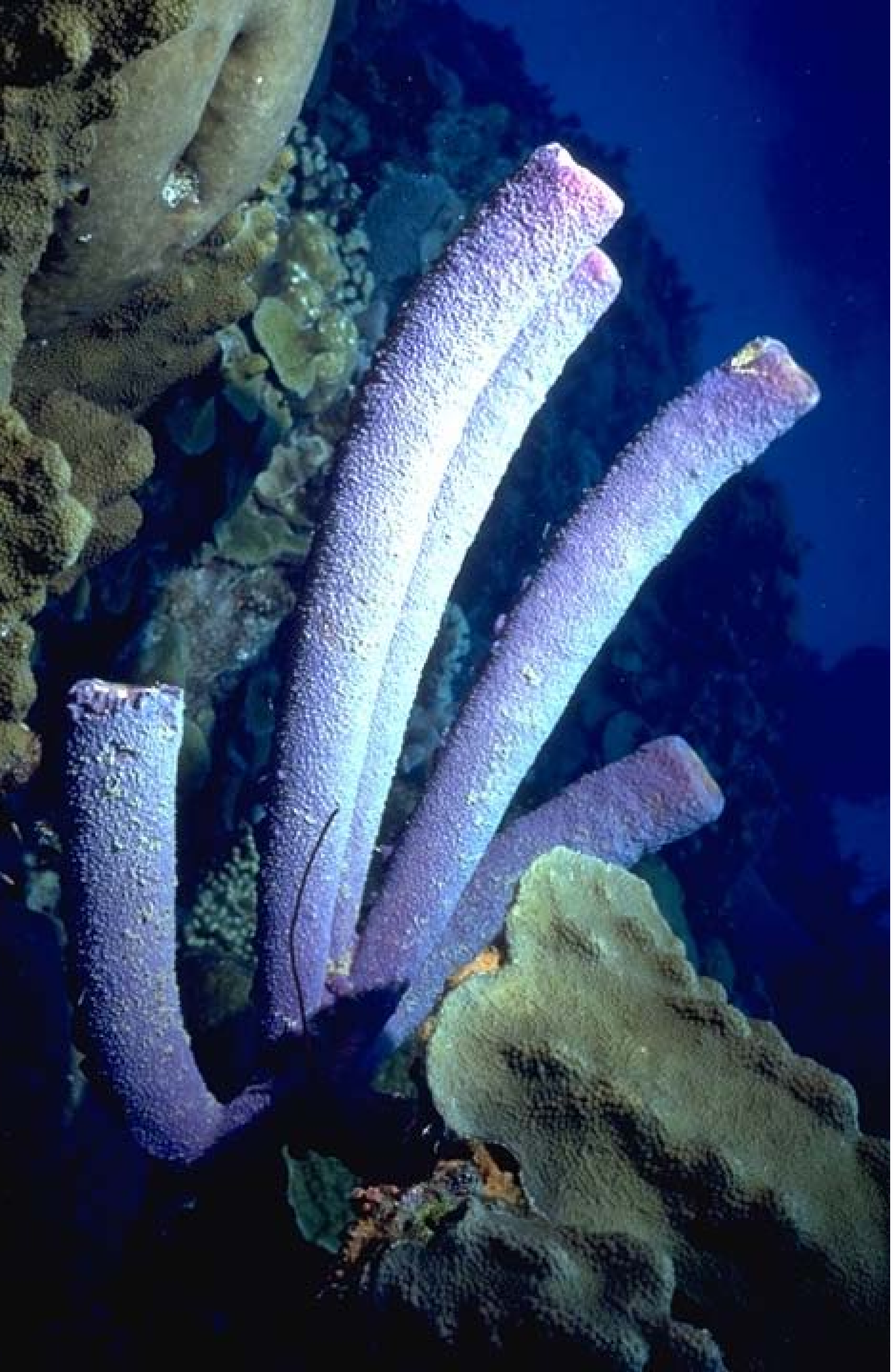

Acknowledgments for collaboration:

Prof. Matthew Collins & Team (UK)

Prof. Serguei L. Molodtsov & Team (Germany)

Prof. Alexander Ereskovsky (France)

Prof. Gert Wörheide & Team (Germany)

Prof. Henry Reiswig (Canada)

Prof. Hartmut Worch & Team (Germany)

Prof. Eike Brunner & Team (Germany)

Prof. Stanislav Gorb & Team (Germany)

Prof. Carsten Werner & Team (Germany)

Prof. Victor Smetacek, Prof. Karen Wiltshire & Team (Germany)

Dr. Konstantin Tabachnick (Russia)

Dr. Paul Simon (Germany)

Dr. Philipp Sapozhnikov (Russia)


Thank you for your attention !